

Emilie Steinbakk Ulriksen  
NTNU  
Norwegian University of  
Science and Technology  
Faculty of Natural Sciences  
Department of Biotechnology and Food Science

Emilie Steinbakk Ulriksen

# Immune cell profiles associated with exposure to phthalates (DEHP and DiNP)

A high-dimensional cell cytometry (CyTOF)  
approach

May 2019





Norwegian University of  
Science and Technology

# **Immune cell profiles associated with exposure to phthalates (DEHP and DiNP)**

A high-dimensional cell cytometry (CyTOF) approach

**Emilie Steinbakk Ulriksen**

Biotechnology

Submission date: May 2019

Supervisor: Eivind Almaas

Co-supervisor: Unni Cecilie Nygaard

Norwegian University of Science and Technology  
Department of Biotechnology and Food Science



# Sammendrag

**Bakgrunn:** Forekomsten av immunrelaterte sykdommer har i løpet av de siste tiårene økt for personer som lever i den vestlige verden. Denne økningen, kan delvis skyldes økt eksponering fra kjemikalier fra hverdags produkter og diet som resultere i en kjemisk cocktail senario. Ftalater er en gruppe av slike hverdags kjemikalier. Mange er karakterisert som endokrine forstyrrende stoffer (EDC) og ftalat eksponering er assosiert med økning i immune relaterte sykdommer som astma og allergi. For øyeblikket er det lite som er kjent om handlings mekanismen (mode of action) for ftalat eksponering på immunceller. Dette er i en stor grad et resultat av kompleksiteten til immunsystemet og tidligere mangel på metoder for å undersøke handlingsmekanismene i høy-dimensjons detalj.

**Mål:** Målet med denne masteroppgaven var å undersøke om høy-dimensjons celle analyse ved bruk av CyTOF kan oppdage assosiasjoner mellom ftalat eksponering og immuncelle profiler hos voksne. Mer spesifikt, var målet å identifisere subpopulasjoner eller funksjonelle karaktertrekk assosiert med DEHP (Di(2-ethylhexyl) phthalate ) og DiNP (Diisononyl phthalate) eksponering.

**Metode:** Perifere blod mononukleære celler fra 28 friske deltakere ble analysert ved bruk av høy-dimensjons CyTOF analyse. Fjorten deltakere, syv damer og syv menn, ble inkludert i de høye og lave DEHP og DiNP eksponeringsgruppene. For hver deltaker ble to prøver kjørt. En prøve var ustimulert og var inkludert for å identifisere hoved populasjoner og subpopulasjoner i detalj, og uttrykk av funksjonelle markører på disse. Den andre prøven ble stimulert med phorbol 12-myristate 13-acetate og ionomycin og var inkludert for å se på hoved populasjoner, noen subpopulasjoner og cytokinuttrykket hos disse. Både manuell «gating», statistiske analyser og data-dreven clustring (unsupervised) ble utført for å identifisere gruppeforskjeller i immun celler hos de høyt og lavt eksponerte.

**Resultat og diskusjon:** I gruppen med høy sammenlignet med lav eksponering for ftalater, observerte vi en økning i mengden av gitte immunceller funnet i det medfødte immun systemet, det vil si Mo og NK-celle subpopulasjoner. Den høyt eksponerte gruppen viste også et konsistent reduserende mønster. Vi fant redusert produksjon av IL-6 og TNF $\alpha$  i samme subpopulasjoner av B-celler i den høyt sammenlignet med den lavt eksponerte gruppen. I tillegg fant vi redusert uttrykk av HLA-DR i  $\gamma\delta$ T-celler og CD69 i underpopulasjoner av Th-celler hos den høyt sammenlignet med den lavt eksponerte gruppen.

**Konklusjon:** Den observerte økningen av celler i det medfødte immunsystemet kan antyde en tendens til høyere inflammasjon i personer med høy ftalat eksponering. Det reduserte uttrykket av IL-6 og TNF $\alpha$  fra samme B-celle subpopulasjoner og redusert uttrykk av aktiveringsmarkører på noen T-celle subpopulasjoner antyder en mulig funksjonell reduserende effekt på celler i det adaptive immun systemet som et resultat av høy ftalat eksponering. Innad i det medfødte og det adaptive immun systemet ser det ut til å være like tendenser i celle mengde og karaktertrekk, dette sammen med tidligere studier antyder en mulig effekt av ftalater på immun celler. Videre studier (eks. genuttrykk og *in vitro* studier) trengs for å bekrefte disse observasjonene.

# Abstract

**Background:** Incidences of immune related diseases have increased during the last decades for people living in the western world. This rise might, in part, be due to the increased exposure to chemicals from common everyday products and diet, resulting in a chemical cocktail exposure scenario. Phthalates are a group of such everyday chemicals. Many phthalates are characterized as endocrine disruptive chemicals (EDC) and phthalate exposure have been associated with increased immune related diseases like asthma and allergies. At the moment, little is known about the mechanism, the mode of action (MoA) of phthalate exposure on immune cells. This is largely due to the complexity of the immune system and previously lacking methods for investigating MoAs in high-dimensional detail.

**Aim:** The overall aim of this Master project was to investigate whether explorative high-dimensional cell analysis by CyTOF can reveal associations between phthalate exposure and immune cell profiles in adults. More specifically, we aimed to identify subpopulations or functional characteristics associated with DEHP (Di(2-ethylhexyl) phthalate ) and DiNP (Diisononyl phthalate). exposure.

**Method:** Peripheral blood mononuclear cells from 28 healthy participants were analyzed using high-dimensional CyTOF analysis. Fourteen participants, seven males and seven females, were included in the groups exposed to high and low levels of the phthalates DEHP and DiNP. For each participant two samples were run. One sample were left unstimulated aiming to, in detail, identify major cell populations and subpopulations of these and analyze the expression of functional markers. The other sample were stimulated with phorbol 12-myristate 13-acetate and ionomycin, aiming to identify major cell populations and their cytokine expression. Both manual gating, statistical analysis and unsupervised clustering were used for identifying group differences for the immune cells of the high and low exposed.

**Results and discussion:** In the group with high compared to the low exposure to phthalates, we observed an increase in the abundance of certain innate immune cells, i.e. Mo and NK-cell subpopulations. This high exposed group also showed a consistent reducing pattern on cells in the adaptive immune system. Reduced production of IL-6 and TNF $\alpha$  in the same subpopulations of B-cells were found in the high compared to the low phthalate exposed group. In addition, the two activation markers HLA-DR and CD69 were found to be reduced in  $\gamma\delta$ T-cells and subpopulations of Th-cells in the high compared to the low exposed group, respectively.

**Conclusion:** The observed increase of innate immune cells could suggest a tendency towards higher inflammation in people exposed to high levels of phthalates. The reduced expression of IL-6 and TNF $\alpha$  from the same B-cell subpopulations and reduced expression of activation markers on some T-cell subpopulations suggests a possible functional reducing effect in adaptive immune cells as a result of high phthalate exposure. The observed similar tendency of cell abundance and functional characteristics of cells within the innate or adaptive immune system along with previous studies does suggest a possible effect of phthalates on immune cells. Further studies (e.g. looking at gene expression and *in vitro* analysis) are needed confirm these effects.

## Forord

Jeg vil begynne med å takke Folkehelseinstituttet ved Trine Husøy og Hubert Dirven for å ha gitt meg muligheten til å delta på EuroMix prosjektet. Uten dere hadde ikke denne masteroppgaven vært mulig. I tillegg vil jeg takke Kanutte Huse på Radiumhospitalet for lån av utstyr og kompetanse relatert til CyTOF og Anette Bølling for hennes bidrag med kunnskap om ftalater. Jeg vil også rette en stor takk til bioingeniørene Hege Hjertholm, Tone Rasmussen, Else-Carin Groeng og Bodil Hasseltvedt for all hjelp på laboratoriet. Spesielt vil jeg takke deg Hege, du har vært en fantastisk labpartner og en god venn gjennom hele masterløpet.

Jeg vil også rette en stor takk til mine veiledere Eivind Almaas og Unni Cecilie Nygaard for deres gode tilbakemeldinger og innspill. Spesielt vil jeg takke deg Unni, du har vært en helt fantastisk veileder. Du har vært tilgjengelig til enhver tid, både for spørsmål, diskusjon og en uformell prat. Maken til innsats skal man lete lenge etter! Din evne til å videreformidle og forklare har gitt meg både en forståelse og interesse for fagfeltet som har vært helt avgjørende for min oppgave. Jeg setter stor pris på all hjelpen du har gitt meg.

Til alle dere på avdeling for toksikologi og risiko, dere har vist meg hvor viktig og gøy samarbeid innen forskning er. Tusen takk for at dere fikk meg til å føle meg velkommen fra dag en, dere er en flott gjeng!

I tillegg til jeg takke mine flotte studiekamerater i Trondheim for alle de fantastiske opplevelsene og de gode minnene dere har gitt meg gjennom studietiden. Til slutt vil jeg takke min fantastiske familie som har stått med meg og støttet meg både gjennom oppturer og nedturer. Dere har vært en klippe gjennom hele studieløpet, og spesielt gjennom masterskrivingen. Jeg hadde ikke klart dette uten deres støtte.

Also, to Friederike Sonnet. Thank you so much Rike for all your help, you have been an amazing support and a great help throughout my master project. You were always available for questions and discussions, and I really appreciate all you have done for me!

Emilie Steinbakk Ulriksen

Oslo/Trondheim, Mai 2019

# Index

1.	Introduction .....	1
1.1.	Immunotoxicology.....	1
1.2.	Phthalates.....	2
1.2.1.	Effect of HMW phthalates .....	3
1.3.	The Immune system.....	4
1.3.1.	The innate immune system .....	5
1.3.2.	The adaptive immune system.....	6
1.3.3.	Cytokines .....	8
1.4.	The new era of high-dimensional technology and Immunotoxicology.....	9
1.4.1.	CyTOF.....	9
2.	Aims and hypothesis .....	11
3.	Material and methods .....	12
3.1.	Subjects (EuroMix) and Ethics.....	12
3.2.	Choice of participants.....	12
3.3.	Choice of experimental design and antibody panels.....	13
3.4.	Antibody conjugation, titration and testing.....	15
3.5.	Sample preparation .....	15
3.5.1.	PBMC preparation .....	15
3.5.2.	Thawing of cells.....	16
3.5.3.	Sample preparation – unstimulated cells (Panel 1) .....	17
3.5.4.	Sample preparation – stimulated cells (Panel 2) .....	17
3.5.5.	CyTOF data acquisition .....	17
3.6.	Reproducibility – between days, PBMC vials and tube parallels .....	18
3.7.	Further development of CyTOF protocol.....	18
3.7.1.	Impact of antibody cocktail freezing and thawing.....	18
3.7.2.	Test of EDTA for increased cell yield.....	18
3.8.	CyTOF statistical analysis (Cytobank) .....	19
3.8.1.	Biaxial gating.....	19
3.8.2.	viSNE .....	21
3.8.3.	CITRUS.....	21
3.8.4.	Statistical analysis (Mann-Whitney test).....	22
4.	Results .....	23



4.1.	Initial methodological investigations.....	23
4.1.1.	Effect of stimulation on cytokine production and marker expressions in Panel 2 .....	24
4.1.2.	Reproducibility - between days, PBMC vials and tube parallels .....	26
4.2.	Participant characteristics .....	27
4.3.	Immune cell profiles associated with phthalate exposure levels.....	30
4.3.1.	Manual biaxial gating .....	30
4.3.2.	Data-driven clustering and group differences (CITRUS results).....	30
4.4.	Further development of CyTOF protocol.....	35
4.4.1.	Freezing and thawing of the antibody cocktail.....	35
4.4.2.	Test of EDTA for increased cell yield.....	37
5.	Discussion .....	38
5.1.	Methodological considerations.....	38
5.1.1.	Reproducibility .....	38
5.1.2.	Effect of stimulation on cytokine production and marker expression in Panel 2 .....	38
5.1.3.	Cytokine signal and background assessment.....	39
5.1.4.	Freezing of antibody cocktail.....	39
5.1.5.	Monocyte numbers and cell yield .....	40
5.1.6.	Statistical tests in the CITRUS algorithm .....	40
5.2.	Phthalates and innate immune cells.....	41
5.3.	Phthalates and adaptive immune cells.....	44
6.	Conclusion and future directions .....	48

References

Appendix

Figures

Tables

# Figures

<b>Figure 1:</b> Immunotoxic exposure are chemicals and substances that might affect the immune response in some way.....	1
<b>Figure 2:</b> Differentiation of a multipotential hematopoietic stem cell into myeloid or lymphoid progenitor cell. ....	5
<b>Figure 3:</b> Th-cell differentiation.....	8
<b>Figure 4:</b> Illustration of CyTOF based analysis of cellular markers .....	10
<b>Figure 5:</b> Mass cytometry panels.....	14
<b>Figure 6:</b> CyTOF PBMC cell preparation process. ....	16
<b>Figure 7:</b> Gating strategy for the data analyses.....	19
<b>Figure 8:</b> Results from the MMM cytokine control experiment for samples from one of the two participants. ....	24
<b>Figure 9:</b> Effect of PMA+IM stimulation results from two parallel samples from one participant are shown. ....	25
<b>Figure 10:</b> The percentage of the major immune cell populations (B-, T-, NK-cells, DC, Mo and subpopulations of T-cells (Th- and Tc-cells)) in unstimulated (A) and stimulated (B) samples, all from one participant (L14). ....	27
<b>Figure 11:</b> The participants chosen for the high and low exposed group resulted in two groups. ....	29
<b>Figure 12:</b> Percentages of the major immune cell populations present in PBMC (T-, B-,NK-cells, DC, Mo and T-cell subpopulations Th- and Tc-cells) for each individual as well as the group median (framed to the right), in unstimulated samples obtained by manual gating according to Table 2. ....	30
<b>Figure 13:</b> CITRUS cell abundance results for unstimulated cells stained with antibody Panel 1 (PAM cv.min statistics are shown). ....	32
<b>Figure 14:</b> CITRUS cell expression level of functional marker results for unstimulated cells stained with antibody Panel 1 (PAM cv.min statistics are shown). ....	33
<b>Figure 15:</b> CITRUS cell abundance results for stimulated cells stained with antibody Panel 2A and 2B (PAM cv.min statistics are shown. ....	34

**Figure 16:** CITRUS cell expression level of functional marker results for stimulated cells stained with antibody Panel 2A and 2B (SAM (FDR <1%) statistics are shown). ..... 35

**Figure 17:** Difference in median marker intensity between the frozen and fresh antibody cocktail for the unstimulated (A) and the stimulated (B) samples. .... 36

**Figure 18:** Percentage of major PBMC cell populations in samples with EDTA treatment (orange) or without EDTA treatment (blue) in stimulated (A, B) and unstimulated (C, D) samples. . ..... 37

**Figure 19:** Summary of the main results for innate immune cells. .... 41

**Figure 20:** Summary of the main results for adaptive immune cells. .... 44

## Tables

**Table 1:** DEHP and DiNP parent compound, first metabolites and oxidized secondary metabolites ..... 3

**Table 2:** Manual biaxial gating was performed on living singlet cells..... 20

**Table 3:** Exposure levels for the molecular corrected sum of DEHP and DiNP and characteristics of the selected participants in the group of high (red) and low (green) exposure levels for DEHP and DiNP<sup>1</sup>. ..... 28

# Abbreviations

$\gamma\delta$ T – gamma-delta T-cells

AoP – Adverse outcome pathway

APC – Antigen presenting cells

B – B-cells

CD – Clusters of differentiation

CSB – Cell Staining Buffer

CytoF – Cytometry by Time of Flight

DC – Dendritic cells

DEHP - Di(2-ethylhexyl) phthalate

DiNP - Diisononyl phthalate

EDC – Endocrine disruptive chemical

EDTA - Ethylenediaminetetra-acetic Acid

HMW – High molecular weight

Ig – Immunoglobulin

IL – Interleukin

IM – Ionomycin,

LMW – Low molecular weight

MHC – Major histocompatibility complex

Mo – Monocytes

MoA – Mode of action

NK – Natural killer cells

PBMC – Peripheral blood mononuclear cells

PMA - Phorbol 12-myristate 13-acetate

PPAR $\gamma$  – Peroxisome proliferator-activated receptor gamma

RT – Room temperature

TCR – T-cell receptor

IFN – Interferon

Tc – Cytotoxic T-cells

Th – Helper T-cells

TNF – Tumor necrosis factor

# 1. Introduction

## 1.1. Immunotoxicology

With all the different components of the immune system working together and relying on precise communication to function properly, it stands to reason that any misregulation of this complex system might have serious consequences [1] (Figure 1).

Immunostimulation is indicated by an over-reactive immune response and might lead to inflammation and chronic diseases such as asthma, allergies and autoimmune diseases [2-4]. Immunosuppression is, on the other hand, not so easily recognized, but may result in increased risk of infections, reduces resistance to cancers and reduced effects of vaccination [5, 6].

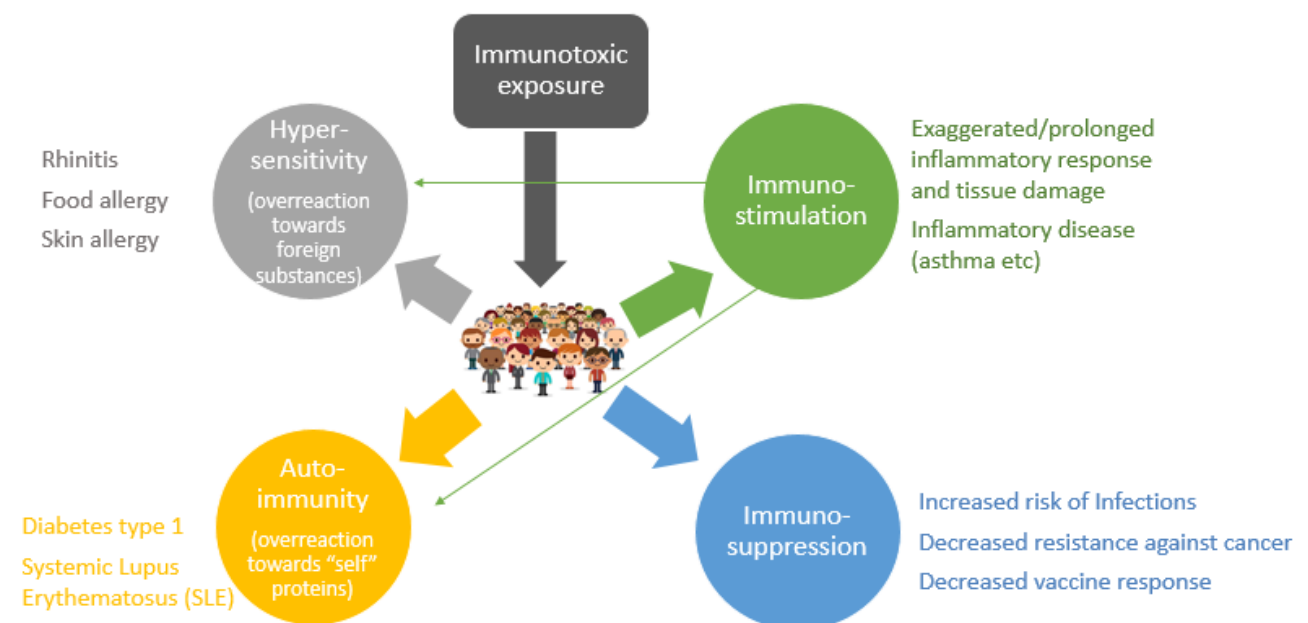


*Figure 1: Immunotoxic exposure are chemicals and substances that might affect the immune response in some way. The main ways the immune system is affected is either through immunosuppression or immunostimulation (thought to contribute to autoimmunity and hypersensitivity). Depending on how the immune system is affected, different disease risks are associated with such dysfunctional immune activity [7].*

The observed increases in immune related diseases in the western world during the last decades have resulted in more focus on the immunological effects of toxicologically assessed chemicals [8-10]. It is hypothesized that this increase in prevalence might be due to western lifestyle, including chemical exposures from everyday products commonly found in the western world [11, 12]. Immunotoxicology is the study of toxic effects on the immune system. The interest in these effects have grown concurrently with the growing awareness of the potential harmful effects that chemicals, including air and water pollutants, food and cosmetic additives and contaminants might have on the human immune system. There is a growing concern that these chemicals might increase or promote immune related diseases and disorders [13].

These concerns are supported by animal, epidemiological and human studies investigating mainly prenatal and early life exposure to certain consumer chemicals in connection to immune-related health outcomes later in life. A number of studies are

reporting a possible link between exposure to chemicals (e.g. phthalates and phenols) from consumer products (dietary contaminants, food packaging, polyvinyl chloride (PVC) containing products, cosmetic and cleaning products etc.) and increased risk of immune related diseases [13-17].

Immunotoxicological endpoints reflecting immune functions have, however, not until recently and only to a limited extent been considered in regulatory risk assessments of chemicals and contaminants. This is, largely, due to the lack of appropriate biological assays and biomarkers to assess such adverse effects on the immune system.

## 1.2. Phthalates

Phthalate esters are a group of synthetic compounds widely used as plasticizers in consumer products, and suspected of having adverse effects on human health [18]. These plasticizers are not chemically bound to the material in which they are used, and may easily leak to the surroundings [19]. Phthalates are found in products ranging from children's toys, PVC flooring, medical equipment, personal care products (PCP) and food products, with a higher leakage into fatty food [20-27].

Phthalates have different properties depending on the length of their carbon backbone chains and are divided into two main groups accordingly. These two are high molecular weight (HMW) phthalates (9-13 carbon backbone atoms) and low molecular weight (LMW) phthalates (3-8 carbon backbone atoms) [28]. LMW phthalates are mainly used in PCP and cosmetic products [20, 22, 29], and HMW phthalates are mainly used as plasticizers in PVC products, including clothing, food packing, medical devices and toys [30].

HMW phthalates are larger lipophilic molecules that needs to be metabolized to a higher degree than LMW phthalates before excretion in urine [31, 32]. Despite this, most of the oxidized HMW phthalate secondary metabolites are secreted within 24 - 44 h after exposure [33-35]. Because of this, a common way to estimate total phthalate exposure is to measure the metabolites in urine and calculate the total sum of parent compound exposure based on these [25].

Due to their common use and wide range of applications, metabolites of especially HMW phthalates are present, to varying degree, in urine samples of all individuals [20, 36]. Quite a few of these HMW phthalates are suspected of having adverse effects in humans and are therefore the focus of several research project. Some of these HMW phthalates, including Di(2-ethylhexyl) phthalate (DEHP) and in recent years Diisononyl phthalate (DiNP), are also found in relatively high amounts in the general population [27, 37-39]. These two HMW phthalates were the focus for this Master project.

Investigation of different exposure routes have found ingestion and inhalation to be the major routes of exposure for HMW phthalates like DEHP and DiNP [23, 27, 37, 40]. These HMW phthalates are found to contaminate human food (primarily meat, fats and dairy products) and indoor environment through dust and air, and by leaching from PVC material [40, 41]. When entering the human body, these HMW phthalates are rapidly metabolized to their primary metabolites before further oxidation to secondary metabolites (Table 1 for DEHP and DiNP) [23, 35, 42, 43].

Table 1: DEHP and DiNP parent compound, first metabolites and oxidized secondary metabolites

Parent compound	First metabolite	Oxidized second metabolite
<b>DEHP</b>	Monoethylhexyl phthalic acid (MEHP)	Mono(2-ethyl-5-hydroxyhexyl) phthalate (MEHHP) Mono(2-ethyl-5-oxohexyl) phthalate (MEOHP)  Mono(2-ethyl-5-carboxypentyl) phthalate (MECPP) Mono(2-carboxymethylhexyl) phthalate (MCMHP)
<b>DiNP</b>	Mono-iso-nonylphthalate (MiNP)	Hydroxyl (oh-MiNP) Oxo (oxo-MiNP) Carboxy (cx-MiNP)

Because of its endocrine mimicking ability, DEHP has, as of 2008, been characterized as an endocrine disruptive chemical (EDC) category 1B by the European Chemical Agency (ECHA) Member State Committee (MSC), and the use of more than or equal to 0.3 % DEHP is prohibited in consumer products [44]. This classification and the determined total daily intake (TDI) value of 50 µg/kg/day set by European food and safety authority (EFSA) and ECHA are mainly based on results from animal studies [45]. The strict regulation of DEHP has led the industry to use DiNP as a substitute plasticizer due to the similar chemical structure of these two chemicals [25, 35, 38]. However, studies have found DiNP to possibly have similar adverse effects as those noted for DEHP [46-48].

### 1.2.1. Effect of HMW phthalates

Some groups of people are exposed to particularly high levels of HMW phthalates [49, 50]. These groups include children, in utero/newborns, since HMW phthalates can cross the placenta and are found in breast milk, and workers in the healthcare system and those working with PVC material [20, 23, 42, 51-56].

One hypothesis is that continuous exposure to phthalate background levels, over time might result in subtle endocrine and reproductive related changes [57]. This notion is supported by animal studies reporting that phthalates, mainly DEHP, have negative effects on the reproductive system and development [20, 58-62]. These findings seem to be applicable to humans, as other studies have found indications that DEHP, among other phthalates and chemicals, might act as an endocrine modulator in humans [36, 45, 53, 63-66]. A cohort study looking at phthalate concentrations in pregnant women in relation to endocrine effects in infants have found similar effects. The study found a significant association between higher DEHP metabolite exposure (especially MEHP) in mother during pregnancy and alterations of reproductive organs of especially male infants [67].

However, recent studies have found that reproductive toxicity might not be the most sensitive endpoint. Phthalates are suspected of acting as adjuvants to promote the development of, or aggravate immune related diseases (i.e. allergies and asthma) [13]. This suspicion is strengthened by studies finding associations between exposure to HMW phthalates and a decrease in lung function and increased asthma and allergy related immune responses (Th-2 cell responses, see section 1.3.2.1.2 below) [68-71]. DEHP and

DiNP exposure have in humans been associations with increased risk of developing asthma and allergies, especially if exposed in utero or during childhood, but also for the general population [20, 22, 37, 72, 73]. It is suggested that this increased risk might be due to a Th2-dominant response [74].

Studies performed in rodents further find that DEHP and DiNP have the potential to enhance ongoing inflammation responses, and increase airway inflammation and skin rashes [75, 76]. This have also been observed in offspring's if the mother was exposed during pregnancy [13, 70, 74].

Human occupational studies involving exposure to phthalate fumes in high concentrations (i.e. working with PVC material and daily exposure to PVC equipment for people working in hospitals) have reported associations between exposure to PVC and higher degree of asthma and respiratory diseases [77-82]. There has also been reported a correlation between plastic-walls in the workplace and plastic material in the home and increased risk of asthma and negative respiratory outcomes [77, 83-86].

Most of these human studies are based on associations between phthalate exposure and health outcomes. There are only a few human studies investigating the underlying mechanism and the immunological processes, i.e. the mode of action (MoA), behind these associations.

In one study comparing allergic to non-allergic individuals there was an increase in interleukin 6 (IL-6) (inflammation cytokine) gene expression and cytokine production when directly exposing the participants to low DEHP concentrations, while higher concentrations led to downregulation of inflammatory cytokines [87]. Similar results were found in studies exposing primary immune cells and immune cell lines to higher monophthalate (metabolites of phthalates) doses. This study found that some monophthalates could increase cytokine production in a concentration dependent manner, but that all measured phthalates suppressed cytokine production at higher concentrations [88].

Other studies looking at immune effects of phthalates found that MEHP could potentially influence histamine release from basophils and might be involved in inducing apoptosis in B-cells. Leading to downregulation of immunoglobulin E (IgE) antibody production and an immunosuppressive effect [89-92]. In addition, MEHP has been found to act through peroxisome proliferator-activated receptors (PPAR's) to induce the production of TNF $\alpha$  (a pro-inflammatory cytokine) from murine monocyte-macrophage cell lines [93].

There is still a need for a more detailed understanding of the underlying mechanisms that potentially drives these adverse health outcomes. Therefore, the immunological effects of phthalates needs more research. The mechanisms are still largely unknown, possibly due to the high complexity of the immune system, and high-dimensional methods are needed to broaden the understanding.

### 1.3. The Immune system

The immune system is the body's defense mechanism against foreign invaders. It consists of an interactive network of lymphoid organs, immune cells, humoral factors, and cytokines working together to keep the organism healthy [94, 95]. The immune



system distinguishes endogenous "self" from atypical or "non-self" through specific molecules present on cell surfaces and eradicate potential harmful molecules and cells not expressing this "self" pattern [96]. A molecule recognized by the immune system as foreign is called an antigen [96].

The best illustration of the necessity of the immune system becomes evident when the system is malfunctioning. Where over-activity can result in allergies and autoimmune diseases, underactivity might results in severe and more frequent infections and immunodeficiency [97].

Humans and vertebrates have two main types of complementary cellular immunity, the innate immune system (not antigen specific) and the acquired, also called the adaptive, immune system (antigen specific). Cells in the innate immune system mainly originate from the myeloid stem cell lineage, while cells in the adaptive immune system mainly originate from common lymphoid progenitor cells, respectively [96, 98]. Cells in the immune system are analytically characterized based on their surface proteins named by clusters of differentiation (CD) numbers. Different CD's are also commonly used to distinguish between different cell subpopulations [99]. The focus of this project was the peripheral blood mononuclear cells (PBMC) (Figure 2), as these are blood cells that can be collected and stored in a living state.

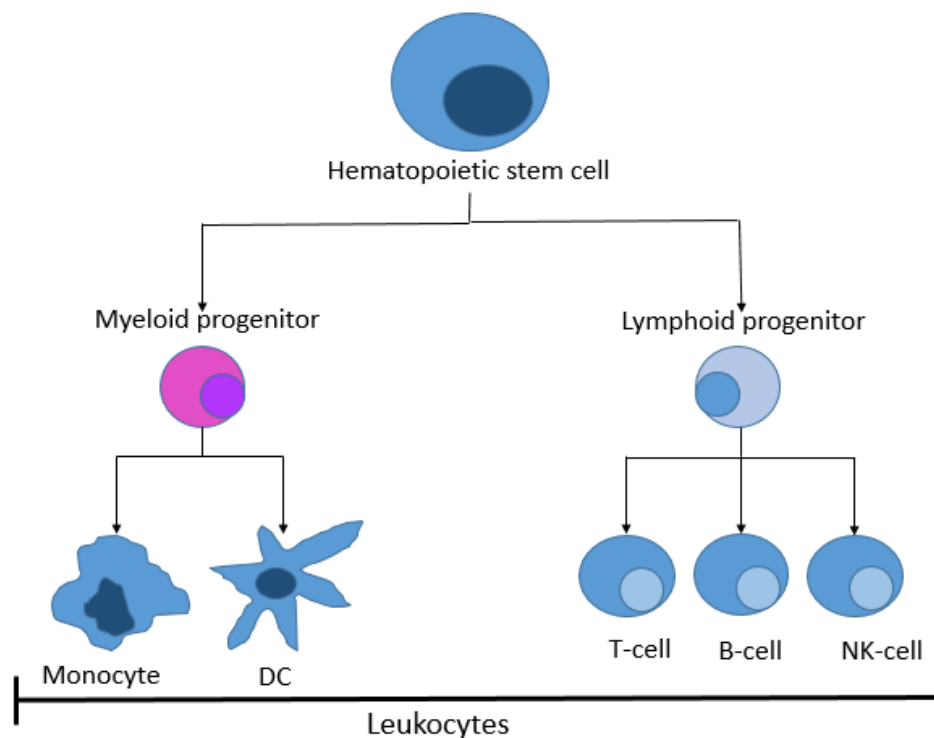


Figure 2: Differentiation of a multipotential hematopoietic stem cell into myeloid or lymphoid progenitor cell. These cells then differentiates into effector leukocyte cells (white blood cells) present in the immune system. The flowchart shows cells found in PBMC.

### 1.3.1. The innate immune system

The innate immune system is inherent and does not require prior exposure to antigens to respond. Cells in this system have germline-encoded pattern recognition receptors (PRR)

designed to recognize widespread antigens with general surface protein pattern. This type of rigid antigen receptor does not provide antigen-specific responses or the possibility to develop cellular memory, but makes the innate cells able to differentiate quickly and act fast (within hours) when antigens are present [100].

#### *1.3.1.1. Cells in the innate immune system*

Monocytes (Mo), Dendritic cells (DC) and Natural killer- (NK-) cells, as well as granulocytes, are cells of the innate immune system. All but granulocytes are preserved after PBMC isolation. Mo and DC belong to a group of large cells that engulf and digest foreign substances, called phagocytes. Mo circulate in blood before migrating to the site of tissue inflammation where they differentiate to macrophages (MØ) [101, 102]. DC belong to a subgroup of cells called antigen presenting cells (APC) [103]. APC carry major histocompatibility complex (MHC) class II molecules which are needed for presenting antigen peptides to T-cells and engage the adaptive immune system, also includes B-cells (see section 1.3.2. below) [96]. NK cells are responsible for removing foreign substances in the body, either by physical cell-to-cell contact or through secretion of cytotoxic molecules (i.e. perforin and granzyme) [104]. These substances includes infected or damaged cells that does not express a "self" MHC class I molecule or antigens coated by antibodies in an antibody-dependent manner [105, 106].

#### **1.3.2. The adaptive immune system**

If the innate defense is unable to immediately remove the invading antigen, the adaptive immune system comes into play. The adaptive immune system does require exposure to an antigen before being able to conduct a specific response towards that particular antigen. This system consists of T- and B- cells (lymphocytes) and can be divided into cell-mediated immunity, which depends on T-cell responses, and humoral immunity, which is the secretion of soluble antigen-specific antibodies from B-cells [107].

The repertoire of individual B- and T-cells can together recognize a very wide range of different antigens. These circulating antigen specific lymphocytes are generated through a differentiation process. This process involves the generation of millions of different receptors through somatic recombination and hypermutations in gene segments that make up the antigen receptors of both T- and B-cells [108].

The adaptive immune system has a delayed response time of four to seven days after the first exposure. This is due to the process required for the differentiation and proliferation of these antigen-specific lymphocyte cells to reach sufficient numbers to efficiently attack the foreign substance. A differentiation process is also necessary for the adaptive immune system's ability to provide cellular memory. This cellular memory is what enables the adaptive immune system to quickly mount a specific attack against the same antigen upon re-exposure. It consist of antigen-specific memory lymphocytes that remain in the body after the antigen is removed [96].

#### *1.3.2.1. Cells in the adaptive immune system*

Even though B-cells, T-cells and their subpopulations are morphologically similar, they have very distinct functional tasks. They are analytically distinguished based on their antigen-specific surface receptors (B- and T-cell receptors, respectively) and surface proteins named by CD numbers.

#### 1.3.2.1.1. B-cells

B-cells make up around 5-15 % of the lymphocytes in blood [99]. They are the major players of the humoral adaptive immune defense where mature B-cells (plasma cells) secrete antibodies after activation via helper T-cells (see section 1.3.2.1.2. below) [107]. One plasma cell is capable of producing large amounts of similar antibodies, all specific to one target [109, 110]. The antibodies produced can either coat their specific antigen and thereby neutralize it, or engage NK-cell, macrophages or the compliment system of the innate immune system to remove the antigen [111].

#### 1.3.2.1.2. T-cells

T-cells make up the cell-mediated immunity in the adaptive immune system and are unable to recognize free antigens. The T-cell receptor (TCR) binds to antigens either presented to them through a MHC class I (CD4+ T-cells) or class II (CD8+ T-cells) molecule. In order to be fully activated, the T-cell also require the binding of either a CD4 (in the case of MHC class II binding) or a CD8 (in the case of MHC class I binding) co-receptor. After specific recognition and binding with a MHC-peptide complex, the CD4+ helper T-cells (Th-cells) and CD8+ cytotoxic T-cells (Tc-cells) can further differentiate into other specialized effector subpopulation cells based on environmental stimuli, mainly from co-stimulatory molecules and cytokines from neighboring cells. Once differentiated, these cells may rapidly proliferate [107, 112].

All nucleated cells have MHC class I molecules on their cell surface but only when this molecule presents a "non-self" peptide will the MHC class I be recognized by the CD8+ T-cell as foreign [113]. Similar to NK-cells in the innate immune system, Tc-cells are able to kill an infected or damaged cell. The binding of a specific non-self peptide (within the MHC class I molecule) to the TCR and CD8 co-receptor activates the Tc-cell resulting in the differentiation into effector cells that are able to kill the cell carrying the foreign peptide [112].

Th-cells help to regulate the immune system through their co-stimulatory molecules and cytokine production and secretion. Naïve helper T-cells may differentiate to different effector subpopulations based on the signals they receive from their environment [114-117]. Among these subpopulations are Th1-, Th2-, Th17-, follicular Th (T<sub>FH</sub>)-, gamma-delta T ( $\gamma\delta$ T)- and regulatory T (T<sub>reg</sub>)-cells, all with distinct cytokine secretion patterns and functions (Figure 3) [114, 116, 118-122].

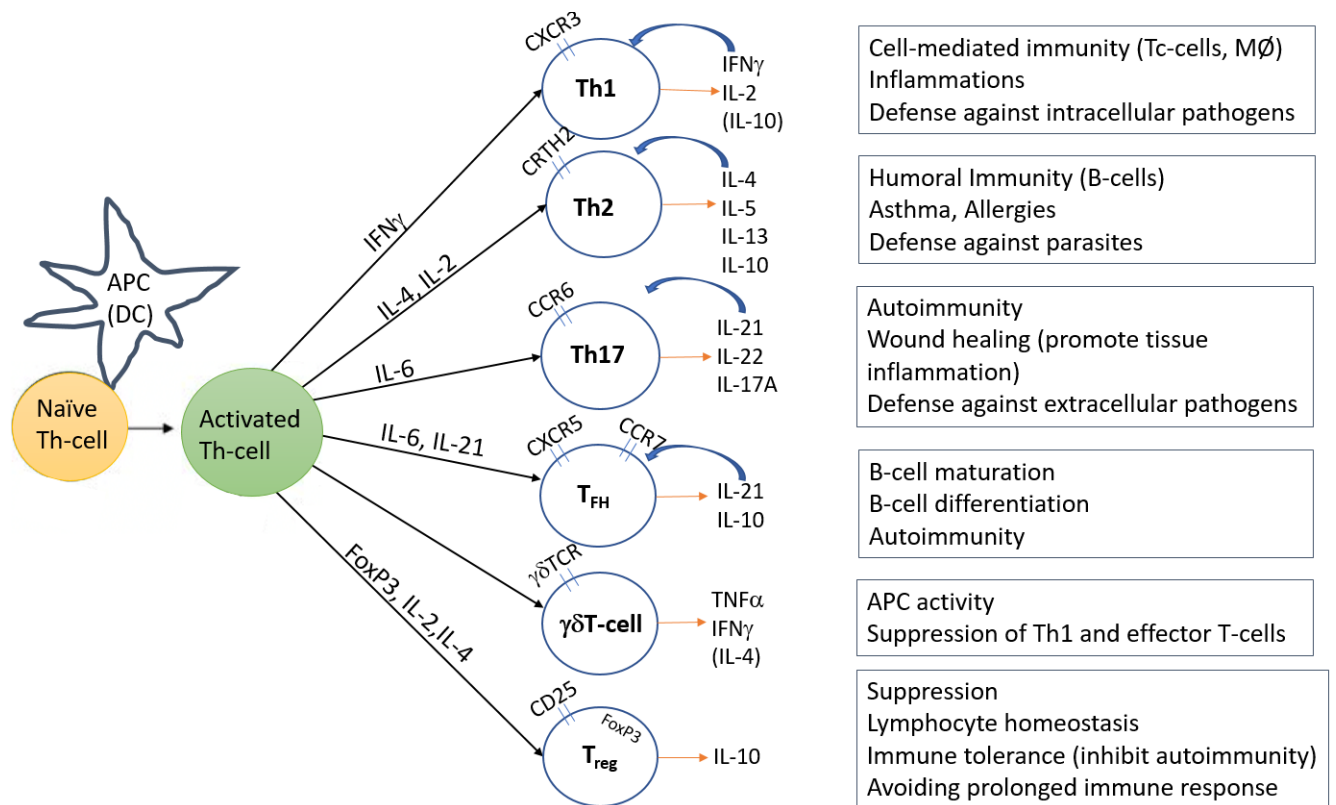


Figure 3: Th-cell differentiation. Antigens are presented to naive helper T-cells by APC. The naive cell then differentiates into an activated T-cell. Based on environmental stimuli (mainly cytokines from surrounding innate and adaptive cells), this activated T-cell will further differentiate into effector T-cells (e.g. Th1-, Th2-, Th17-, T<sub>FH</sub>-, γδT- and regulatory T<sub>reg</sub>-cells) that secrete specific cytokines and have different functions in immune responses.

### 1.3.3. Cytokines

The signaling in the immune system is done by cell-to-cell contact, through chemokines or by cytokines functioning as soluble chemical messengers, orchestrating this complex system [107]. Cytokines are small proteins produced and secreted by cells in response to stimuli, like specific antigens, pathogen associated molecules, chemicals or other cytokines. In the immune system, cytokines are important for the communication between different cells (both within and between the innate and adaptive immune system) and signaling to cells to dictate effector, memory and functional qualities [107].

These small molecules are not produced to target specific antigens, but rather to deliver their signals through cell surface receptors to provoke a specific response in the cell [99]. Cytokines can be produced by different cell types and influence responses in a variety of different cells that bear or upregulate that particular cytokine receptor (Appendix Table 1) [123]. Cytokines consist of a diversity of Interleukins (IL), interferons (IFN) and tumor necrosis factors (TNF) [99, 124]. Depending on the cell they act upon, they can be either pro-inflammatory or anti-inflammatory [123], or can direct the immune response to a variety of different response patterns and thus promote various adverse health effects (e.g. Figure 3)

## 1.4. The new era of high-dimensional technology and Immunotoxicology

The immune system can be viewed as a complex machinery where every component works together to orchestrate the appropriate response against foreign cells and molecules. The rise of high-dimensional technology has made it possible to investigate in detail the components that make up this machinery and how they act together to achieve the end goal of keeping the organism healthy. Thus, such technology increases the chances for more comprehensive immunotoxicological evaluation in future risk assessments.

The recent technological developments that have made it possible for immunologists to get a more detailed picture of the components in the immune system is resulting in a greater understanding of the processes leading to adverse health outcomes [125]. This MoA focus has encouraged the adverse outcome pathway (AOP) approach that provides insight into the molecular initiating event for a toxicant, and key events in the mechanistic pathways that might lead to adverse effects on the immune system [126].

While adverse effects have been associated with immunotoxic compounds in epidemiological and animal studies, *in vitro* studies are important for establishing causality through identification of the MoA of the AOP by looking at the direct effect of chemicals on specific cells and cellular mechanisms. Such studies are, with the standardization of methods and new technology, becoming more common when evaluating toxicological effects on the immune system [127, 128]. However, to efficiently identify immunotoxicity by *in vitro* studies, it is helpful to know what markers to test for and which cell types that are likely to be affected. Some of the opportunities and advantages arising from these new high-dimension technologies are the ability to identify and characterize new or rare cell populations and to identify potential biomarkers that can be tested *in vitro* using human cell lines [125, 129]. We hypothesize that cytometry by time of flight (CyTOF) and other high-dimensional techniques and data analyzing tools will provide insight into the MoA for chemicals of interest and which components in the immune system they might affect.

### 1.4.1. CyTOF

Mass cytometry (also referred to as cytometry by time-of-flight [CyTOF]) is a relatively new method for detailed analysis of cells on a single-cell level (referred to as «deep profiling»). CyTOF allows for the detection of both surface and intracellular markers with high sensitivity. Making it possible to classify cell subpopulations and their activation status while simultaneously detecting functional markers like intracellular cytokines, signaling pathways and proliferation for each single cell. This new high-dimension analysis have already provided new knowledge about diseases progress and immune system functions, among others [130-142].

In mass cytometry, cells are stained with antibodies that are conjugated to stable rare earth metal isotopes and TOF-mass spectrometry (TOF-MS) is used for quantitative detection of the metals. Once cells are injected into the instrument, the nebulizer transforms each cell into aerosol single-cell droplets. These single-cell droplets are then directed to the inductively coupled argon plasma (ICP) where the molecular bonds are broken. The resulting ion cloud is subsequently directed through the quadrupole where low mass ions are removed. This leaves the elemental isotopes with high mass to be

measured by the TOF mass analyzer. The detector is set to detect only heavy elemental ions, excluding atomic ions from cellular elements and from the argon plasma that might remain after the quadrupole. This results in minimal background noise and thus reliable quantitative readings of the labelled tags. The amount of each metal isotope (i.e. specific antibody) per cell is summarized and returned as an flow cytometry standard (FCS) file for each sample (Figure 4) [143].

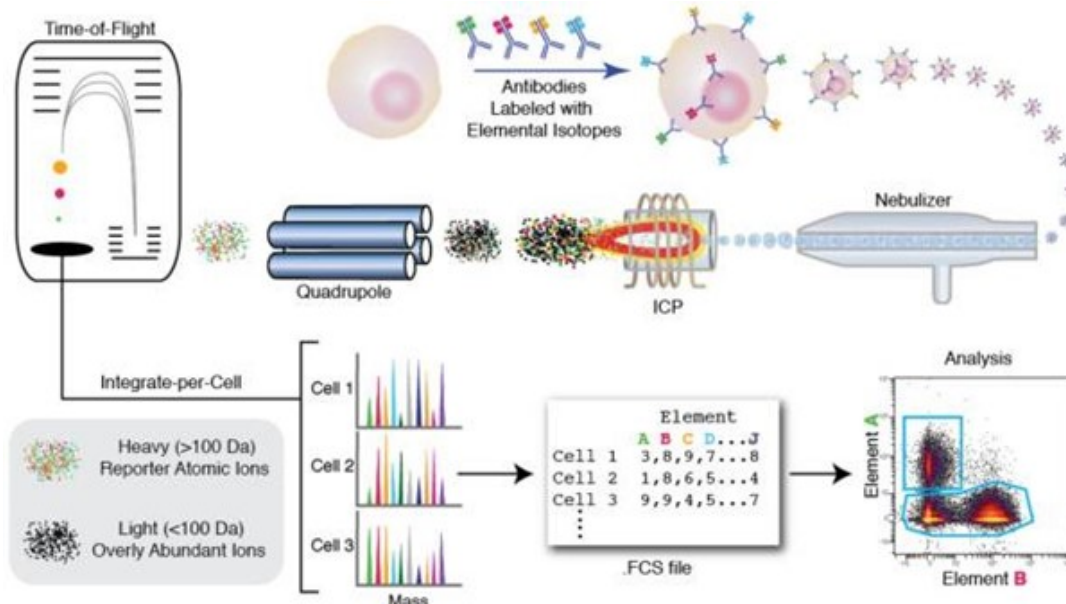


Figure 4: Illustration of CyTOF based analysis of cellular markers. Antibodies are tagged with metal isotopes before staining the cells with antibodies of interest. The stained cells are lead through a nebulizer to be transformed to aerosol single cell droplets. The droplets are lead through the ICP to be atomized and ionized. The Quadrupole then removes the low mass ions, leaving the high mass ions to be measured by the TOF mass analyzer. The quantitative metal mass results from each sample are return as an FCS file, ready to be analyzed by available computational programs [143].

The use of these non-biological metal isotopes provides precise mass resolution and discrete isotopic peaks with no significant overlap between channels. This resolution is what makes it theoretically possible to measure 70-100 parameters on one single cell at the same time. The high number of markers and the possibility to customize the antibody panels to the researchers needs makes it possible to analyze phenotypic and functional markers, both extracellular and intracellular, simultaneously [131]. Due to limitations with the purification of elemental metals, the technology is today limited to around 50 parameters per samples. Compared to fluorescence flow cytometry this is still a great improvement, as in flow cytometry commonly the measurements of 10-12 parameters are performed, although up to 21 parameters are currently possible [143-145].

## 2. Aims and hypothesis

The overall aim of this Master project was to investigate whether explorative high-dimensional cell analysis by CyTOF can reveal associations between phthalate exposure and immune cell profiles in adults. More specifically, we aimed to identify subpopulations or functional characteristics associated with DEHP and DiNP exposure.

Measurements in human samples find that most adult are, to a varying degree, exposed to phthalates, especially DEHP and DiNP, and studies have found associations between exposure and altered immune responses. Our hypothesis is that exposure to phthalate mixtures can lead to altered immune responses in innate and adaptive immune cells. To test this hypothesis we investigated PBMC from adult individuals with high or low exposure estimates for DEHP and DiNP by use of high-dimensional CyTOF analysis and unsupervised clustering algorithms.

We chose to focus on the following research questions:

- Are there subpopulations of cells that differ significantly between the high DEHP and DiNP exposed group and the low exposed group?
  - Does the number of immune cell populations differ between the two groups?
  - Does the expression of activation markers or combinations of markers on the cells differ between the two groups?
- After PMA+IM stimulation, are there cell subpopulations with significantly different cytokine expression between the high DEHP and DiNP exposed group and the low exposed group?

## 3. Material and methods

### 3.1. Subjects (EuroMix) and Ethics

Participants from a Norwegian human biomonitoring study as part of the EU EuroMix project were used in this master project. For each participant, there were available urinary phenol and phthalate metabolite concentrations, blood samples and isolated PBMC, detailed food and PCP diary and a short questionnaire regarding general health (Husøy et al. submitted). All data were registered under the EuroMix study at the Norwegian institute of public health (NIPH). The EuroMix project was funded by the Horizon 2020 Framework Program of the European Union. All participants signed a written informed consent form.

In brief, 144 adult participants aged 24-72 years old (100 women and 44 men) participated in the EuroMix study at NIPH. At two different 24 h periods, 2-3 weeks apart, the participants were asked to collect all urine in separate containers. At the end of each 24 h period, blood samples were collected. The urinary samples collected from 6 am-12 pm, 12 pm-6 pm and 6 pm-6 am (next morning) were pooled in three batches. Then kept at -80 °C until analyzed for phenol and phthalate metabolite concentrations by on-line column switching liquid chromatography coupled to tandem mass spectrometry (HPLC-MS-MS) as described elsewhere [146]. In addition to the biological samples, each participant was asked to keep a detailed food and PCP diary for the 24 h period. In this diary, the participants documented in detail the type, the amount, and the brand for the food consumed plus the type and number of applications of the PCP used in the period.

The mean value of the resulting urine metabolite concentrations from the three pools, measured to be over the limit of detection (LOD), was subsequently adjusted for specific gravity (SG). The average of these three SG-adjusted concentration values was then used to make one 24 h urine sample for one participant.

For each participant, PBMC were isolated from the ethylenediaminetetra-acetic acid (EDTA) blood sample within one hour after collection and counted before being placed in liquid nitrogen (isolation procedure described in 3.5.1 below). Only PBMC and the results from phenol and phthalate metabolite measurements from the first 24 h period were used in this study.

### 3.2. Choice of participants

To investigate cell profiles associated with high and low exposure levels of phthalates, we aimed to select for participants with the highest phthalate exposure levels and compare these to participants with the lowest phthalate exposure levels. The justification for combining data from two different phthalates (DEHP and DiNP) were their similar industrial use and chemical structure, thus these are assumed to have similar effects in the body [38].

To estimate the urine concentration of DEHP and DiNP metabolites, the measured concentration for DEHP and DiNP metabolites were corrected for molecular weight by multiplying with 1000 and dividing on the molecular weight of the metabolite. Thereafter, concentration of the DEHP and DiNP parent compounds were estimated by adding the corrected concentrations of all DEHP and DiNP metabolites. The participants were selected into two groups mainly based on high and low DEHP and DiNP estimated



concentrations in urine (Appendix Table 2). Secondly, from the potential high and low DEHP and DiNP candidates, the other phenols and phthalate concentrations were considered (Appendix Table 3-4). For the candidates with high DEHP and DiNP estimated exposure concentrations, we chose to select those with high concentration of the remaining phthalate metabolites and phenols. For the candidates with low DEHP and DiNP estimated exposure levels, participants were selected to also have low concentrations of the other phthalate metabolites and phenols.

Among the possible candidates for the high and low exposed group, participants were also selected to have the group average and median of age and weight as similar as possible between the high and low exposed groups. Considerations were also made to ensure that the number of males and females in each group was the same. This was to reduce factorable noise from these possibly confounding factors.

### 3.3. Choice of experimental design and antibody panels

Two panels of metal-conjugated antibodies were used for analyzing specific cell subpopulations and functional characteristics of the cells. Panel 1 was used to stain unstimulated cells and consisted of 36 antibodies targeting surface markers (Figure 5A and Appendix Table 5). This panel was designed to identify the major cell populations (T-cells (including Th- and Tc-cells), B-cells, NK-cells, Mo cells and DC) and, in detail, their subpopulations in PBMC (some are listed in Table 2). As mentioned previously, these populations are suggested to play an important role in the regulation of the immune response and the development of asthma and allergies. In addition, Panel 1 included antibodies specific to activation markers and co-stimulatory molecule markers used to identify cell activation status.

A)

**Unstimulated cells (Panel 1)**

<b>Cell population identification markers</b> CD45 CD3 CD4 CD8 gdTCR  CD45RA CD19 IgD IgG  CD33 CD14 CD56  CD123 (IL-3R) CD161  IL-33R/ST2 CD127	CD25 HLA-DR  CCR6 CXCR5  CCR7 CD11c  CD16	<b>Migration, adherence, activation markers</b> CD69 CD38 CD11b  CD294 CXCR3 CCR4  CD371 CD24 CD163  CD23
		<b>Co-stimulatory</b> CD27 CD28 CD134

B)

**PMA+IM stimulated cells (Panel 2A and 2B)**

<b>Cell population identification markers</b> CD45 CD3 FoxP3  CD4 CD8 CD45RA  CD19 CD14 CD56  CD161 (CD33) CD127	CD11c CCR7  CD25 HLA-DR  CXCR5 CD16	<b>Migration, adherence, activation markers</b> CD23 BAFF-R
	<b>Co-stimulatory</b> CD154	
	<b>Cytokines</b> IL-2 IL-22 IL-5 TNF $\alpha$ IL-10 IL-13 IL-17A IL-4 IFN $\gamma$ IL-6 IL-21	

Figure 5: Mass cytometry panels. A) The markers used for surface staining (Panel 1) and B) the markers used for surface (Panel 2A in orange) and intracellular (Panel 2B in blue) staining. The markers are surface markers used for identification of known cell populations, Fc-receptors, Co-stimulatory molecules or migration, adherence or activation markers or a combination. For the stimulated samples, the cytokines included in this sample is also illustrated.

Panel 2 was used to stain stimulated cells and consisted of 20 antibodies targeting surface molecules (Panel 2A) and 12 antibodies targeting intracellular proteins (Panel 2B) (Figure 5B and Appendix Table 5). Panel 2 was designed to identify major immune cell populations (T-cells (including Th- and Tc-cells), B-cells, NK-cells, Mo cells and DC) based on surface markers (Panel 2A) and to identify T<sub>reg</sub>-cells and analyze cytokine production (Panel 2B, respectively) after stimulation. Cells stained with this panel were stimulated with phorbol 12-myristate 13-acetate (PMA) and ionomycin (IM) to induce cytokine production and treated with Brefeldin A (BFA) to hinder secretion, resulting in accumulation of the proteins inside the cells (PMA+IM stimulation). Staining with Panel 2B was performed after fixation and permeabilization of the cells (Figure 6).

To assess the effect of the stimulation on phenotype markers and cell function, stimulation control was performed on two parallel samples from the same participant. Both were stained according to the protocol for stimulated cells (using Panel 2A and 2B) (see section 3.5.4. below), but only one were stimulated with PMA+IM for 4 h. The

marker expressions in the stimulated sample were compared to the marker expressions in the other unstimulated sample from the same participant.

### 3.4. Antibody conjugation, titration and testing

Most of the antibodies used in this experiment were pre-conjugated with the metal tags provided by Fluidigm. Other antibodies (IgG, IL-10, IL-13, IL33R, IL-6, CD154 (CD40L), BAFF-R (CD268), and CD161) were self-conjugated with the Maxpar<sup>®</sup> X8 Antibody Labelling Kits [Fluidigm, CA, USA] according to the manufacturer's instruction. The self-conjugated antibodies were, based on titration results, diluted to optimal concentration in PBS-based Antibody Stabilization Solution [Candor Bioscience, Germany] and stored at 4 °C.

A mass minus many (MMM) control was performed for the cytokines to confirm that any observed cytokine production were not due to spillovers from other channels or background noise. This was done with samples from two participant with two parallels. Both parallels were stimulated according to protocol, but one were stained with both Panel 2A and Panel 2B and the other with only Panel 2A and not the Panel 2B cytokine antibodies.

### 3.5. Sample preparation

#### 3.5.1. PBMC preparation

20 mL EDTA blood was diluted in equal amounts of physiological saline solution (total volume of 40 mL), and then slowly added to a 50 mL conical tube with Ficoll (about  $\frac{3}{4}$  of the blood/saline solution) before being centrifuged (800x g, 25 min, RT). The mononuclear cell band was collected by pipette and transferred to a new 50 mL tube, up to 40 mL PBS was added to the cells, mixed and pelleted (429x g, 10 min, RT) to remove the platelets. The supernatant (containing the platelets) was discarded and the cell pellet resuspended in the residual volume. Following this, the cells were washed twice with 40 mL PBS (429x g, 10 min, RT) before being resuspended in PBS and counted. The cells were pelleted (429x g, 10 min, RT) before ice-cold freezing media (1500  $\mu$ L FBS and 1500  $\mu$ L FBS+20% DMSO) were added to a final volume of 3 mL freezing media. The cell solution was then aliquoted into three cryotubes (1 mL in each) for freezing at -80 °C for 24 h before being transferred to liquid nitrogen.

### 3.5.2. Thawing of cells

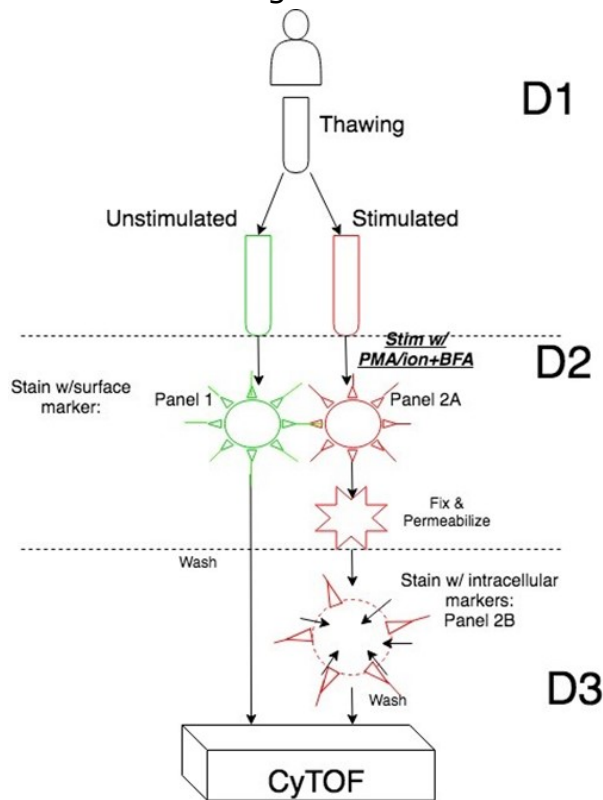


Figure 6: CyTOF PBMC cell preparation process. Two parallels were run for each participant, one unstimulated (green) and one stimulated (red). The main steps for each day (D1, D2 and D3) are illustrated for both parallels.

For each participant, cryopreserved PBMC were thawed in a water bath before gently being transferred into a 50 mL tube using a 1mL pipette. 9 mL of the pre-warmed benzonase medium (1:10 000 benzonase in cell culture medium (containing RPMI, 10% FCS, 1% Ionomycin) (CCM)) were added to prevent clumping of cells during thawing [147, 148]. The cells were pelleted (300x g, 10 min, RT) and gently resuspended in residual volume after discarding the supernatant. This step was repeated one time with 10 mL of the benzonase medium. Cells were then washed with CCM and pelleted (300x g, 5 min, RT) before being counted using a Bürker counting chamber. Following this, CMM was used to adjust the viable cell numbers to  $5 \cdot 10^6$  cells/mL (according to the equation below) and  $3 \cdot 10^6$  cells (600  $\mu$ l) were transferred to two polystyrene tubes (one for unstimulated cells and one for cell stimulation) (Figure 6). The cells were left overnight at 37 °C in a CO<sub>2</sub> incubator.

The following equation were used after counting in Burker chamber to calculate the number of cells present in each sample after the thawing procedure:

$$\frac{\# \text{ of cells}}{3} * 10^4 * \text{dilution factor} * \text{volume of resuspension volume} = \text{total number of cells in sample}$$

### 3.5.3. Sample preparation – unstimulated cells (Panel 1)

PBMC from one of the two polystyrene tubes were pelleted (300x g, 5 min, RT) before being washed with 3 mL PBS and pelleted again (300x g, 5 min, RT). Cells were resuspended to 1 million cells/mL using similar amounts of PBS and 2x Cell-ID™ Cisplatin (for 3 million cells: 150µL PBS and 150µL 2x Cell-ID™ Cisplatin were used) and incubated for 5 min at RT. Following the incubation, cells were washed with 1.5 mL Maxpar® Cell Staining Buffer (CSB) [Fluidigm, CA, USA] and pelleted (300x g, 5 min, RT) before being stained with 50 µL antibody cocktail, containing 0.5 µL of each antibody in Panel 1 (Appendix Table 5) in CSB, and left on ice for 30 min. After staining, cells were washed twice with 2 mL CSB and pelleted (300x g, 5 min, RT) before 1 mL of 1x Intercalator solution (4000x Cell-ID™ Intercalator-Ir [Fluidigm] diluted in 1:4000 Maxpar® Fix and Perm Buffer [Fluidigm]) was added for identification of nucleated cells. The cells were then incubated overnight at 4 °C.

The following day, cells were washed twice with 2 mL PBS and pelleted (800x g, 5 min, RT), the pellet was left at RT until CyTOF data acquisition.

### 3.5.4. Sample preparation – stimulated cells (Panel 2)

The PBMC in the second polystyrene tube were stimulated (CO<sub>2</sub> incubator, 4 h, 37 °C) with 6 µL PMA+IM stimulation solution containing CCM and the equivalent of 20 ng/mL PMA [Sigma-Aldrich Norway As, Oslo, Norway], 1µg/mL ionomycin [Sigma-Aldrich] and 10 µg/mL BFA [BioLegend, CA, USA]. After stimulation, cells were pelleted (300x g, 5 min, RT) and the supernatant was gently removed by aspiration due to the fragile state of the cells after stimulation. Cells were then washed with 3 mL PBS and pelleted (300x g, 5 min, RT).

Following this, cells were resuspended to 1 million cells/mL using similar amounts of PBS and 2x Cell-ID™ Cisplatin (for the 3 million cells: 150µL PBS and 150µL 2x Cell-ID™ Cisplatin were used) and incubated for 5 min at RT. Next, cells were washed with 1.5 mL CSB (300x g, 5 min, RT) before staining with 50 µL surface antibody cocktail, containing 0.5 µL of all but one (1 µL of CD161) of Panel 2A surface antibodies (Appendix Table 5) and CSB, and left on ice for 30 min. After staining, the cells were washed twice with 2 mL CSB (300x g, 5 min, RT) and fixated by adding 1 mL fix solution (Maxpar® Fix I Buffer (5x) [Fluidigm] diluted 1:5 in PBS) and incubated for 20 min at RT. Following the incubation, cells were washed with 1 mL PBS (800x g, 5 min, RT) and permeabilized by adding 1 mL ice-cold methanol (MeOH) and left overnight at -20 °C.

The following day, cells were rehydrated, first by washing with 1 mL PBS (800x g, 5 min, RT) and then with 2 mL Maxpar® Perm-S buffer [Fluidigm] (800x g, 5 min, RT). After rehydration, cells were stained with 50 µL intracellular antibody cocktail, containing 0.5 µL of each of the Panel 2B intracellular antibodies (Appendix Table 5) and Maxpar® Perm-S Buffer [Fluidigm], and incubated in RT for 30 min. Following the incubation, the cells were washed twice with 2 mL CSB (800x g, 5 min, RT) before adding 1 mL of the 1x Intercalator solution and incubating for 20 min at RT. Cells were then washed twice with 2 mL PBS (800x g, 5 min, RT) and left pelleted until CyTOF run.

### 3.5.5. CyTOF data acquisition

The CyTOF data were acquired using the CyTOF II instrument [Fluidigm] equipped with a SuperSampler system [Victorian Airship & Scientific Apparatus]. Before use, the

instrument was tuned and calibrated and cleaning procedures were performed according to manufacturer's advice. Argon gas ( $\geq 99.999\%$ ) was used to generate the plasma and to nebulize the cell suspension.

Right before data acquisition, cells were resuspended in Maxpar<sup>®</sup> Water [Fluidigm] to a concentration of  $2.5 - 5 \times 10^5$  cells/mL. The cells were then filtered into Falcon cell strainer cap tubes to avoid clogging of the machine and a 1:10 (of the final resuspension volume) volume of the EQ<sup>™</sup> Four Element Calibration Beads [Fluidigm] were added to the sample for normalization.

The cell suspension were measured at a rate of 300-600 events/second. To ensure the appropriate mass sensitivity, the EQ beads were checked to have a Eu153 median intensity of  $\geq 1000$ . To avoid spillover between samples, the machine was washed with water (minimum 3 min) between samples before starting with the next sample. If necessary, additional wash solution was used between the samples before cleaning with water.

The resulting raw data (FCS files) were normalized by a bead based normalization tool [Helios software 6.5.358, Fluidigm]. The normalized files were analyzed in Cytobank [Cytobank Inc.] using biaxial gating, viSNE and CITRUS.

### 3.6. Reproducibility – between days, PBMC vials and tube parallels

To get an indication of the reproducibility in our studies, two new vials from one of the participants previously analyzed (participant L14) were prepared according to the same protocol as described above (Section 3.5). Additionally, one of these vials were split into two staining tubes, all with  $3 \times 10^6$  cells (600  $\mu$ l). This was done to evaluate reproducibility between days (looking at potential differences in CyTOF machine and lab-technical performance variation from day to day (performed three months apart)), between vials of frozen cells (looking at variations due to individual cell aliquoting, freezing and thawing) and between tubes with cells from the same vial (evaluating potential technical variance that might affect the results).

### 3.7. Further development of CyTOF protocol

#### 3.7.1. Impact of antibody cocktail freezing and thawing

To investigate the impact of freezing on the antibody cocktail, an extra antibody cocktail for an unstimulated and stimulated sample were prepared and frozen in  $-80$  °C freezer for use the following week. The frozen antibody cocktail was tested along with a freshly prepared antibody cocktail on samples from the same participant. All other steps in the protocol (described in 3.5 above) were the same.

#### 3.7.2. Test of EDTA for increased cell yield

To investigate the impact of EDTA on cell adherence to tubes and each other, the EDTA test was performed on cells from one participant. EDTA was added to an extra parallel tube of both the stimulated and unstimulated samples after the 4 h PMA+IM stimulation period, to a final concentration of 2 mM. The cells were incubated for 15 min with EDTA before continuing with the washing and following protocol procedure as described in the

sample preparation section above (3.5.3 and 3.5.4). In addition to the added EDTA, the wash buffer used also contained 2 mM EDTA.

### 3.8. CyTOF statistical analysis (Cytobank)

Each sample data was normalized using the FCS processing program in the Fluidigm CyTOF Software 6.7 for Windows [Fluidigm] before performing statistical analysis. The statistical analysis was done for populations were doublets, dead cells and calibration beads had been manually gated out. Leaving the intact living singlet cells population or subpopulations within this population to be analyzed (Figure 7).

#### 3.8.1. Biaxial gating

Manual biaxial gating was done to exclude doublets, exclude EQ beads used for normalization, remove cisplatin-containing dead cells and exclude non-existing double positive cells (CD19+CD3+ and CD19+CD14+) (Figure 7). The resulting "living singlet cells" were used for further analysis. Further cell population and subpopulation gating were done according to characteristic extracellular markers (Table 2), respectively.

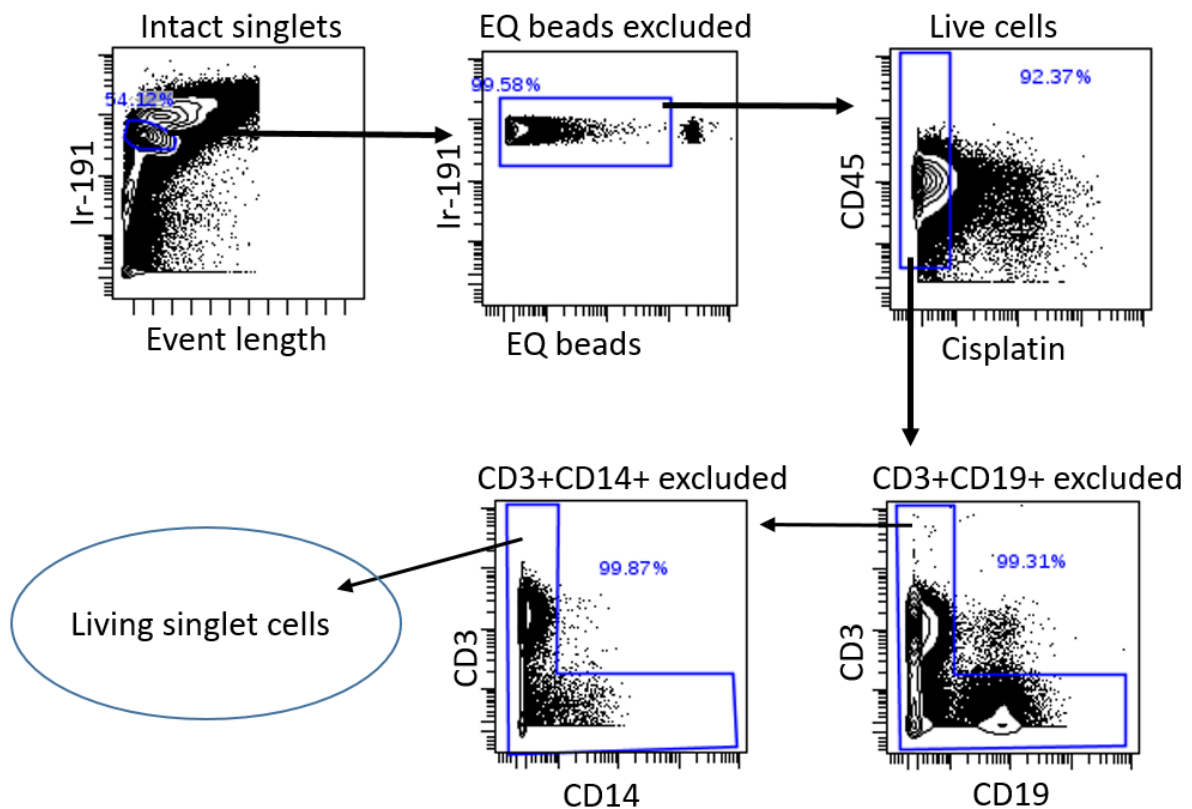


Figure 7: Gating strategy for the data analyses. Firstly, singlet cells were selected based on event length and intercalator (cell identification) content. Secondly, EQ beads used for normalization were excluded before dead cells containing cisplatin (stains DNA only for dead cells) were excluded. Finally, non-existing double positive CD3+CD19+ and CD3+CD14+ cells were excluded, resulting in the living singlet cells gate used for all further analyses ("Living singlet cells").

Table 2: Manual biaxial gating was performed on living singlet cells. The main cell populations (in bold) and subpopulations found in PBMC samples were determined based on the following combination of markers, as established in literature.

<b>Cell populations:</b>	<b>Characteristic Markers:</b>
<b>T-cells</b>	<b>CD3+CD19-</b>
<b>Th-cells</b>	CD3+CD4+
Naïve	CD3+CD4+CD45RA+CCR7+ (CD25-)
Effector	CD3+CD4+CD45RA+CCR7-
Central memory	CD3+CD4+CD45RA-CCR7+
Effector memory	CD3+CD4+CD45RA-CCR7-
$\gamma\delta$ T-cell	CD3+CD4+ $\gamma\delta$ TCR+
T <sub>reg</sub>	CD3+CD4+CD25+FoxP3+
<b>Tc-cells</b>	CD3+CD8+
Naïve	CD3+CD8+CD45RA+CCR7+
Effector	CD3+CD8+CD45RA+CCR7-
Central memory	CD3+CD8+CD45RA-CCR7+
Effector memory	CD3+CD8+CD45RA-CCR7-
<b>B-cells</b>	<b>CD19+CD3-</b>
Double negative	CD19+IgD-CD27-
Naïve	CD19+IgD+CD27- (BAFF-R+CXCR5+HLA-DR+)
Pre-Switch Memory	CD19+IgD+CD27+
Post-Switch Memory	CD19+IgD-CD27+
<b>Innate immune cells</b>	<b>CD3-CD19-</b>
<b>DC</b>	<b>CD56-CD14-CD16+HLA-DR+</b>
pDC <sup>1</sup>	CD56-CD14-CD16+HLA-DR+CD11c-CD123+
mDC <sup>2</sup>	CD56-CD14-CD16+HLA-DR+CD11c+CD123-
<b>NK-cells</b>	<b>CD33*+CD56+</b>
NK-cells	CD33*+CD56+CD16+
NK-cells	CD33*+CD56+CD16-
Mature resting cytotoxic	CD33*+CD56+CD45RA+CD38+CD69-
Pro-inflammatory	CD33+CD56+CD161+
NK-like	CD33*+CD56+CD11c+
<b>Monocytes</b>	<b>CD56-HLA-DR+CD33*+CD14+CD16+</b>
Classical	CD56-HLA-DR+CD33*+CD14+++CD16-
Intermediate	CD56-HLA-DR+CD33*+CD14+++CD16+
Non-classical	CD56-HLA-DR+CD33*+CD14 <sup>dim</sup> CD16++

\*The CD33 marker were only used for gating the unstimulated samples due to faulty double positive CD33+CD3+ expression on cells observed in the stimulated samples.

<sup>1</sup> Plasmacytoid DC (pDC)

<sup>2</sup> Myeloid DC (mDC)



### 3.8.2. viSNE

For visual representation of all the parameters, we used a viSNE 2D plot on aspects of the analysis where this was appropriate. viSNE is a visualization tool based on the t-Distributed Stochastic Neighboring Embedding (t-SNE) algorithm used to map high-dimension mass cytometry data (e.g. from CyTOF) to a 2D structure without losing the high-dimension structure [149]. Each dot in the viSNE plot represents one cell and cells that are clustered close together are, based on the markers included in the clustering, phenotypically similar [150]. The viSNE analysis was run in Cytobank using default settings (iteration = 100, perplexity = 30, theta = 0.5) to generate the viSNE maps. For clustering, all 36 markers in the unstimulated samples (Panel 1) and 31 markers (all except CD33 (see section 4.1.1. below)) in the stimulated samples (Panel 2A and 2B) were used.

### 3.8.3. CITRUS

To compare the high and low exposed groups and analyze for significant differences, CITRUS analysis was performed. CITRUS (cluster identification, characterization, and regression) is an unsupervised data-driven clustering algorithm used to identify subpopulations in high-dimensional datasets. The algorithm randomly selects a user-defined number of cells from all samples, combine these to one representable dataset and then hierarchically clusters cells that are phenotypically similar based on marker similarities. A minimum cluster size threshold (MCST) value, set by the user, determines the percent of cells needed to be present in a cluster in order for it to be marked for further analysis [150, 151].

CITRUS then splits the clustered data back to individual sample components. On a per sample basis for each cluster, the proportion of cells in that particular cluster (abundance) and/or the median expression of specific markers (chosen by the user) for the cells in each cluster are calculated. Looking for clusters that differ significantly between the user defined experimental conditions (i.e. differences between high and low exposed groups) [150, 151].

We performed abundance analysis to look at differences between cell numbers in the high and low exposed groups. For the unstimulated samples, we used all markers (Panel 1) for clustering. For the stimulated samples, we used all markers except CD33 (see section 4.1.1. below) (Panel 2A and 2B) for clustering. We performed the expression level analysis on activation markers in the unstimulated cells (CD69, CD134, CD123, CD28, CD23, CD25, CD163, CD371 and HLA-DR) and cytokines and functional markers in the stimulated cells (IL-2, IL-22, IL-5, TNF $\alpha$ , IL-10, IL-13, IL-17A, FoxP3, IL-4, IFN $\gamma$ , IL-6, IL-21, CD23, CD25 and BAFF-R). Sampling was set to equal and we tested different minimum cluster sizes before deciding on a minimum cluster size of 2 %, resulting in presentable CITRUS trees (not too cramped and not too scarce). The default CITRUS settings were used for Cross-validation fold (CVF) of 5, False discovery rate (FDR) of 1 % and global normalization scales.

Differences in cluster expression levels and abundance features were calculated mainly by use of the predictive model PAM (prediction analysis of microarrays) and with the correlative SAM (significant analysis of microarrays) model where exported data were available. The PAM algorithm is designed for making predictions from gene expression

data [152] and will as a result probably require large datasets to achieve reliable error rates. SAM is a non-parametric test designed to identify cluster properties that can be associated with an experimental group and to calculate robust false discovery rates for high-dimensional datasets [142, 153].

Each node in the resulting CITRUS trees represents a cluster of phenotypically similar cells. Descriptions of the clusters in this study will focus on markers with high or medium expression. The markers with very low or no expression will generally not be included for each cluster but can be found in the appendix (Appendix Table 6-7 for all markers (unstimulated and stimulated) and Appendix Table 8-9 for functional markers and cytokines).

All CITRUS analyses are based on sampling of 5000 random events per file (total of 140 000 events) from the living singlet cells population, and confirmed with at least three repetitions. Additionally, the main analyses was repeated with 10 000 and 25 000 random events per file (total of 280 000 and 700 000 events).

#### 3.8.4. Statistical analysis (Mann-Whitney test)

To evaluate if the results comparing the two independent high and low exposed groups were statistical significantly different, non-parametric Mann-Whitney test was performed. This is an alternative to the independent sample t-test that can be used if the sample size is small (<30) and the data is not assumed to be normally distributed [154, 155].

The Mann-Whitney test does not use the original observation values, but ranks the values and uses this ranking to evaluate the differences between the two groups. The test provides a p-value for  $H_0$ : the groups have equal distribution of values against  $H_1$ : the distribution of values are not equal, i.e. that one group have higher distribution values than the other group [155]. Since this is a non-parametric test, it does not give indications of parameters like the mean difference, but rather indicates if one group distribution is shifted either more to the left or the right compared to the other [156]. The two-sided test was performed to evaluate if there were any significant differences in shift between the two populations, not specifying if the interest was in either a positive or a negative shift (one-sided test) [157].

## 4. Results

To investigate associations between high exposure levels of phthalates and immune cells, we used mass cytometry analysis and unsupervised computational programs designed for processing high-dimension data to broadly assess changes in immune cell abundance and functional characteristics. For each participant, we analyzed two parallel samples, one unstimulated and one stimulated with PMA+IM. We used the unstimulated sample (stained with Panel 1) for detailed phenotyping of cell subpopulations and to analyze the expression of activation markers in these. We used the stimulated sample (stained with Panel 2A and 2B) for analyzing mainly cytokine production, and some functional markers, in the major cell populations.

### 4.1. Initial methodological investigations

In the titration of the in-house conjugated antibodies IL-6, CD154 and IL-33R, the optimal amount for adequate antibody solution was 0.25  $\mu\text{L}$  while for BAFF-R, it was 0.125  $\mu\text{L}$  and for CD161 the optimal amount was 0.5  $\mu\text{L}$  of the original 0.5 mg/mL stock solution. The antibody solutions were accordingly diluted in stabilization buffer and the optimal concentrations were further used for all experiments.

The mass minus many (MMM) cytokine controls was to identify the background signal for each cytokine channel to compare with the signal in the stained sample. The result mostly showed a clear negative population without any expression for the cytokines in the sample only stained with Panel 2A (surface markers) (Figure 8). This confirmed the specificity of the staining, i.e. the cytokine signal observed would in fact be the cytokine expressions and not unspecific staining or a signal from neighboring channels ( $\pm 1$  mass channel) or an oxidation channel (signals from oxidized isotopes that will appear in the +16 mass channel). We did however note some background for IL-10 and IL-4. The neighboring mass channel for IL-10 is CD45RA and for IL-4, the  $\pm 1$  mass channel is FoxP3 and CD23, and the +16 mass channel is CD11c. All of these have relatively dominant expression and these background signals could therefore be indications of spillover.

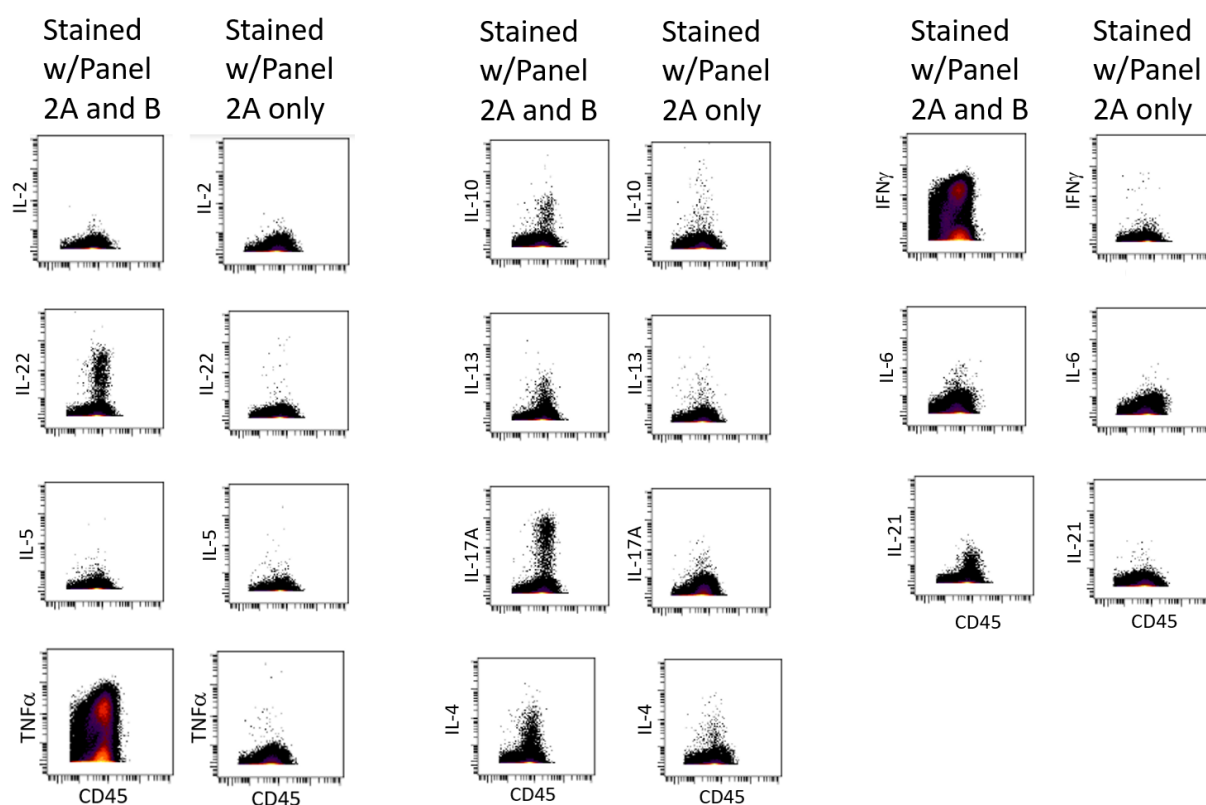


Figure 8: Results from the MMM cytokine control experiment for samples from one of the two participants. The parallel in the left column were stained with antibodies to surface markers (Panel 2A) and intracellular markers (Panel 2B), and the parallel sample in the right column were stained only with antibodies to surface markers (Panel 2A). Each dot represents one cell and both axes show the amount of the respective metal-conjugated antibody per cell on a logarithmic scale. The plots show expression of CD45 on the x-axis and the expression of the different markers on the y-axis, respectively, for all living singlet cells.

#### 4.1.1. Effect of stimulation on cytokine production and marker expressions in Panel 2

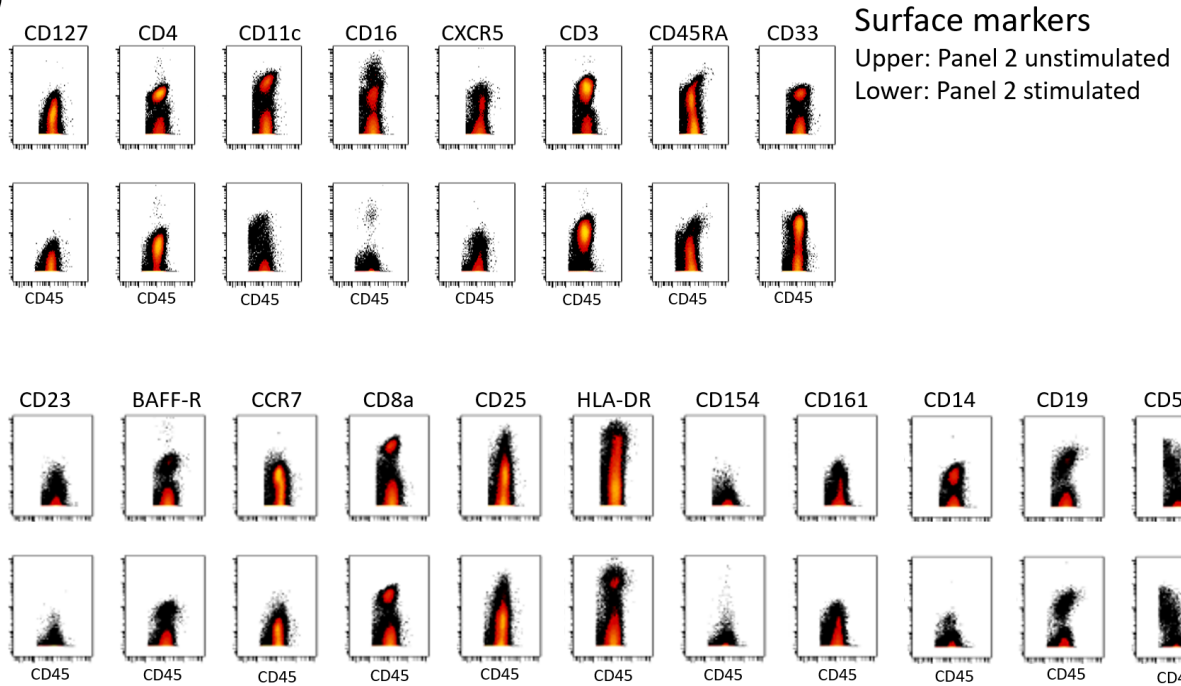
To evaluate the effect of the stimulation step on cytokine production and marker expression, we compared a stimulated and an unstimulated sample from the same participant. The rest of the protocol was the same (including staining with Panel 2A and 2B), making PMA+IM stimulation the only variable between the two samples.

For the surface markers (Panel 2A), most markers had similar expression. However, the stimulation showed a clear reducing effect on the expression of CD14 and CD16, and a somewhat reduced expression of CD11c, CXCR5 and CD23 (Figure 9A). In addition, the expression of CD33 in the stimulated sample demonstrated a strong increase in the percentage of double positive CD3+CD33+ cells (25-40 %). This marker combination is not known to be present in nature to this extent [158-161]. CD33 was therefore excluded from all further statistical analysis on the stimulated samples.

For the intracellular markers (Panel 2B), the stimulation clearly induced expression of IL-22, IL-5, TNF $\alpha$ , IL-13, IL17A, IL-4, IFN $\gamma$  and IL-21, while it had little or no effect on the expression of IL-2 and IL-6 (Figure 9B). In addition, IL-10 was not affected by the

stimulation, but were spontaneously expressed in the unstimulated samples or affected by spillover (as described in section 4.1 above).

A)



B)

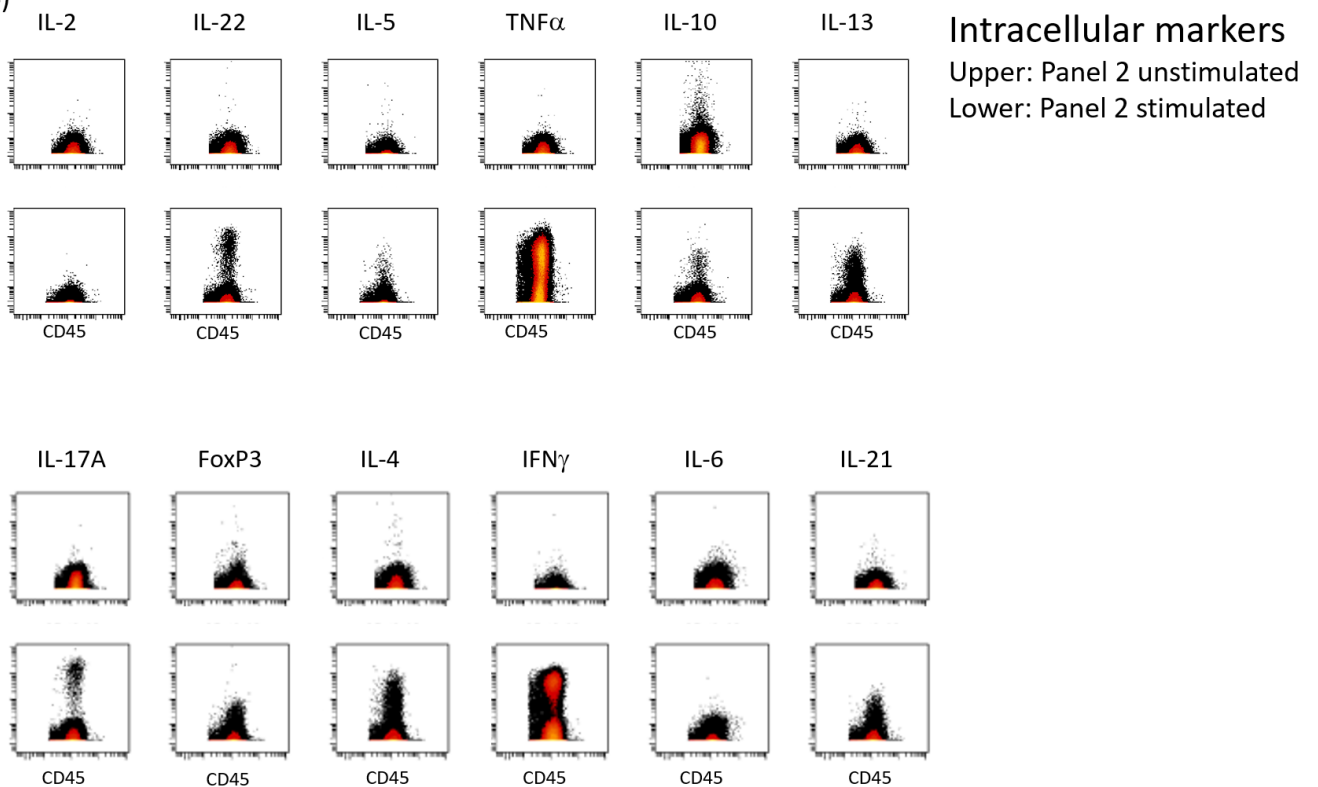


Figure 9: Effect of PMA+IM stimulation results from two parallel samples from one participant are shown. Both parallels were stained with the same antibody cocktails, but only one of the two parallels were treated for 4 h with PMA+IM stimulation. A) Surface markers (Panel 2A). B) Intracellular markers (Panel 2B). Each dot represents one cell and both axes show the amount of the respective metal-conjugated antibody on a logarithmic scale. The plots show the expression of CD45 on the x-axis and the expression of the different markers on the y-axis, respectively, for all living singlet cells. The stimulated samples are present in the lower row and the unstimulated are presented in the upper row.

#### 4.1.2. Reproducibility - between days, PBMC vials and tube parallels

Comparison of one participant's sample between days (D1 and D2, about three months apart) revealed minor differences in the percentage of the major cell populations present in the unstimulated sample (Figure 10A). The largest difference was observed for Th- and Tc-cells in the stimulated samples, where the samples run on D1 showed an approximate 10 % difference in cell numbers between days (Figure 10B).

Comparison between different vials from the same participant (D2A and D2B), prepared on the same day, had some small difference in the percentages (1-2%) of NK-cells, Mo and DC in the unstimulated samples (Figure 10A). This pattern was not seen for the stimulated samples, where we observed minor differences for the major cell populations (Figure 10B).

Looking at differences within the same vial of cells, but prepared in two tubes (D2B.1 and D2B.2), we observed minor differences within the same vial in both the unstimulated and stimulated samples (Figure 10).

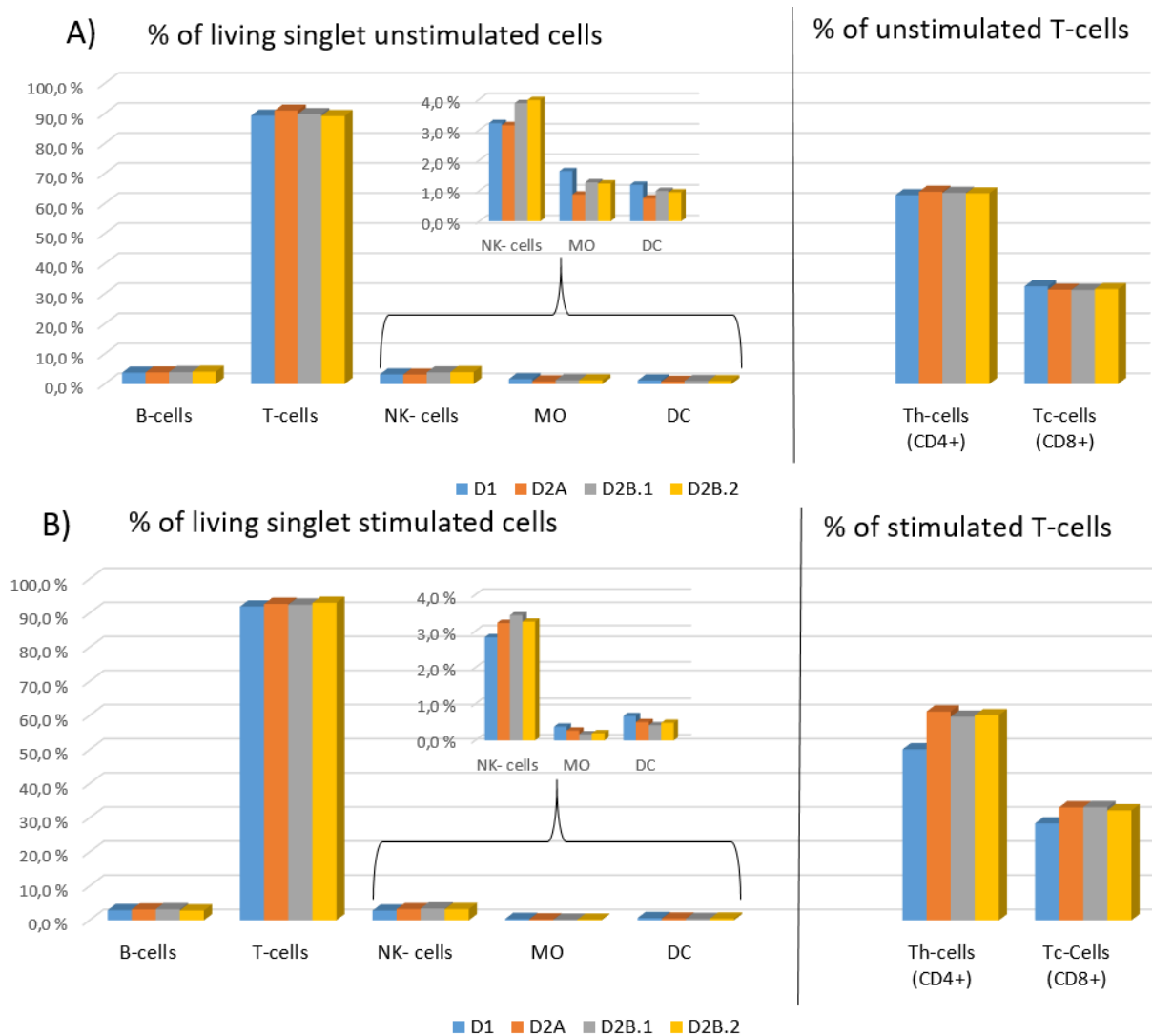


Figure 10: The percentage of the major immune cell populations (B-, T-, NK-cells, DC, Mo and subpopulations of T-cells (Th- and Tc-cells)) in unstimulated (A) and stimulated (B) samples, all from one participant (L14). Results are shown for Vial 1 and Vial 2 from the same day (D2A and D2B), for two parallels from Vial 2 (D2B.1 and D2B.2) and for a Vial analyzed and prepared on another day (D1). The percentages were calculated from live singlet cell populations or from parent population for the subpopulations.

## 4.2. Participant characteristics

We chose the samples in this study mainly based on the participant's DEHP and DiNP estimated urine metabolite concentrations. The combined estimated exposure levels of DEHP and DiNP, and some other characteristics for all participants chosen are shown in Table 3. This resulted in two distinct groups of participants where the estimated values for the high exposed group ranged between 189.9 – 1071.2 ng/mL, while for the low exposed group, the range was between 48.4 – 80.1 ng/mL. A Mann-Whitney test confirmed a statistically significant difference between the high and low exposed groups ( $p < 0.0001$ ) (Figure 11A).

Table 3: Exposure levels for the molecular corrected sum of DEHP and DiNP and characteristics of the selected participants in the group of high (red) and low (green) exposure levels for DEHP and DiNP<sup>1</sup>.

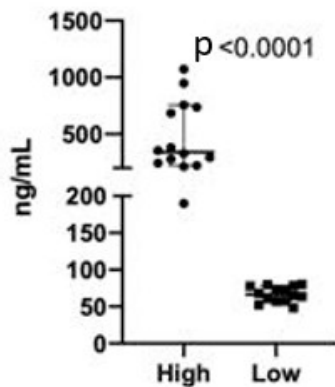
Participants	Sum DEHP & DiNP (µg/mL)	Sex	Age	Weight
<b>High Exposed</b>				
<b>H1</b>	294,6	F	32	60
<b>H2</b>	222,5	M	34	81
<b>H3</b>	212	F	52	71
<b>H4</b>	757,4	M	55	97
<b>H5</b>	328,5	M	60	82
<b>H6</b>	737,6	M	38	105
<b>H7</b>	189,9	M	34	91
<b>H8</b>	244,4	F	53	NA
<b>H9</b>	279,8	F	35	53
<b>H10</b>	684,1	F	42	75
<b>H11</b>	354,9	F	25	70
<b>H12</b>	1071,2	F	46	65
<b>H13</b>	948,6	M	40	81
<b>H14</b>	381,6	M	64	76
<b>Sex<sup>2</sup></b>		50		
<b>Median</b>	341,7		41	76
<b>Low exposed</b>				
<b>L1</b>	71,6	F	32	64
<b>L2</b>	78,7	M	32	74
<b>L3</b>	52,4	F	44	60
<b>L4</b>	77,8	M	60	76
<b>L5</b>	60,7	F	41	57
<b>L6</b>	65,1	F	40	70
<b>L7</b>	71,9	F	40	78
<b>L8</b>	68,2	M	52	75
<b>L9</b>	57,3	M	25	80
<b>L10</b>	48,4	F	62	80
<b>L11</b>	79,9	M	26	89
<b>L12</b>	57	M	51	90
<b>L13</b>	80,1	M	57	94
<b>L14</b>	63,7	F	25	60
<b>Sex<sup>2</sup></b>		50		
<b>Median</b>	66,6		40,5	75,5

<sup>1</sup> The molecular corrected sum of DEHP and DiNP metabolites combined for each participant (MEP, MiBP, MnBP, MBzP, MEHP, MEHHP, MEOHP, MECPP, MMCHP, oh-MiNP, oxo-MiNP, cx-MiNP, oh-MINCH, oxo-MINCH and oh-MPHP). The median for estimated exposure levels, age and weight are calculated within the high and the low exposed group. (F: females, M: males)

<sup>2</sup> Percentage of females and males in the group



## A) DEHP and DiNP exposure



## B)

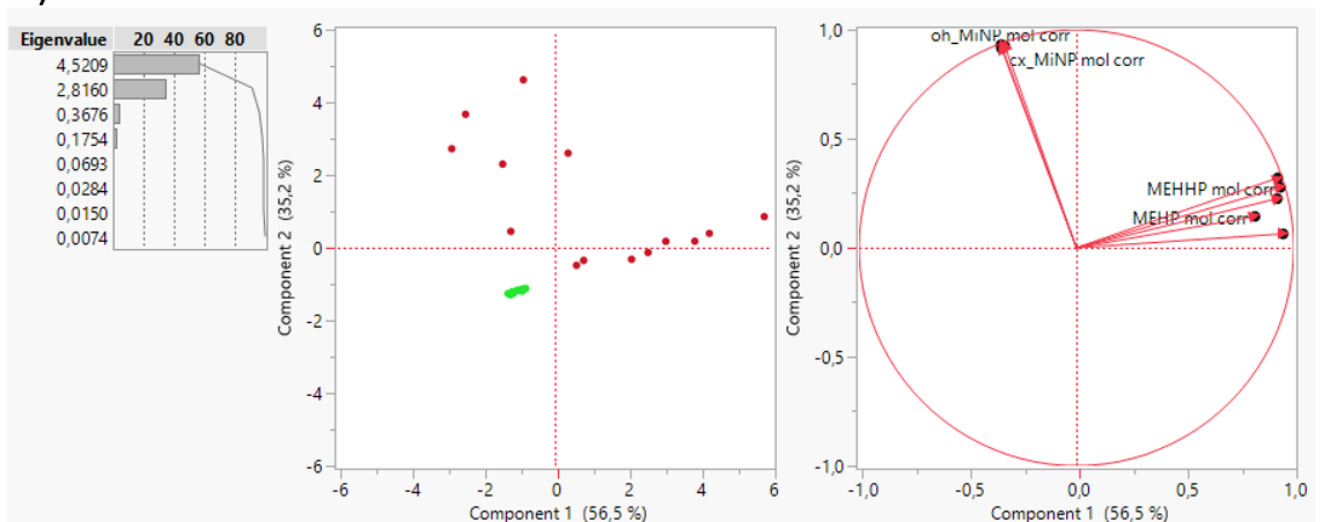


Figure 11: The participants chosen for the high and low exposed group resulted in two groups. A) The corrected molecular weight values for DEHP and DiNP in the participants (dots) in the high compared low exposed groups are shown. The lines indicate the group median and the difference between the 75<sup>th</sup> and the 25<sup>th</sup> percentiles (the interquartile range (IQR)). A Mann-Whitely test confirmed significant differences between the two groups ( $p < 0.0001$ ). B) In the plot of the two first principal components of the PCA analysis, the participants in the high (red) and low (green) DEHP and DiNP exposure group show two-three distinct groups. The plot to the right illustrates how the metabolites from DEHP and DiNP contribute to driving the scattering along the two axes.

To find which component that accounted for most of the variation in exposure level observed between the high and low exposed individuals in the two groups, we performed a principal component analysis (PCA) for all the DEHP and DiNP metabolites measured for all the participants in the two groups. In the low exposed group, all the participants were clustered together near the center, while the high exposed individuals were more scattered along the PCA1 and PCA2 (Figure 11B). The two distinct scatters were mainly driven by the metabolites from DEHP and DiNP, respectively.

## 4.3. Immune cell profiles associated with phthalate exposure levels

### 4.3.1. Manual biaxial gating

Manually biaxial gating (according to markers in Table 2) was done to assess the percentages of the major immune cell populations (T-, B-,NK-cells, Mo cells and DC) and major T-cell subpopulations(Th- and Tc-cells) present in PBMC (Figure 12). Due to the effect that stimulation, fixation and permeabilization have on some of the surface markers used to identify cell populations, the percentage of immune cell populations were only calculated from the unstimulated samples. A Statistically significantly higher percentage of Mo was observed in the high compared to the low exposed group (two-tailed Mann-Whitney test;  $p=0.0042$ ), but were not observed for the Mo subpopulations (Appendix Figure 1) or Mo activation markers (data not shown). Even though not significant, we found a lower percentage of non-classical Mo and a slightly higher percentage of intermediate and classical Mo in the high compared to the low exposed group (Appendix Figure 1). For DC, T-, B- and NK-cells main populations and subpopulations, there was no statistically significant differences between the two groups (Appendix Figure 2-5).

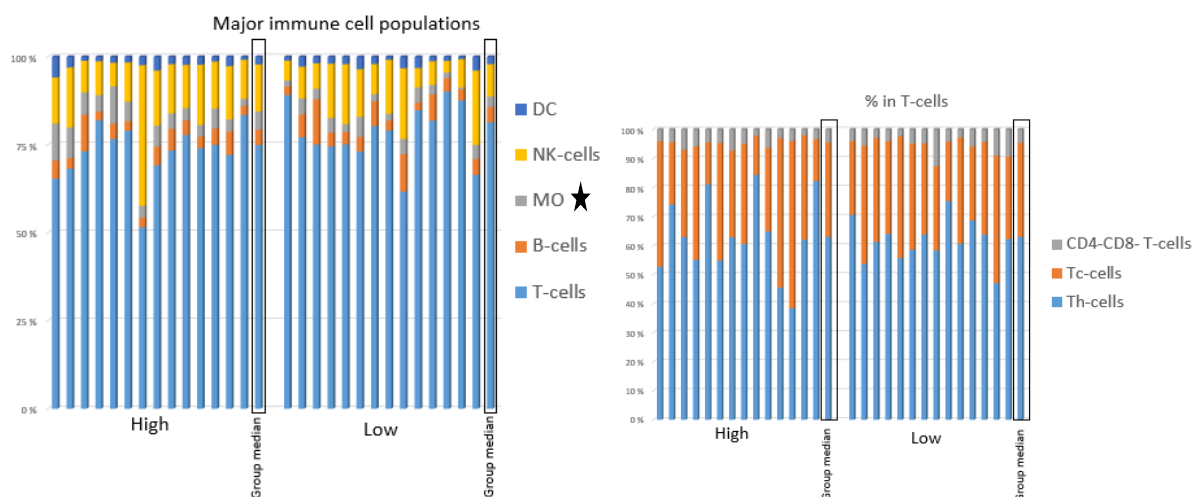


Figure 12: Percentages of the major immune cell populations present in PBMC (T-, B-,NK-cells, DC, Mo and T-cell subpopulations Th- and Tc-cells) for each individual as well as the group median (framed to the right), in unstimulated samples obtained by manual gating according to Table 2. \* illustrates the PBMC subpopulation with statistically significantly different cell numbers in the high and low exposed group.

### 4.3.2. Data-driven clustering and group differences (CITRUS results)

We performed the CITRUS analysis to identify characteristics that were significantly different between the two groups of participants with estimated high or low phthalate exposure levels. In cases where multiple nodes in the same three branch are significantly different between the two groups, only the nodes furthest away (the "end" node) from the top of the hierarchy (the center node) are presented and characterized. This is to capture the characteristics for the significantly different cell cluster in that given branch. These end nodes are given names based on the cellular subpopulations they belong to (characterized by marker expressions in the CITRUS trees (Appendix Figure 6) and CITRUS histograms). The characterization markers are presented in brackets for each subpopulation and illustration of the marker expression for all markers can be found in

the histograms depicted in the Figure C from each run and Appendix Table 6 and 7. The histograms show the relative presence of all the markers used for clustering in the significant nodes.

The CITRUS analysis mainly returned PAM statistics, but where SAM results were returned these are presented. The model error rate for group prediction in the PAM results were not significant for any of the CITRUS runs, probably because the PAM model ideally requires more data to be reliable. However, we still consider the results exploratory relevant for the identification of group differences within the various cell nodes.

In this study, we had too few participants to analyze differences between genders for the high and low DEHP and DiNP exposed groups. The CITRUS algorithm requires minimum eight participants in each group to perform a reliable and robust analysis [162]. We only had seven for each gender in the high and low exposed group, when running CITRUS with these participants we received unreliable results where almost every cell cluster were characterized as significantly different (data not shown). We did not find these results to be trustworthy and concluded that more participants were needed for more accurate within gender results. However, we performed a viSNE analysis to evaluate whether we by eye could observe any systematic major differences between the high and low exposed groups within each sex, this was not the case (data not shown). In addition, we had intentionally included an equal number of males and females within each group to exclude any possible gender bias.

#### 4.3.2.1. Unstimulated cells – Panel 1

##### 4.3.2.1.1. Abundance

When unstimulated cells were clustered based on all surface markers (Panel 1, Appendix Table 5), PAM identified five main branches of cell clusters as significantly different between the high and low phthalate exposure groups (PAM statistics; Figure 13). Three branches were T-cell clusters (results presented for the cell cluster nodes Th#1, Tc#1 and Tc#2) had a significantly lower abundance in the high compared to the low exposed group (Figure 13A and B). We characterized these clusters based on their marker expression, only positive markers are presented (Figure 13C and Appendix 3) for Tc#1: CD3<sup>high</sup>CD8<sup>high</sup>CD45RA<sup>high</sup>CD127<sup>high</sup>CD69<sup>low</sup>CD183<sup>high</sup>CD28<sup>high</sup>CD27<sup>high</sup>CD294<sup>high</sup>CD24<sup>low</sup>CD197<sup>high</sup>IL-33R<sup>high</sup>CD38<sup>med/high</sup>, Tc#2: CD3<sup>high</sup>CD8<sup>high</sup>CD45RA<sup>high</sup>CD127<sup>med</sup>CD183<sup>high</sup>CD28<sup>high</sup>CD27<sup>high</sup>CD294<sup>high</sup>CD24<sup>med</sup>CD197<sup>high</sup>HLA-DR<sup>low</sup>IL-33R<sup>high</sup>CD38<sup>med/high</sup> and Th#1: CD127<sup>high</sup>CD69<sup>low</sup>CD4<sup>high</sup>IgD<sup>low</sup>CD194<sup>med</sup> $\gamma\delta$ TCR<sup>low</sup>CD185<sup>high</sup>CD3<sup>high</sup>CD45RA<sup>low/med</sup>CD183<sup>med</sup>CD161<sup>low</sup>CD28<sup>high</sup>CD27<sup>high</sup>CD294<sup>med</sup>CD197<sup>high</sup>CD25<sup>med</sup>CD38<sup>low/med</sup>.

A branch of NK-cell subpopulations (NK#1) and Mo subpopulations (MO#1) had significantly higher cell abundance in the high exposed than in the low exposed group (Figure 13A and B). We characterized these subpopulations based on marker expression (Figure 13C and Appendix Table 6) for NK#1:

CD56<sup>high</sup>CD16<sup>high</sup>CD69<sup>med</sup>CD11c<sup>high</sup>CD3<sup>low</sup>CD45RA<sup>high</sup>CD183(CXCR3)<sup>med</sup>CD161<sup>med</sup>CD28<sup>low</sup>CD23<sup>low</sup>CD8<sup>high</sup>IL-33R<sup>low</sup>CD38<sup>high</sup>CD371<sup>med</sup>CD11b<sup>low</sup> and for MO#1: CD14<sup>high</sup>CD16<sup>high</sup>CD33<sup>high</sup>CD69<sup>high</sup>CD11c<sup>high</sup>CD194(CCR4)<sup>low</sup>CD123<sup>high</sup>CD3<sup>low/med</sup>CD45RA<sup>med</sup>CD183<sup>low</sup>CD161<sup>low</sup>CD28<sup>low/med</sup>CD294<sup>med</sup>CD163<sup>low</sup>CD24<sup>low</sup>CD8<sup>med</sup>HLA-DR<sup>high</sup>IL33R<sup>high</sup>CD38<sup>high</sup>CD371<sup>high</sup>IgG<sup>high</sup>CD11b<sup>high</sup>CD4<sup>high</sup>.

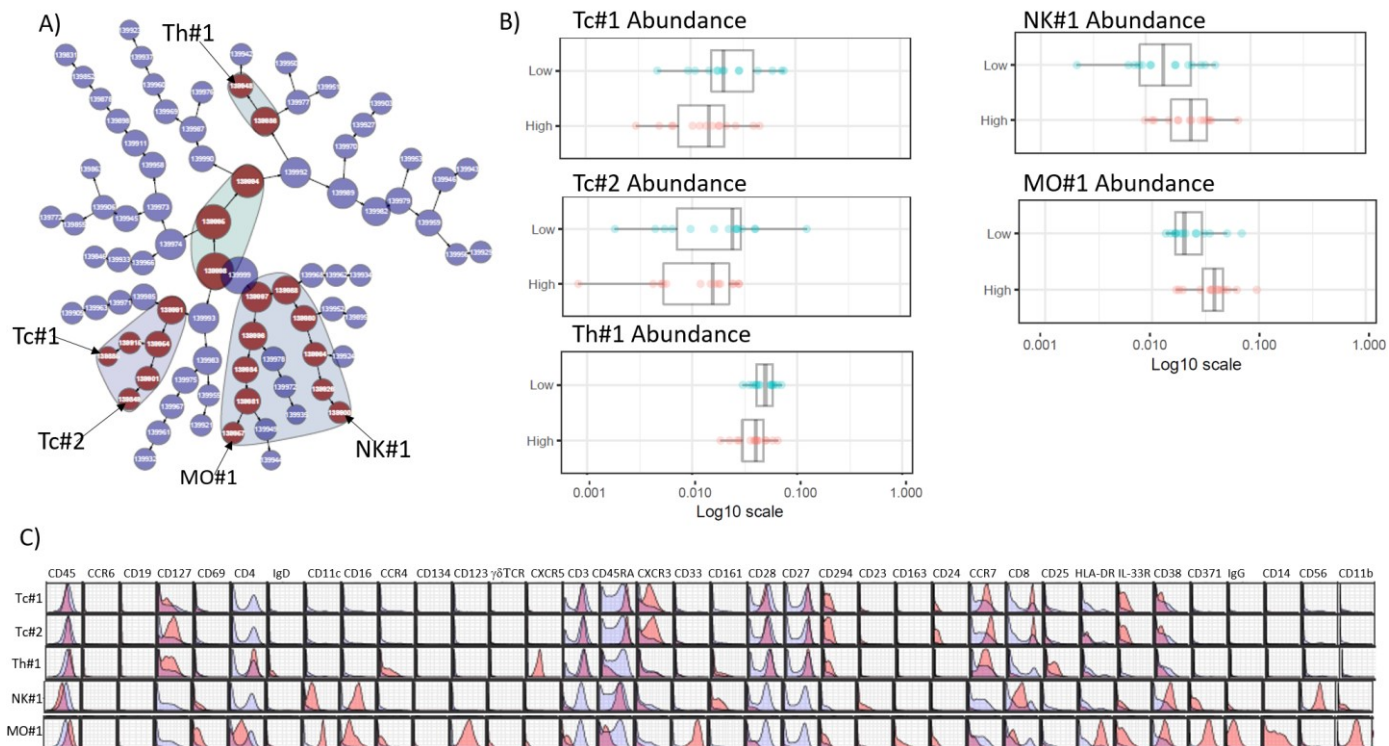


Figure 13: CITRUS cell abundance results for unstimulated cells stained with antibody Panel 1 (PAM cv.min statistics are shown). The results were generated based on sampling of 5000 randomly selected events per file and the use of all 36 surface markers in Panel 1 (Appendix Table 5) for clustering. A) The CITRUS three results with the cell cluster populations with significantly different cell abundance in the high and low exposed group marked red. The results for the named populations (indicated by arrows) are further displayed: B) For the five selected cell subpopulations, box plots from the CITRUS analysis illustrate the cell abundance for each participant (represented as one dot) and the box represents the median and the IQR. C) CITRUS histograms of all the markers in the panel for the five selected subpopulations. Marker expression for cells in that particular node are colored in red, while the respective marker expressions for all other cells are colored blue.

#### 4.3.2.1.2. Marker expression levels

We investigated the difference in marker expression intensity per cell for CD371, CD69, HLA-DR, CD134, CD123, CD28, CD23, CD25 and CD163. In the high versus the low exposed group, there was a statistically significant reduced expression of the activation marker CD69 in a subpopulation of naïve Th-cells (Th#2), a reduced HLA-DR expression in  $\gamma\delta$ T-cells (gdT) and an increase in CD371 in a subpopulation of NK-cells (NK#2) (PAM statistics; Figure 14A and B). The remaining activation markers included in the marker expression level analysis did not show any statistical significant difference in expression between the high and low exposed groups (data not shown).

We characterized these subpopulations based on the following marker expressions (Figure 14C and Appendix Table 6), for Th#2:

$CD127^{high}CD4^{high}IgD^{low}CD3^{high}CD45RA^{high}CD183(CXCR3)^{med}CD28^{high}CD27^{high}$

$CD8^{med}CD294^{high}CD197(CCR7)^{high}CD8^{med}IL-33R^{low}CD38^{high}$ , gdT:

$\gamma\delta TCR^{high}CD3^{high}CD127^{low}CD11c^{low}CD16^{low}CD45RA^{high}CD183(CXCR3)^{high}CD161^{low}$

$CD28^{low}CD8^{med}HLA-DR^{med}$  and NK#2:

$CD11c^{med}CD16^{low}CD194^{low}CD161^{low}CD28^{low}CD8^{low}HLA-DR^{low}CD38^{high}CD56^{high}CD11b^{low}$ .

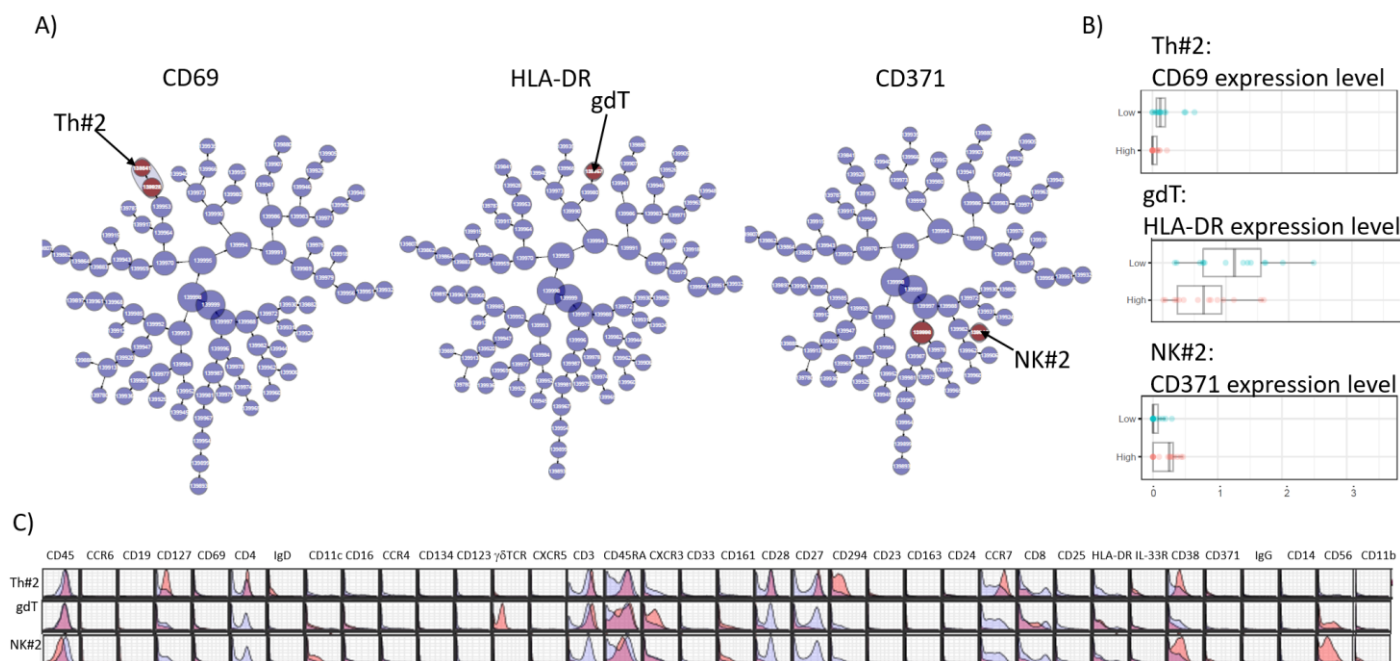


Figure 14: CITRUS cell expression level of functional marker results for unstimulated cells stained with antibody Panel 1 (PAM cv.min statistics are shown). The results were generated based on sampling of 5000 randomly selected events per file and the use of all 36 surface markers in Panel 1 (Appendix Table 5) for clustering. A) The CITRUS three results with the cell cluster populations with significantly different marker expression level per cell in the high and low exposed group marked red. The results for the named populations (indicated by arrows) are further displayed: B) For the three selected cell subpopulations, box plots from the CITRUS analysis illustrate the marker expression level for each participant (represented as one dot) and the box represents the median and the IQR. C) CITRUS histograms of all the markers in the panel for the three selected subpopulations. Marker expression for cells in that particular node are colored in red, while the respective marker expressions for all other cells are colored blue.

#### 4.3.2.2. Stimulated cells – Panel 2A and 2B

##### 4.3.2.2.1. Abundance

After stimulation with PMA+IM, the cells from individuals in the high exposed group showed a significantly lower abundance of a subpopulation of Tc-cells (Tc#3) and a higher abundance of a subpopulation of NK cells (NK#3) compared to the low exposed group (PAM statistics; Figure 15A and B). We characterized the Tc#3 subpopulation by its marker expression (Figure 15C and Appendix Table 7):

$CD3^{high}CD8^{high}CD127^{med}45RA^{high}CD197(CCR7)^{high}HLA-DR^{low}TNF\alpha^{low}IL-6^{med}$ , and the NK#3 subpopulation:  $CD56^{high}CD11c^{high}CD45RA^{high}IFN\gamma^{high}CD8^{low}HLA-DR^{low}CD161^{high}$ .

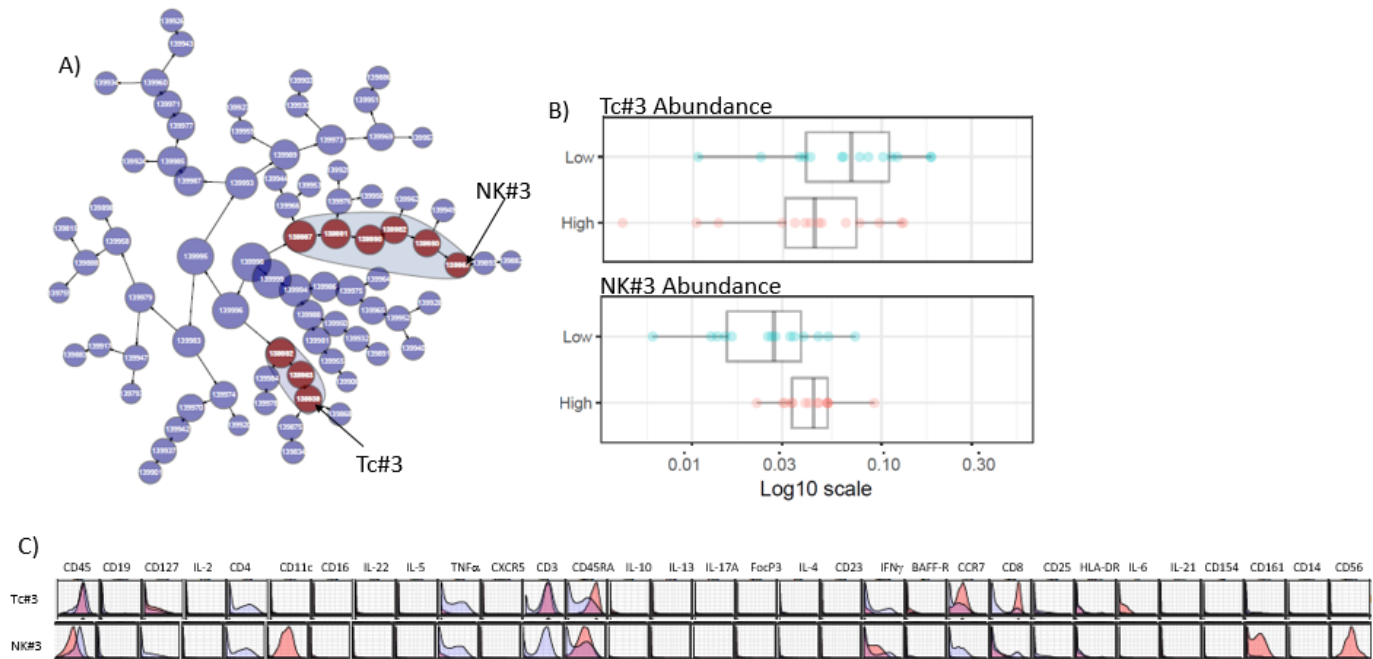


Figure 15: CITRUS cell abundance results for stimulated cells stained with antibody Panel 2A and 2B (PAM cv.min statistics are shown). The results were generated based on sampling of 5000 randomly selected events per file and the use of together 31 surface and intracellular markers (CD33 excluded) in Panel 2A and 2B (Appendix Table 5) for clustering. A) The CITRUS three results with the cell cluster populations with significantly different cell abundance in the high and low exposed group marked red. The results for the named populations (indicated by arrows) are further displayed: B) For the two selected cell subpopulations, box plots from the CITRUS analysis illustrate the cell abundance for each participant (represented as one dot) and the box represents the median and the IQR. C) CITRUS histograms of all the markers in the panel (except CD33) for the two selected subpopulations. Marker expression for cells in that particular node are colored in red, while the respective marker expressions for all other cells are colored blue.

#### 4.3.2.2. Intracellular marker expression levels

When looking at marker expression per cell for the cytokines and functional markers (IL-2, IL-22, IL-5, IL-10, IL-13, IL-17A, FoxP3, IL-4, IL-21, CD23, CD25 and BAFF-R) in the PMA+IM stimulated samples, SAM found a significantly reduced expression of both IL-6 and TNF $\alpha$  in a branch of subpopulations of naive B-cells (results presented for B#2) for the high compared to the low exposed group (SAM statistics; Figure 16A and B).

The “child node” of B#2, the end node of the significant B-cell branch (B#1) had a significantly lower expression of IL-6 only (not TNF $\alpha$ ) in the high compared to the low exposed group. B#1 and B#2 was characterized based on marker expression (Figure 16C and Appendix Table 7) B#1: CD19<sup>high</sup>CD185(CXCR5)<sup>high</sup>CD45RA<sup>high</sup>BAFF-R<sup>high</sup>CD197(CCR7)<sup>high</sup>CD8<sup>low</sup>CD25<sup>low</sup>HLA-DR<sup>high</sup>TNF $\alpha$ <sup>high</sup>IL-6<sup>high</sup>. B#2: CD19<sup>high</sup>CD185(CXCR5)<sup>high</sup>CD45RA<sup>high</sup>BAFFR<sup>high</sup>CD197(CCR7)<sup>high</sup>CD8<sup>low</sup>CD25<sup>low</sup>HLA-DR<sup>high</sup>TNF $\alpha$ <sup>med</sup>IL-6<sup>high</sup>. B#1 showed a higher expression level of CD25, TNF $\alpha$  and IL-6 compared to the parent B#2 node.

In the high exposed group, we also observed a significantly reduced expression of TNF $\alpha$  in a subpopulation of Th-cells (Th#3) (Figure 16A and B). We characterized the Th#3 node based on marker expression (Figure 16C and Appendix Table 7): CD3<sup>high</sup>CD4<sup>high</sup>CD45RA<sup>high</sup>CD197(CCR7)<sup>high</sup>IL-6<sup>low</sup>. For the remaining cytokine and functional markers (IL-2, IL-22, IL-5, IL-10, IL-13, IL-17A, FoxP3, IL-4, IL-21, CD23,

CD25 and BAFF-R), we found no statistically significant difference in expression profile between the groups (data not shown).

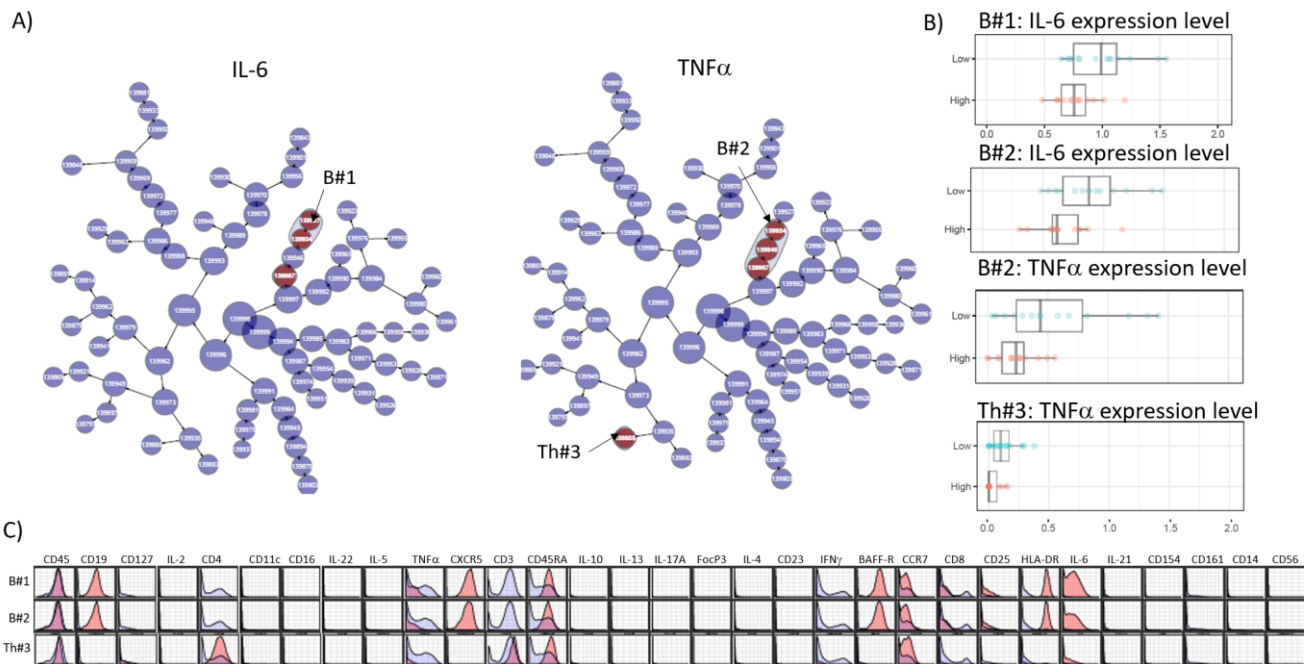


Figure 16: CITRUS cell expression level of functional marker results for stimulated cells stained with antibody Panel 2A and 2B (SAM (FDR <1%) statistics are shown). The results were generated based on sampling of 5000 randomly selected events per file and the use of together 31 surface and intracellular markers (CD33 excluded) in Panel 2A and 2B (Appendix Table 5) for clustering. A) The CITRUS three results with the cell cluster populations with significantly different marker expression level per cell in the high and low exposed group marked red. The results for the named populations (indicated by arrows) are further displayed: B) For the four selected cell subpopulations, box plots from the CITRUS analysis illustrate the marker expression level for each participant (represented as one dot) and the box represents the median and the IQR. C) CITRUS histograms of all the markers in the panel for the four selected subpopulations. Marker expression for cells in that particular node are colored in red, while the respective marker expressions for all other cells are colored blue.

## 4.4. Further development of CyTOF protocol

### 4.4.1. Freezing and thawing of the antibody cocktail

For future, larger experiments, it may reduce variability to use the same antibody cocktail for all samples. Therefore, we investigated the impact of one-time freezing and thawing of the antibody cocktail. The result showed no visual differences in volume between the frozen and fresh antibody cocktail. After manual gating for the major cell populations in the unstimulated sample, we observed little differences between the amounts of cells in the frozen vs the fresh cocktail. The difference in percentage between the frozen and the fresh antibody cocktail was for T-cells 77.16 % against 77.74 %, for B-cells 2.92 % against 2.68 % and for cells in the innate immune system (NK, Mo and DC) 17.81 % against 17.46 %.

Similarly, for the stimulated samples, the differences between the frozen and fresh antibody cocktail in the manually gated major cell populations were minor. For T-cells, the difference between the frozen and fresh antibody cocktail was 72.91 % against 72.57

%, for B-cells 4.26 % against 4.61 % and for innate immune cells (NK, Mo and DC) 22.63 % against 22.74 %.

We further compared the marker expression based on median marker intensity for all living singlet cells combined and the expression was generally similar for the frozen and fresh antibody cocktails (Figure 17). In the unstimulated sample, exceptions were noted for CD45 and CD4 that showed a slightly higher expression in the sample with the frozen antibody cocktail and for CD3 that showed a slightly lower expression in the frozen antibody samples. In the stimulated sample, the frozen antibody cocktail gave a higher expression of CD3.

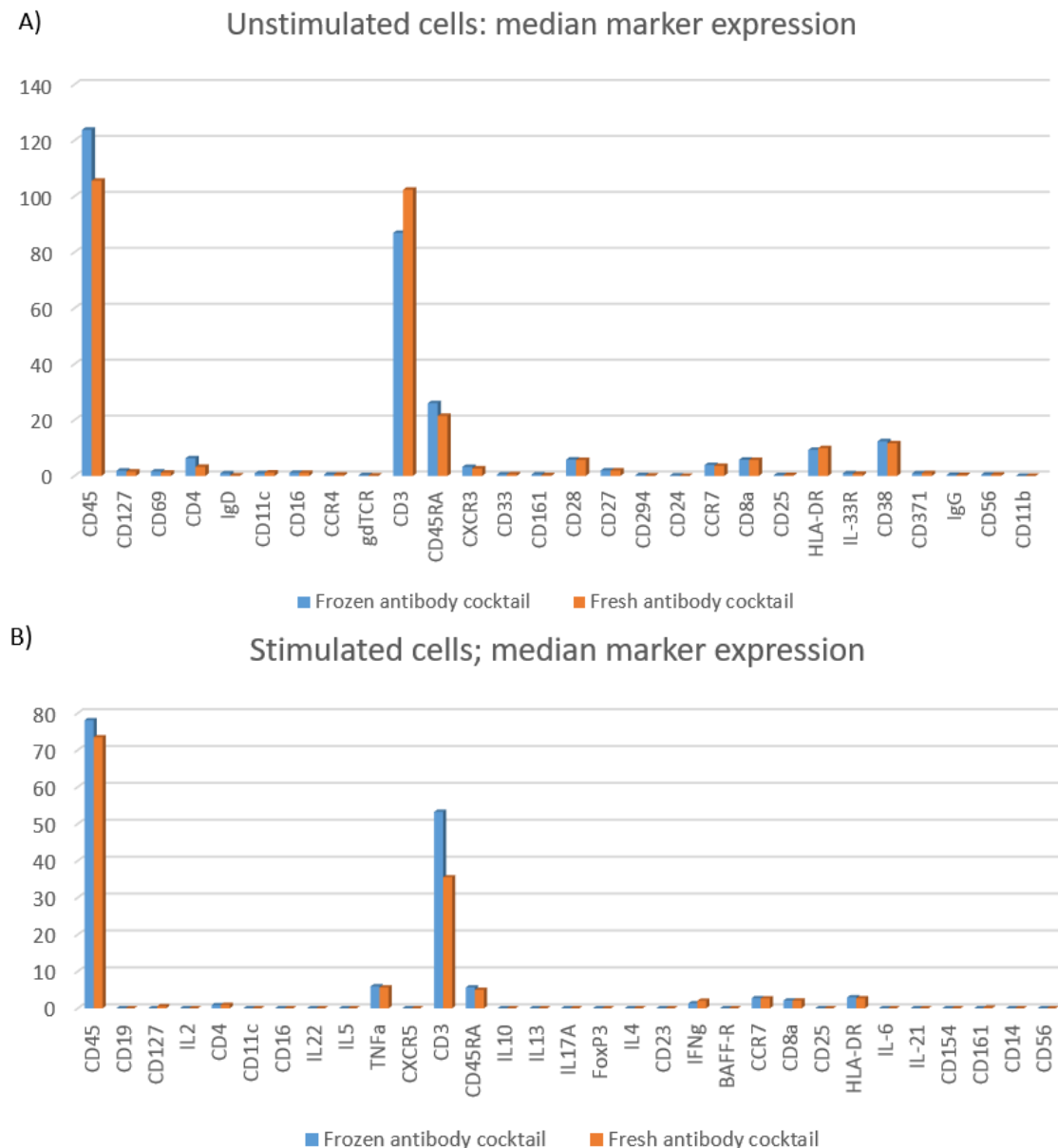


Figure 17: Difference in median marker intensity between the frozen and fresh antibody cocktail for the unstimulated (A) and the stimulated (B) samples. The graph show the median marker intensity for each marker in the living singlet cells population.



#### 4.4.2. Test of EDTA for increased cell yield

After starting the present experiment, we learned that EDTA are used in several other labs with the aim of increasing cell yield by preventing cells from sticking to each other and the material that contains them [163-165]. We therefore compared a sample treated and washed with the EDTA buffer with a sample from the same individual, following our original protocol for stimulated and unstimulated cells. In the EDTA treated samples, the general cell counts were slightly higher, increasing with about 10%, both in the unstimulated and stimulated cells (Figure 18A and C). In the unstimulated sample treated with EDTA, we observed a slightly higher percentage of NK, Mo and DC, while in the stimulated sample treated with EDTA, we observed a slightly lower percentage of Mo and DC (Figure 18B and D).

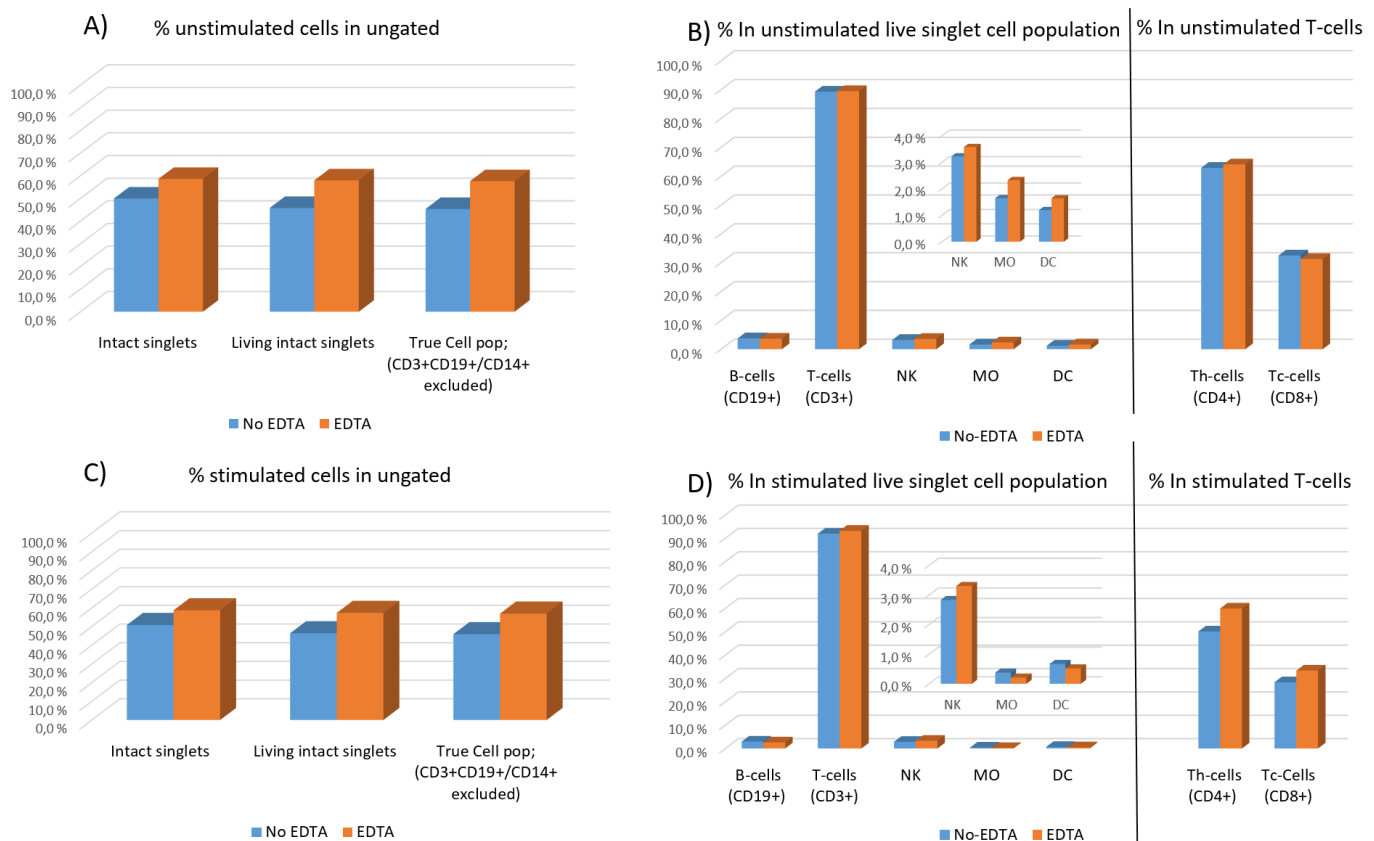


Figure 18: Percentage of major PBMC cell populations in samples with EDTA treatment (orange) or without EDTA treatment (blue) in stimulated (A, B) and unstimulated (C, D) samples. Data from one participant are shown.

## 5. Discussion

In this study, we aimed to evaluate whether DEHP and DiNP showed any effects on the human immune system, which part of the immune system that were most affected and to look for potential biomarkers associated with exposure that could be used in future *in vitro* studies. As far as we know, we are the first to combine high-dimensional mass cytometry analysis with exposure level assessment for such purpose. The combination of an extensive and explorative analysis of immune cell phenotypes on a single cell level with computational analyzing tools revealed new combinations of cell subpopulations, effects on activation markers and cytokine expression profiles (IL-6 and TNF $\alpha$ ) associated with high exposure estimates for DEHP and DiNP.

### 5.1. Methodological considerations

#### 5.1.1. Reproducibility

Due to the high cost and labor-intensive work behind CyTOF analyses, only one technical replicate was included per participant. It is therefore useful to know the technical variability of the method, thus we looked at how well the reproducibility was between days, vials and tubes for the same participant. Although cautions have to be taken when concluding based on only one test, our results indicate that the reproducibility between days, vials and tubes were generally high. For unstimulated cells, we observed some difference in the percentages of NK-cells, Mo and DC, but these cells were present in low amounts and the differences were less than 1 %. Some of these variations could be due to cells, in particular Mo, sticking to the tube wall or other cells during incubation and/or stimulation, and thus not being included in the gating for living singlet cells during the initial manual gating (see section 5.1.5 below).

The only difference observed that was higher than 1-2 % was the differences of Th- and Tc-cells in the stimulated samples, which seemed to vary most between days, not between vials or tubes. Parameters that might give such batch effects can be different concentrations during antibody staining, stimulation, instrument variation etc. For each run in the main experiment, we compared all samples (3-4 samples were thawed, stained and acquired on the same day), and did not see any clear batch effect on any of the markers. However, any potential difference in batch effect can be minimized by introducing a standard cell sample for each participant and normalize each sample accordingly. We did not do this in this experiment due to unavailability of suitable standard with sufficient cells and vials. However, for each run we randomly included samples from both groups and gender, therefore we have no reason to think that any variation between batches, vials or tubes would be group-specific. We therefore expect the presented result to be actual differences related to the investigated groups, and not due to batch effect or other experimental variations.

#### 5.1.2. Effect of stimulation on cytokine production and marker expression in Panel 2

To evaluate the impact of the PMA+IM stimulation on both surface and intracellular expression of the markers in Panel 2, we compared a stimulated sample with an unstimulated sample, both stained with Panel 2A and 2B. We found CD14 and CD16 expression to be clearly reduced as a result of the PMA+IM stimulation, probably affecting the gating and statistical analysis of Mo and DC in the stimulated samples (recognizes by use of the CD14 and CD16 markers). In addition, the effect of stimulation

on the CD33 marker indicated that this marker is not useful when using the PMA+IM stimulation. For most of the cytokines (IL-22, TNF $\alpha$ , IL-13, IL-17A, IL-4, IFN $\gamma$  and IL21) we found PMA+IM to induce cytokine production.

In order to trigger the production of the other cytokines (IL-2, IL-6 and IL-10), and maybe overcome the negative effect observed for CD14, CD16 and CD33, other stimulants (i.e. Phytohaemagglutinin (PHA), Lipopolysaccharide (LPS) or Pokeweed-Mitogen (PWM)) might be more adequate [166, 167]. We did this evaluation to observe the general effect of PMA+IM stimulation on the markers in Panel 2A and 2B, the observations are therefore based on measurements from the live singlet cells population and are not reflecting the effect of stimulation on specific cell subpopulations.

### 5.1.3. Cytokine signal and background assessment

To investigate whether the observed induction of cytokines in fact were cytokine expression and not unspecific background noise, and to be able to set the cytokine gate correctly in relation to the background signal, we performed a MMM control. We found the overall specificity of all cytokines, except IL-10 and IL-4, to be good with little spillover from other channels. In our results, we did not see any effect of these two cytokines and therefore chose not to pursue this finding. However, for future studies, this finding should be considered when choosing metal tags for panel design.

### 5.1.4. Freezing of antibody cocktail

Since this was a small study, we did not prepare one antibody batch to be use in all samples, but prepared each antibody cocktail for each time. For future experiments, between days, vials and tube differences might be reduced by using aliquots from one large frozen antibody cocktail batch that can be thawed when necessary [168]. If applicable, this approach would be favorable for larger studies. However, before including this procedure in a standardized CyTOF labeling protocol, we did an initial test to investigate whether freezing had any effect on the antibody cocktail volume or the detection of the different markers.

We found no effect on the antibody cocktail volume caused by one-time freezing and thawing. For the marker intensity, we found some markers (CD45, CD3 and CD4) to be affected by the freezing. These effects are, however, minor and comparison based on median marker intensity will also not reflect the true marker expression in each cell subpopulation.

The results from the manual gating suggests that the ability to gate cell subpopulations correctly was not affected by the changes observed in median for CD3 and CD4. Finally, we ran a viSNE analysis comparing the frozen and fresh cocktail samples, visually confirming that no cell subpopulations were absent or had considerably reduced expression of some of the markers (Appendix Figure 7 and 8).

These minor differences between the frozen and fresh antibody cocktail staining indicates that freezing does not influence the antibody specificity and affinity or decreases the volume in any significant amount. We therefore recommend this protocol for future use in CyTOF staining protocols for larger cohort studies.

### 5.1.5. Monocyte numbers and cell yield

Although the observed low levels of Mo are similar to what have been reported in other studies [169], a relatively low Mo count may partly be due to a variable number of Mo, and possibly other cells, remaining on the tube walls after incubation and stimulation. Upon activation, Mo rely on adhesion to endothelial cells and will as a result upregulate the expression of surface proteins needed for adhesion [170, 171]. EDTA can be used as a chelator and affect the ions that are necessary for proper cell adhesion function [172]. By reducing cell adhesion capacity, the cells will be less likely to stick together or to other material and thus reduce the likelihood of these cells remaining in the tubes or being excluded as doublets during gating.

The observed variations in cell subpopulations were found to be within the normal tube-to-tube variation range and thus could also be due to stimulation or other factors, not necessarily EDTA. Additionally, the lower percentages observed in the stimulated samples for Mo cells and DC is most likely due to the reduced detection of the CD14 and CD16 markers after stimulation. Similar effects of stimulation have been observed in other studies [173-175], and have consequences for further gating of Mo and DC. We gated on DC from CD16+ cells and Mo are gated as CD14+CD16+ cells.

Even though we only tested the EDTA procedure for one participant, the results indicate that the EDTA treatment did not affect the relative number of Mo or other major cell subpopulations in our samples. The main differences were observed for the general cell yield and would thus be expected to be equal for both groups. Suggesting that the results we present on phthalate associated effect on cell populations would not have been considerably affected by the presence of EDTA and thus supports the validity of the results reported.

### 5.1.6. Statistical tests in the CITRUS algorithm

The CITRUS algorithm constructs trees of cell nodes based on hierarchical clustering and subsequently, PAM evaluates the predictive quality or SAM evaluates the correlative quality to the groups of each feature in each node independently. When identifying clusters that independently displayed different characteristics between the high and low exposed groups, PAM, and only a few cases of SAM, were returned. This could indicate that any variability in one group are not related to variability in the other group (correlative) as would be expected if looking at one disease group vs a control group. Instead, the PAM model gives indications of the minimum set of features that best predicts the groups (i.e. high and low exposed) [176].

The quality of the predictive PAM statistical CITRUS analysis is determined based on the CVF and the model error rate. If the CVF is high, meaning that the data is divided into many subsets, and the resulting model error rate is not good, then the PAM model cannot reliably predict whether a sample is in the high or low exposed group [150, 151]. We decided to use a low FDR threshold (of 1%) to minimize the likelihood of including too many false positive features. We also decided to use a CVF of 5 to make sure that we had enough training sets for the predicative model, but also that we did not divide the dataset into too many smaller components resulting in a validation set with insufficient amount of data to confidentially evaluate the model.

Even though some of the CITRUS results were questionable due to high variation within each group and some overlap between the groups, the overall consistent results across several CITRUS runs makes the findings more reliable. For the main PAM results, since this was an explorative study with few participants, and we were not specifically looking for predictive features, we used the statistical reports on group differences even though the model error rate was not good. For future studies, increasing the number of participants might accommodate the needs of the PAM model.

For the correlative SAM statistics, the results does not return a model error rate, as this is an indication of how well the identified features are predictive of the group characteristics. For the SAM results, the model returns all features that are included when the FDR is 1%, 5% and 10%. When using the SAM results, we used the results with a 1% FDR. This was to ensure equality between the SAM and PAM criteria and thus between the results.

## 5.2. Phthalates and innate immune cells

In the group exposed to high levels of DEHP and DiNP, the statistically significantly different subpopulations of cells in the innate immune system (related to NK-cells and Mo) show a consistent pattern, all with a higher abundance than in the low exposed group. The main findings are summarized in Figure 19.

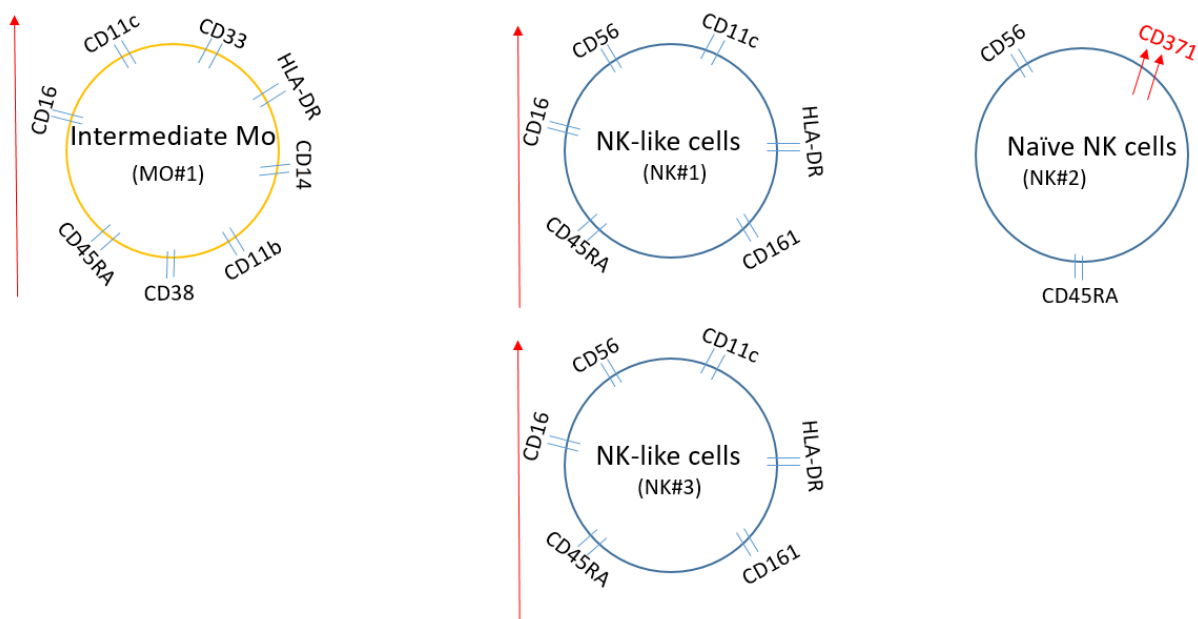


Figure 19: Summary of the main results for innate immune cells. Each "circle" represent one identified cell cluster (name in brackets) that were significantly different between the group exposed to high levels of DEHP and DiNP phthalates compared to the low exposed group. The red arrows indicate the observed significant increase in cell abundance or marker expression (when present on the cell circle line) in the high exposed group compared to the low exposed group. Other markers included on each cell circle illustrates the markers characterizing each cell circle.

Firstly, the CITRUS algorithm found a significantly higher abundance of several subpopulations of Mo (including MO#1) in the high compared to the low exposed group.

This finding was supported by the manual gating on the entire Mo population, also showing a statistically significant higher abundance in the high exposed group.

The high expression of CD33, CD11b and HLA-DR characterized MO#1 as an intermediate Mo subpopulation [177]. HLA-DR expression have been found to be upregulated by pathogens in Mo cells, the high HLA-DR expression in MO#1 thus indicates that this is an activated subpopulation [178]. Intermediate Mo have previously been found to have pro-inflammatory functions and to be increased during inflammation and infection [177, 179, 180]. The MO#1 subpopulation also expressed high levels of several markers that previously have been found to be upregulated during disease state (including CD38, CD11c and CD45RA) [181-185].

Studies have found CD14+CD16+ Mo levels in blood to be increased in inflammatory diseases [186, 187]. An increase in Mo count has also been found to be related to myelosuppressed states (e.g. aplastic anemia), recovery from myelosuppression and in hematologic malignancies (myeloid leukemia and particularly Hodgkin disease) [188, 189].

Other studies have found that phthalates, especially DEHP, are able to enhance TNF $\alpha$  production from Mo cells and macrophages and thus initiate an inflammatory state in the innate immune system [190]. In addition, another study suggests that phthalates influences early inflammatory phases by enhancing mast cell degranulation and eosinophilic infiltration, which could lead to the development of allergic asthma [191].

The downregulation of the monocyte markers (CD14 and CD16) and the problem with the CD33 marker in the stimulated samples (see section 4.1.1. above) probably affected the clustering and identification of the Mo subpopulations and their cytokine expression. Cytokine expression from Mo cells is therefore not reliable for this study. In addition, we did not investigate mast cells or eosinophils in this study, as these are not present in PBMC. However, the mentioned studies together with our observation of increased Mo subpopulations, supports the notion of a possible increased risk of early inflammation in the innate immune system due to phthalate exposure.

In addition to increased Mo abundance, the cell numbers in several NK-cell subpopulations were significantly higher in the high compared to the low exposed group (including NK#1 and NK#3 in the unstimulated and stimulated samples, respectively). NK#1, NK#3 and the group of parent-child subpopulations were characterized as NK-like cells based on the high expression of both CD56 and CD11c, these cells have been reported to help the proliferation of  $\gamma\delta$ T-cells [192]. The expression of the CD11c adhesion molecule in addition to the absence of CCR7 (in NK#1, not measured for NK#3) and high HLA-DR expression indicates that these cells primarily migrate to acute inflammatory sites [192, 193]. Further, by looking at the marker expression from the CITRUS tree, we found that almost all the significantly different subpopulations of NK-like cells also expressed CD161 (data not shown). Expression of CD161 on NK-cells are found to indicate a pro-inflammatory state in which these cells are able to respond to cytokines and contribute to inflammatory disease development [194]. The consistent observations of increased number of both NK-cells and Mo cells in the high exposed group suggests that high exposure to phthalates could promote pro-inflammatory innate immune cells.

Even though the expression was low, in the high exposed group we observed a significant increase in the expression of CD371 (CLEC14A, MICL) on another subpopulation of NK-cells (NK#2) (CD45RA+ CD16-). These cells did not express CD11c and therefore belong to a different NK-cell subpopulation than NK#1 and NK#3. CD371 is a C-type lectin-like receptor (CLR) that belongs to the PRR family and binds carbohydrates [195]. The receptor is mostly found on myeloid cells and are mainly involved in the recognition of MHC I and related molecules [196]. The function of CD371 is not well documented, but the receptor is assumed to have an inhibitory role [197]. On NK-cells, CD371 has been found to be important in regulating cytotoxicity and cytokine production and are downregulated during cellular activation [196]. Although the expression of CD371 in this subpopulation is low, the significant reduction may indicate a less active NK-cell subpopulation in the high exposed group. However, the lack of CD16 and the high CD45RA expression does indicate that the NK#2 population is a naïve NK-cell subpopulation [198], and naïve NK-cells have weak functional abilities [199, 200].

As mentioned earlier, phthalates are rapidly metabolize and are not thought to remain long in the body. The reported increased abundance of innate immune cell subpopulations and enhanced expression of inflammatory related markers on some of these cells are in accordance with literature, and might suggests a stimulatory effect and a continued low grade inflammatory state in people with high DEHP and DiNP exposure.

### 5.3. Phthalates and adaptive immune cells

In the group exposed to high levels of DEHP and DiNP, all observed differences in relative cell numbers, cytokine production and activation markers for the adaptive immune cells were found to exhibit a consistent decreasing pattern (Figure 20).

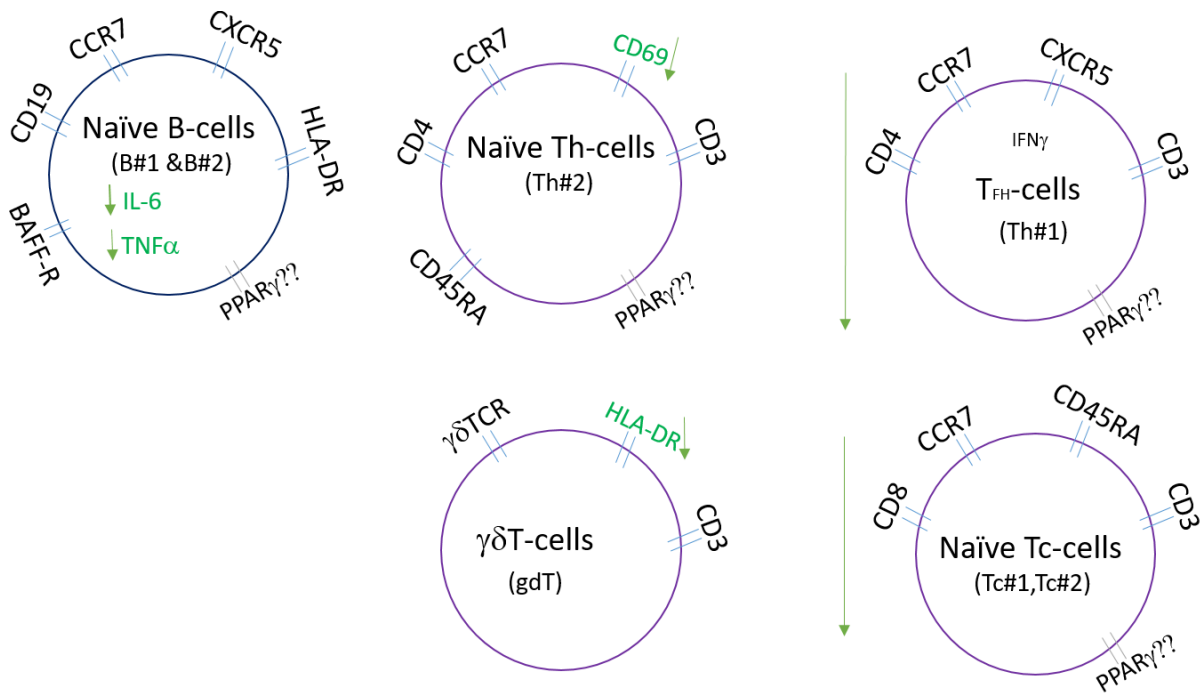


Figure 20: Summary of the main results for adaptive immune cells. Each "circle" represent one identified cell cluster (name in brackets) that were significantly different between the group exposed to high levels of DEHP and DiNP phthalates compared to the low exposed group. The green arrows indicate the observed significant decrease in cell abundance, marker expression (when present on the cell circle line) or cytokine production (when inside the cell circle) in the high exposed group compared to the low exposed group. Other markers included on each cell circle illustrates the markers characterizing each cell circle. PPAR $\gamma$  expressions were not measured in this study, but are included on the cluster of cells that are suspected of expressing this receptor based on other surface markers.

In subpopulations of naïve B-cells (including B#1 and B#2), we observed a statistically significantly reduced production of IL-6 and TNF $\alpha$ , two important pro-inflammatory cytokines, in the high exposed compared to the low exposed group. In a previous study, these two cytokines have been attributed to two different B-cell subpopulations. Among others, Be-2 (primed by Th2-cells) were found to produce IL-6 while Be-1 (primed by Th1-cells) were found to produce TNF $\alpha$ , respectively [201]. In this study, we found both cytokines to be expressed in relatively high amounts in the same B-cell subpopulations and both appeared to be reduced in the same cells.

IL-6 and TNF $\alpha$  are found to be important in B-cell function, and neutralization of these led to reduced B-cell proliferation [202]. Interestingly, lack of B-cell derived IL-6 has been reported to prevent follicular helper T-cell (T<sub>FH</sub>) differentiation [203, 204]. This is in consistence with our observed reduced IL-6 production in subpopulations of B-cells and



the observed reduced number of T<sub>FH</sub>-cells. B-cell derived TNF $\alpha$  have been reported to be important for controlling development of follicular DC and some stromal cells in the spleen [201]. Whether the apparently reduced expression of these cytokines in B-cells in the high phthalate exposed group could lead to such subsequent suppressive effects cannot be answered by the present study.

We also found a reduced TNF $\alpha$  expression in a subpopulation of Th-cells (Th#3) in the high exposed group. This is in agreement with another study, where phthalate monoesters were found to reduce the secretion of TNF $\alpha$  from T-cells [34]. TNF $\alpha$  is a known pro-inflammatory cytokine that also seems to be important in the development of asthma and allergies [205, 206]. Low TNF $\alpha$  levels have been linked to autoimmunity and defective T-cell maturation [207], and the authors suggest that this might result in autoreactive T-cells due to inadequate self-antigen processing.

TNF $\alpha$  is known to interact with and influence many different receptors on different cells. Interestingly, binding of TNF $\alpha$  to PPAR-gamma (PPAR $\gamma$ ) has been found to inhibit its activity [208] and thus potentially reduce inflammatory responses. PPAR $\gamma$  is expressed on various immune cells, and have an especially high expression in tissues with high B-cell numbers (i.e. spleen, lymph nodes and bone marrow) [209]. PPAR $\gamma$  is an important nuclear receptor that controls the expression of a large number of genes and are found to be involved in the pathogenesis of inflammation [210]. Interestingly, PPAR $\gamma$  have been found to be expressed in higher levels in airway tissue of patients with asthma [211], and its functional role in explaining the associations between phthalate exposure and asthma has been discussed by Bølling et al. [40].

PPAR's are activated by lipophilic ligands and studies have found that esters with long and/or branched side chains, like HMW phthalates, are more effective at activating PPAR than esters with short or straight chains [212]. Other studies have found that phthalate monoesters are able to act as PPAR agonists and that MEHP, the active metabolite of DEHP, are able to activate PPAR $\gamma$  [209, 213]. One of these studies found that high MEHP concentrations could lead to B-cell apoptosis, while lower concentrations lead to reduced B-cell growth and found this to indicate an immunosuppressive role of phthalate metabolites [209]. Activation of PPAR $\gamma$  are also found to suppress IL-6 expression in PBMC and brain cells [214, 215]. Such findings are in consistence with other studies that finds phthalates to be able to alter gene expression [216, 217].

These studies supports our observation of suppressed cytokine (TNF $\alpha$  and IL-6) production in B-cell subpopulations and TNF $\alpha$  in a subpopulation of Th-cells after PMA+IM stimulation in the high exposed group. Taken together, it is tempting to hypothesize that exposure to phthalates may affect PPAR $\gamma$  activation by acting as antagonists and thus directly activate the PPAR $\gamma$  and/or by reducing TNF $\alpha$  expression (here in subpopulations of B- and T-cells) and thus limiting the inhibitory activity of TNF $\alpha$ . We did not measure PPAR $\gamma$  expression in the cells, but PPAR $\gamma$  gene expression are currently being assessed in white blood cells from the same participants in an ongoing study.

Interestingly, we found that all subpopulations investigated in this study, that in the high exposed group showed reduction in cell numbers, activation markers and cytokine production, except  $\gamma\delta$ T-cells, also expressed high levels of CCR7. CCR7 is known to be important in the return of lymphocytes to the lymph nodes, where, as mentioned, PPAR $\gamma$  expression on immune cells are found to be particularly high [218]. The gene expression

study is expected to provide more information about the relation between phthalates and PPAR $\gamma$ .

The reducing effect were also evident in activation markers related to subpopulations of T-cells. In the high exposed group, we observed a reduced expression of HLA-DR on  $\gamma\delta$ T-cells. HLA-DR has been reported to be an activation marker on these cells, and are found to be upregulated during disease (e.g. chronic inflammation and autoimmune diseases) [219, 220].  $\delta$ T-cells are important in forming the primary immune response and in the production of cytokines that signals for appropriate Th-response [117]. In this study, we did not measure the cytokine production of  $\gamma\delta$ T-cells, but the reported upregulation of HLA-DR on  $\gamma\delta$ T-cells during disease state suggests a functional role in these cells.

In the high exposed group, we also observed a lower expression of CD69, an early T-cell activation marker, in subpopulations of naïve Th-cells (including Th#2) compared to the low exposed group. CD69 is quickly induced after TCR stimulation and are found to be upregulated on active T-cells [221]. The decrease in HLA-DR expression on  $\gamma\delta$ T-cells and CD69 expression on naïve Th-cell subpopulations is in consistence with the general decrease in adaptive immune cell functions and cell counts observed in this study.

Based on our results, we cannot conclude whether the observed inverse associations between phthalate exposure and cytokine and functional marker expression could lead to suppressive effects of cells in the innate and adaptive immune system or modified cell maturation. However, the consistent results and the accumulative effect on PPAR $\gamma$  from both phthalate exposure and reduced TNF $\alpha$  inhibitory effect could suggest a mechanism for phthalate exposure to cause reduced adaptive immune responses. Further studies are needed to investigate this aspect.

For T-cells, we also observed a slight reduction in abundance of several cell subpopulations in the high exposed group. In the high compared to the low exposed group, we found a slight decrease in the relative number of subpopulations of naïve Tc-cells in both the stimulated and unstimulated samples (including Tc#1, Tc#2 and Tc#3) and subsets of central memory (CM) Th-cells (including Th#1) in the unstimulated samples. Similarly, a decrease in T-cells and related activation markers has in other studies been linked to immunosuppressive effect after exposure to other lipophilic chemicals like Trichloroethylene (TCE), Bisphenol A (BPA) and mercury [222-224]. The authors hypothesized that the observed immunosuppressive effect could result in reduced immune capacity [222] and a possible increased risk of autoimmune diseases [223, 224].

CM T-cells are able to renew themselves and are thought to be important for maintaining the memory cell pool [225]. These cells are mainly located in lymphoid organs where they are activated by DC before proliferating to effector Th-cells [226, 227]. However, the expression of CXCR5 on the Th#1 subpopulation characterizes it as follicular B helper T-cells (T<sub>FH</sub>). Thus indicating that these cells also are able to migrate to B-cell follicles and help in B-cell differentiation [228-230]. After antigen encountering, only a few cells transiently migrate from the T-cell area to the B-cell follicle in peripheral lymph nodes. These cells are important for helping B-cells in producing sufficient amounts of antibodies [228, 231]. The expression of CXCR5 and CCR7 on the Th#1 cell population suggests that this subpopulation represent these transition cells.

Despite being significantly different, on group level, the abundance of the T-cell showed considerable overlapping values for individuals in the two groups. Meaning that the reduction in T-cell populations were quite subtle. In addition, inter-individual variations and fluctuations in T-cell count is common in healthy individuals and could be influenced by many factors, including stress, age, race, sex, time of collection etc. [232]. Even though many of these factors are accounted for in this study, by equal numbers of each gender in the two groups and approximately the same age range, it is not to say that other factors could influence cell count. For these reasons, and due to the subtle changes observed, abundance of T-cell subpopulations will on an individual level not be the most reliable biomarker. We therefore find our results on the expression of functional markers like cytokine and activation markers in particular cell subpopulations to be the markers with strongest potential to be biomarkers of effect and suggest that these markers should be explored in further studies.

The overall consistency of our findings and the agreement with other studies are interesting. All the significant findings in adaptive immune cell populations are pointing in the same direction, towards suppressive or reduced responses: reduced cytokine production in B-cell subpopulation, reduced activation in subpopulation of Th-cells (CD69 in Th#2), reduced activation in  $\gamma\delta$ T-cells (HLA-DR in gdT) and reduced number of Th- and Tc- subpopulations. This might suggest that phthalate exposure either directly or indirectly could lead to reduced adaptive immune responses.

## 6. Conclusion and future directions

In conclusion, for the high exposed DEHP and DiNP group we found an increase in subpopulations of Mo and NK-cells, cells related to the innate immune system, suggesting a possible stimulating effect of DEHP and DiNP on these cells. In the stimulated samples we found a decrease in cytokine production from B-cells (IL-6 and TNF $\alpha$ ) and Th-cells (TNF $\alpha$ ) in the high compared to the low exposed group. Additionally for adaptive immune cells, a decrease was observed for activation markers for  $\gamma\delta$ T-cells and Th-cells, and slight decrease in cell numbers for subpopulations of Th- and Tc-cells. Together, this could suggest a possible suppressive effect of DEHP and DiNP on the adaptive immune cells. Our exploratory study illustrated that mass cytometry can be used for identifying cell subpopulations and functional and phenotypic characteristics of innate and adaptive immune cells that differs between high and low exposed groups.

This was a preliminary study, aiming to contribute to the understanding of the immunological effects of phthalates on immune cells, and demonstrate the usefulness of high-dimensional methods like mass cytometry for this purpose. The present results provides a basis for such studies by identifying cell populations and markers of particular interest and potential biomarkers of effect for phthalate exposure. This was, however, a small study, and both replicating and supplementing studies (e.g. *in vitro* and gene expression studies) are needed to confirm and extend the present findings and address whether DEHP and DiNP have effects on cells in the innate and adaptive immune system and potential adverse consequences.

The ongoing gene expression analysis will contribute to supplementing the findings from this study. It is also important to keep in mind that other factors (e.g. other chemicals, health state etc.) could have influenced the present results on immune cell abundance and functions. Therefore, for future studies, *in vitro* testing of immune cells should be conducted, with both phthalate parent and metabolite compounds, to analyze direct effects. Such experimental studies will strengthen the biological plausibility and the causal link between phthalate exposure and immune effects.

Studies suggests that exposure to DEHP and DiNP during pregnancy and for newborns and infants are associated with adverse immune health outcomes in adolescence and adulthood. This study was performed on adult healthy participants, thus we do not know whether our results are relevant to the early life exposure effects. The large amount of information generated from a small sample volume, and our demonstration of the possibility for identifying functional immune cell features associated with phthalate exposure levels, suggests that mass cytometry is a suitable method also for studies in small children. It would therefore be interesting to perform a similar study on PBMC from newborns or children to better understand the immunological effects of phthalates on early life immune cells in relation to early life phthalate exposure.

# References

1. Davis, M.M., C.M. Tato, and D. Furman, *Systems immunology: just getting started*. Nat Immunol, 2017. **18**(7): p. 725-732.
2. Haland, G., et al., *Reduced lung function at birth and the risk of asthma at 10 years of age*. N.Engl.J Med, 2006. **355**(16): p. 1682-1689.
3. Lodrup Carlsen, K.C., et al., *Asthma in every fifth child in Oslo, Norway: a 10-year follow up of a birth cohort study*. Allergy, 2006. **61**(4): p. 454-460.
4. Schmidt, C.W., *Questions persist: environmental factors in autoimmune disease*. Environ Health Perspect, 2011. **119**(6): p. A249-A253.
5. Kravchenko, J., et al., *Chemical compounds from anthropogenic environment and immune evasion mechanisms: potential interactions*. Carcinogenesis, 2015. **36 Suppl 1**: p. S111-27.
6. Jusko, T.A., et al., *A Birth Cohort Study of Maternal and Infant Serum PCB-153 and DDE Concentrations and Responses to Infant Tuberculosis Vaccination*. Environ Health Perspect, 2016. **124**(6): p. 813-821.
7. International Program on Chemical Safety (IPCS), W.H.O.W. *Guidance for immunotoxicity risk assessments for chemicals* Harmonization Project Document No. 10 2012 [cited 2019 05.07.2019].
8. MacGillivray, D.M. and T.R. Kollmann, *The role of environmental factors in modulating immune responses in early life*. Frontiers in immunology, 2014. **5**: p. 434-434.
9. Herbert, O.C., et al., *Western lifestyle and increased prevalence of atopic diseases: an example from a small papua new guinean island*. The World Allergy Organization journal, 2009. **2**(7): p. 130-137.
10. Quinn, M., *Origins of Western diseases*. Journal of the Royal Society of Medicine, 2011. **104**(11): p. 449-456.
11. Holgate, S.T., *The epidemic of asthma and allergy*. Journal of the Royal Society of Medicine, 2004. **97**(3): p. 103-110.
12. Bauchau, V. and S.R. Durham, *Prevalence and rate of diagnosis of allergic rhinitis in Europe*. 2004. **24**(5): p. 758-764.
13. Kimber, I. and R.J. Dearman, *An assessment of the ability of phthalates to influence immune and allergic responses*. Toxicology, 2010. **271**(3): p. 73-82.
14. Stolevik, S.B., et al., *Prenatal exposure to polychlorinated biphenyls and dioxins is associated with increased risk of wheeze and infections in infants*. Food Chem Toxicol, 2011. **49**(8): p. 1843-8.
15. Granum, B., et al., *Pre-natal exposure to perfluoroalkyl substances may be associated with altered vaccine antibody levels and immune-related health outcomes in early childhood*. J Immunotoxicol, 2013. **10**(4): p. 373-9.
16. Tageldin, M., et al., *Influence of indoor respiratory irritants on the course of bronchial asthma*. Egyptian Journal of Chest Diseases and Tuberculosis, 2014. **63**(2): p. 291-298.
17. Cuervo, A., et al., *Phenolic compounds from red wine and coffee are associated with specific intestinal microorganisms in allergic subjects*. Food & Function, 2016. **7**(1): p. 104-109.
18. Phthalates, N.R.C.U.C.o.t.H.R.o., *Summary*, in *Phthalates and Cumulative Risk Assessment: The Tasks Ahead*, W.D.N.A.P. (US), Editor. 2008.
19. Phthalates, N.R.C.U.C.o.t.H.R.o., *Phthalate Exposure Assessment in Humans.*, in *Phthalates and Cumulative Risk Assessment: The Tasks Ahead.*, W.D.N.A.P. (US), Editor. 2008.
20. Robinson, L. and R. Miller, *The Impact of Bisphenol A and Phthalates on Allergy, Asthma, and Immune Function: a Review of Latest Findings*. Curr Environ Health Rep, 2015. **2**(4): p. 379-87.
21. Dodson Robin, E., et al., *Endocrine Disruptors and Asthma-Associated Chemicals in Consumer Products*. Environmental Health Perspectives, 2012. **120**(7): p. 935-943.

22. North, M.L., et al., *Effects of phthalates on the development and expression of allergic disease and asthma*. *Ann Allergy Asthma Immunol*, 2014. **112**(6): p. 496-502.
23. Kavlock, R., et al., *NTP Center for the Evaluation of Risks to Human Reproduction: phthalates expert panel report on the reproductive and developmental toxicity of di(2-ethylhexyl) phthalate*. *Reproductive Toxicology*, 2002. **16**(5): p. 529-653.
24. Rudel, R.A., et al., *Food packaging and bisphenol A and bis(2-ethylhexyl) phthalate exposure: findings from a dietary intervention*. *Environmental health perspectives*, 2011. **119**(7): p. 914-920.
25. Johns, L.E., et al., *Exposure assessment issues in epidemiology studies of phthalates*. *Environ Int*, 2015. **85**: p. 27-39.
26. MacGill, M. *Food container plastics linked to hypertension*. 2015.
27. Wormuth, M., et al., *What Are the Sources of Exposure to Eight Frequently Used Phthalic Acid Esters in Europeans?* 2006. **26**(3): p. 803-824.
28. Frederiksen, H., N.E. Skakkebaek, and A.M. Andersson, *Metabolism of phthalates in humans*. *Mol Nutr Food Res*, 2007. **51**(7): p. 899-911.
29. Buckley, J.P., et al., *Consumer product exposures associated with urinary phthalate levels in pregnant women*. *J Expo Sci Environ Epidemiol*, 2012. **22**(5): p. 468-75.
30. Lyche, J.L., *Chapter 48 - Phthalates*, in *Reproductive and Developmental Toxicology*, R.C. Gupta, Editor. 2011, Academic Press: San Diego. p. 637-655.
31. Hauser, R. and A.M. Calafat, *Phthalates and Human Health*. 2005. **62**(11): p. 806-818.
32. Lyche, J.L., et al., *Reproductive and Developmental Toxicity of Phthalates*. *Journal of Toxicology and Environmental Health, Part B*, 2009. **12**(4): p. 225-249.
33. Koch, H.M., Bolt, H.M., Preuss, R. et al. , *New metabolites of di(2-ethylhexyl)phthalate (DEHP) in human urine and serum after single oral doses of deuterium-labelled DEHP*. Springer-Verlag, 2005. **79**(7): p. 367–376.
34. Hansen, J.F., et al., *Influence of phthalates on in vitro innate and adaptive immune responses*. *PloS one*, 2015. **10**(6): p. e0131168-e0131168.
35. Koch, H.M. and J. Angerer, *Di-iso-nonylphthalate (DINP) metabolites in human urine after a single oral dose of deuterium-labelled DINP*. *Int J Hyg Environ Health*, 2007. **210**(1): p. 9-19.
36. Grindler, N.M., et al., *Exposure to Phthalate, an Endocrine Disrupting Chemical, Alters the First Trimester Placental Methylome and Transcriptome in Women*. *Scientific Reports*, 2018. **8**(1): p. 6086.
37. Bornehag, C.G., et al., *The association between asthma and allergic symptoms in children and phthalates in house dust: a nested case-control study*. *Environ Health Perspect*, 2004. **112**(14): p. 1393-7.
38. Eljezi, T., et al., *In vitro cytotoxic effects of secondary metabolites of DEHP and its alternative plasticizers DINCH and DINP on a L929 cell line*. *International Journal of Hygiene and Environmental Health*, 2019. **222**(3): p. 583-589.
39. Darbre, P.D., *Chapter 1 - What Are Endocrine Disruptors and Where Are They Found?*, in *Endocrine Disruption and Human Health*, P.D. Darbre, Editor. 2015, Academic Press: Boston. p. 3-26.
40. Kocbach Bolling, A., et al., *Pulmonary phthalate exposure and asthma - is PPAR a plausible mechanistic link?* *Excli j*, 2013. **12**: p. 733-59.
41. Serrano, S.E., et al., *Phthalates and diet: a review of the food monitoring and epidemiology data*. *Environmental health : a global access science source*, 2014. **13**(1): p. 43-43.
42. Latini, G., C. De Felice, and A. Verrotti, *Plasticizers, infant nutrition and reproductive health*. *Reprod Toxicol*, 2004. **19**(1): p. 27-33.
43. Silva, M.J., et al., *Measurement of eight urinary metabolites of di(2-ethylhexyl) phthalate as biomarkers for human exposure assessment*. *Biomarkers*, 2006. **11**(1): p. 1-13.
44. (ECHA), E.C.A., *Communication from the Commission on the finalisation of the restriction process on the four phthalates (DEHP, DBP, BBP and DIBP) under Regulation (EC) No 1907/2006 of the European Parliament and of the Council concerning Registration,*

- Evaluation, Authorisation and Restriction of Chemicals (REACH)*, EU, Editor. 2014, Official Journal of the European Union: Euro-Lex.
45. Sharma, R.P., M. Schuhmacher, and V. Kumar, *Development of a human physiologically based pharmacokinetic (PBPK) model for phthalate (DEHP) and its metabolites: A bottom up modeling approach*. *Toxicology Letters*, 2018. **296**: p. 152-162.
  46. Chen, X., et al., *Toxicity and estrogenic endocrine disrupting activity of phthalates and their mixtures*. *Int J Environ Res Public Health*, 2014. **11**(3): p. 3156-68.
  47. Boberg, J., et al., *Reproductive and behavioral effects of diisononyl phthalate (DINP) in perinatally exposed rats*. *Reproductive Toxicology*, 2011. **31**(2): p. 200-209.
  48. Barakat, R., et al., *Prenatal exposure to an environmentally relevant phthalate mixture disrupts testicular steroidogenesis in adult male mice*. *Environmental Research*, 2019. **172**: p. 194-201.
  49. Lyche, J.L., et al., *Reproductive and developmental toxicity of phthalates*. *J Toxicol Environ Health B Crit Rev*, 2009. **12**(4): p. 225-49.
  50. Wittassek, M., et al., *Assessing exposure to phthalates – The human biomonitoring approach*. 2011. **55**(1): p. 7-31.
  51. Sullivan, P.J., F.J. Agardy, and J.J.J. Clark, *CHAPTER 4 - Living with the Risk of Polluted Water*, in *The Environmental Science of Drinking Water*, P.J. Sullivan, F.J. Agardy, and J.J.J. Clark, Editors. 2005, Butterworth-Heinemann: Burlington. p. 143-196.
  52. Sathyanarayana, S., et al., *Baby Care Products: Possible Sources of Infant Phthalate Exposure*. 2008. **121**(2): p. e260-e268.
  53. Carlstedt, F., B.A. Jonsson, and C.G. Bornehag, *PVC flooring is related to human uptake of phthalates in infants*. *Indoor Air*, 2013. **23**(1): p. 32-9.
  54. Lottrup, G., et al., *Possible impact of phthalates on infant reproductive health*. *Int J Androl*, 2006. **29**(1): p. 172-80; discussion 181-5.
  55. Koch, H.M., R. Preuss, and J. Angerer, *Di(2-ethylhexyl)phthalate (DEHP): human metabolism and internal exposure-- an update and latest results*. *Int J Androl*, 2006. **29**(1): p. 155-65; discussion 181-5.
  56. Tickner, J.A., et al., *Health risks posed by use of Di-2-ethylhexyl phthalate (DEHP) in PVC medical devices: a critical review*. *Am J Ind Med*, 2001. **39**(1): p. 100-11.
  57. Meeker, J.D., S. Sathyanarayana, and S.H. Swan, *Phthalates and other additives in plastics: human exposure and associated health outcomes*. *Philos Trans R Soc Lond B Biol Sci*, 2009. **364**(1526): p. 2097-113.
  58. Skinner, M.K., *Endocrine disruptors in 2015: Epigenetic transgenerational inheritance*. *Nature reviews. Endocrinology*, 2016. **12**(2): p. 68-70.
  59. Quinlivan, K.M., et al., *Transgenerational Effects of Di-(2-Ethylhexyl) Phthalate (DEHP) on Stress Hormones and Behavior*. *Endocrinology*, 2015. **156**(9): p. 3077-83.
  60. Roh, J.Y., et al., *Toxic effects of di(2-ethylhexyl)phthalate on mortality, growth, reproduction and stress-related gene expression in the soil nematode *Caenorhabditis elegans**. *Toxicology*, 2007. **237**(1-3): p. 126-33.
  61. Yin, J., et al., *Di (2-ethylhexyl) phthalate-induced reproductive toxicity involved in dna damage-dependent oocyte apoptosis and oxidative stress in *Caenorhabditis elegans**. *Ecotoxicol Environ Saf*, 2018. **163**: p. 298-306.
  62. Li, S.W., C.M. How, and V.H. Liao, *Prolonged exposure of di(2-ethylhexyl) phthalate induces multigenerational toxic effects in *Caenorhabditis elegans**. *Sci Total Environ*, 2018. **634**: p. 260-266.
  63. De Toni, L., et al., *Phthalates and heavy metals as endocrine disruptors in food: A study on pre-packed coffee products*. *Toxicology reports*, 2017. **4**: p. 234-239.
  64. Swan, S.H., et al., *Decrease in anogenital distance among male infants with prenatal phthalate exposure*. *Environ Health Perspect*, 2005. **113**(8): p. 1056-61.
  65. Fisher, J.S., *Environmental anti-androgens and male reproductive health: focus on phthalates and testicular dysgenesis syndrome*. *Reproduction*, 2004. **127**(3): p. 305-15.

66. Jurewicz, J. and W. Hanke, *Exposure to phthalates: Reproductive outcome and children health. A review of epidemiological studies*. International Journal of Occupational Medicine and Environmental Health, 2011. **24**(2): p. 115-141.
67. Swan, S.H., *Environmental phthalate exposure in relation to reproductive outcomes and other health endpoints in humans*. Environ Res, 2008. **108**(2): p. 177-84.
68. Hussain, I., J.A. Marsh, and R.R. Dietert, *Developmental Immunotoxicology of Di-(2-Ethylhexyl)phthalate (DEHP): Age-Based Assessment in the Female Rat AU - Piepenbrink, Michael S*. Journal of Immunotoxicology, 2005. **2**(1): p. 21-31.
69. Nishioka, J., et al., *Di-(2-ethylhexyl) phthalate induces production of inflammatory molecules in human macrophages*. Inflamm Res, 2012. **61**(1): p. 69-78.
70. Takano, H., et al., *Di-(2-ethylhexyl) phthalate enhances atopic dermatitis-like skin lesions in mice*. Environmental health perspectives, 2006. **114**(8): p. 1266-1269.
71. Inoue, K.-I., et al., *Effects of airway exposure to di-(2-ethylhexyl) phthalate on allergic rhinitis AU - He, Miao*. Immunopharmacology and Immunotoxicology, 2013. **35**(3): p. 390-395.
72. Kolarik, B., et al., *The association between phthalates in dust and allergic diseases among Bulgarian children*. Environ Health Perspect, 2008. **116**(1): p. 98-103.
73. Bertelsen, R.J., et al., *Urinary biomarkers for phthalates associated with asthma in Norwegian children*. Environmental health perspectives, 2013. **121**(2): p. 251-256.
74. Yanagisawa, R., et al., *Effects of maternal exposure to di-(2-ethylhexyl) phthalate during fetal and/or neonatal periods on atopic dermatitis in male offspring*. Environ Health Perspect, 2008. **116**(9): p. 1136-41.
75. Sadakane, K., et al., *Effects of oral administration of di-(2-ethylhexyl) and diisononyl phthalates on atopic dermatitis in NC/Nga mice*. Immunopharmacol Immunotoxicol, 2014. **36**(1): p. 61-9.
76. Koike, E., et al., *Di-(2-ethylhexyl) phthalate affects immune cells from atopic prone mice in vitro*. Toxicology, 2009. **259**(1-2): p. 54-60.
77. Norback, D., et al., *Asthma symptoms in relation to measured building dampness in upper concrete floor construction, and 2-ethyl-1-hexanol in indoor air*. International Journal of Tuberculosis and Lung Disease, 2000. **4**(11): p. 1016-1025.
78. Polakoff, P.L., N. Leroy Lapp, and R. Reger, *Polyvinyl chloride pyrolysis products a potential cause for respiratory impairment*. Archives of Environmental Health, 1975. **30**(6): p. 269-271.
79. Eisen, E.A., D.H. Wegman, and T.J. Smith, *Across-shift changes in the pulmonary function of meat-wrappers and other workers in the retail food industry*. Scandinavian Journal of Work, Environment and Health, 1985. **11**(1): p. 21-26.
80. Markowitz, J.S., *Self-reported short- and long-term respiratory effects among pvc-exposed firefighters*. Archives of Environmental Health, 1989. **44**(1): p. 30-33.
81. Nielsen, J., et al., *Small airways function in workers processing polyvinylchloride*. International Archives of Occupational and Environmental Health, 1989. **61**(7): p. 427-430.
82. Brooks, S.M. and R. Vandervort, *Polyvinyl chloride film thermal decomposition products as an occupational illness: 2. clinical studies*. Journal of Occupational Medicine, 1977. **19**(3): p. 192-196.
83. Jaakkola, J.J.K., et al., *Asthma, Wheezing, and Allergies in Russian Schoolchildren in Relation to New Surface Materials in the Home*. 2004. **94**(4): p. 560-562.
84. Jaakkola, J.J., P.K. Verkasalo, and N. Jaakkola, *Plastic wall materials in the home and respiratory health in young children*. American journal of public health, 2000. **90**(5): p. 797-799.
85. Tuomainen, A., M. Seuri, and A. Sieppi, *Indoor air quality and health problems associated with damp floor coverings*. International Archives of Occupational and Environmental Health, 2004. **77**(3): p. 222-226.
86. Jaakkola, J.J.K., A. Ieromnimon, and M.S. Jaakkola, *Interior surface materials and asthma in adults: A population-based incident case-control study*. American Journal of Epidemiology, 2006. **164**(8): p. 742-749.



87. Deutsche, T., et al., *A Controlled Challenge Study on Di(2-ethylhexyl) Phthalate (DEHP) in House Dust and the Immune Response in Human Nasal Mucosa of Allergic Subjects*. Environmental Health Perspectives, 2008. **116**(11): p. 1487-1493.
88. Jepsen, K.F., A. Abildtrup, and S.T. Larsen, *Monophthalates promote IL-6 and IL-8 production in the human epithelial cell line A549*. Toxicology in Vitro, 2004. **18**(3): p. 265-269.
89. Glue, C., et al., *Phthalates potentiate the response of allergic effector cells*. Basic Clin Pharmacol Toxicol, 2005. **96**(2): p. 140-2.
90. Bissonnette, S.L., et al., *An Endogenous Prostaglandin Enhances Environmental Phthalate-Induced Apoptosis in Bone Marrow B Cells: Activation of Distinct but Overlapping Pathways*. 2008. **181**(3): p. 1728-1736.
91. Schlezinger, J.J., et al., *An L-Tyrosine Derivative and PPAR $\gamma$  Agonist, GW7845, Activates a Multifaceted Caspase Cascade in Bone Marrow B Cells*. Toxicological Sciences, 2007. **98**(1): p. 125-136.
92. Schlezinger, J.J., et al., *Environmental and endogenous peroxisome proliferator-activated receptor  $\gamma$  agonists induce bone marrow B cell growth arrest and apoptosis: Interactions between mono(2-ethylhexyl)phthalate, 9-cis-retinoic acid, and 15-deoxy- $\Delta$ 12,14-prostaglandin J2*. Journal of Immunology, 2004. **173**(5): p. 3165-3177.
93. Kocbach Bølling, A., et al., *Mono-2-ethylhexylphthalate (MEHP) induces TNF- $\alpha$  release and macrophage differentiation through different signalling pathways in RAW264.7 cells*. Toxicology Letters, 2012. **209**(1): p. 43-50.
94. Quie, P.G., *Humoral factors in host defense against microbial invaders*. Scand J Infect Dis Suppl, 1982. **31**: p. 34-40.
95. Lowe, J.S. and P.G. Anderson, *Chapter 8 - Immune System*, in *Stevens & Lowe's Human Histology (Fourth Edition) (Fourth Edition)*, J.S. Lowe and P.G. Anderson, Editors. 2015, Mosby: Philadelphia. p. 123-142.
96. Kuby, J.A.O.J.P.S.A.S.P.P.J.J., *Kuby immunology 7th edition*. 2013, New York: W.H. Freeman, ©2013.
97. Parkin, J. and B. Cohen, *An overview of the immune system*. Lancet, 2001. **357**(9270): p. 1777-89.
98. Rothenberg, E.V., *Lineage determination in the immune system*. Immunological reviews, 2010. **238**(1): p. 5-11.
99. Peter J. Delves, P. *Cellular Components of the Immune System*. Biology of the Immune System 2018.
100. Hato, T. and P.C. Dagher, *How the Innate Immune System Senses Trouble and Causes Trouble*. Clinical journal of the American Society of Nephrology : CJASN, 2015. **10**(8): p. 1459-1469.
101. van Furth, R. and H. Beekhuizen, *Monocytes*, in *Encyclopedia of Immunology (Second Edition)*, P.J. Delves, Editor. 1998, Elsevier: Oxford. p. 1750-1754.
102. Kinne, R.W., B. Stuhl Müller, and G.R. Burmester, *CHAPTER 8C - Macrophages*, in *Rheumatoid Arthritis*, M.C. Hochberg, et al., Editors. 2009, Mosby: Philadelphia. p. 107-115.
103. Luckashenak, N. and L.C. Eisenlohr, *Chapter 5 - Dendritic Cells: Antigen Processing and Presentation*, in *Cancer Immunotherapy (Second Edition)*, G.C. Prendergast and E.M. Jaffee, Editors. 2013, Academic Press: San Diego. p. 55-70.
104. Paul, S. and G. Lal, *The Molecular Mechanism of Natural Killer Cells Function and Its Importance in Cancer Immunotherapy*. Frontiers in immunology, 2017. **8**: p. 1124-1124.
105. Actor, J.K., *6 - Innate Immunity*, in *Elsevier's Integrated Review Immunology and Microbiology (Second Edition)*, J.K. Actor, Editor. 2012, W.B. Saunders: Philadelphia. p. 43-51.
106. Katz, S.C., et al., *Chapter 10 - Liver immunology*, in *Blumgart's Surgery of the Liver, Biliary Tract and Pancreas, 2-Volume Set (Sixth Edition)*, W.R. Jarnagin, Editor. 2017, Content Repository Only!: Philadelphia. p. 173-187.e2.
107. Cologne, G.I.f.Q.a.E.i.H.C.I., *The innate and adaptive immune systems*, in *InformedHealth.org [Internet]*. 2010: <https://www.ncbi.nlm.nih.gov/books/NBK279396/>.
108. Reinhard, E.V. and M.B. Barbara, *Innate vs acquired immunity*

*Oxford Textbook of Rheumatology*. Oxford, UK.

109. Sanz, I., et al., *Phenotypic and functional heterogeneity of human memory B cells*. *Seminars in immunology*, 2008. **20**(1): p. 67-82.
110. Caraux, A., et al., *Circulating human B and plasma cells. Age-associated changes in counts and detailed characterization of circulating normal CD138- and CD138+ plasma cells*. *Haematologica*, 2010. **95**(6): p. 1016-1020.
111. Forthal, D.N., *Functions of Antibodies*. *Microbiology spectrum*, 2014. **2**(4): p. 1-17.
112. Yakimchuk, K. *Development and specific markers of T and B lymphocytes*. 2016.
113. Germain, R.N., *T-cell development and the CD4–CD8 lineage decision*. *Nature Reviews Immunology*, 2002. **2**: p. 309.
114. Alberts B, J.A., Lewis J, et al., *Molecular Biology of the Cell. 4th edition*. Helper T Cells and Lymphocyte Activation., ed. N.Y.G. Science; 2002.
115. Fujihashi, K., P.N. Boyaka, and J.R. McGhee, *19 - Host defenses at mucosal surfaces*, in *Clinical Immunology (Third Edition)*, R.R. Rich, et al., Editors. 2008, Mosby: Edinburgh. p. 287-303.
116. Nakayamada, S., et al., *Helper T cell diversity and plasticity*. *Current Opinion in Immunology*, 2012. **24**(3): p. 297-302.
117. Ferrick, D.A., et al., *Differential production of interferon- $\gamma$  and interleukin-4 in response to Th1- and Th2-stimulating pathogens by  $\gamma\delta$  T cells in vivo*. *Nature*, 1995. **373**(6511): p. 255-257.
118. Kolls, J.K., *Th17 cells in mucosal immunity and tissue inflammation*. *Seminars in immunopathology*, 2010. **32**(1): p. 1-2.
119. Seder, R.A. and J.R. Mascola, *2 - IMMUNOLOGY: PART A. Basic Immunology of Vaccine Development*, in *The Vaccine Book*, B.R. Bloom and P.-H. Lambert, Editors. 2003, Academic Press: San Diego. p. 51-72.
120. Wing, K. and S. Sakaguchi, *16 - Regulatory T cells*, in *Clinical Immunology (Third Edition)*, R.R. Rich, et al., Editors. 2008, Mosby: Edinburgh. p. 249-258.
121. Bettelli, E., et al., *Reciprocal developmental pathways for the generation of pathogenic effector TH17 and regulatory T cells*. *Nature*, 2006. **441**: p. 235.
122. Iyer, S.S. and G. Cheng, *Role of interleukin 10 transcriptional regulation in inflammation and autoimmune disease*. *Critical reviews in immunology*, 2012. **32**(1): p. 23-63.
123. Zhang, J.-M. and J. An, *Cytokines, inflammation, and pain*. *International anesthesiology clinics*, 2007. **45**(2): p. 27-37.
124. Peter J. Delves, P. *Molecular Components of the Immune System*. *Biology of the Immune System* 2018 05.10.2019]; Available from: <https://www.msmanuals.com/professional/immunology-allergic-disorders/biology-of-the-immune-system/molecular-components-of-the-immune-system#v28603723>.
125. Germolec, D., et al., *Immunotoxicology: A brief history, current status and strategies for future immunotoxicity assessment*. *Current Opinion in Toxicology*, 2017. **5**: p. 55-59.
126. Kleinstreuer, N.C., et al., *Adverse outcome pathways: From research to regulation scientific workshop report*. *Regul Toxicol Pharmacol*, 2016. **76**: p. 39-50.
127. Nowak, K., E. Jabłońska, and W. Ratajczak-Wrona, *Immunomodulatory effects of synthetic endocrine disrupting chemicals on the development and functions of human immune cells*. *Environment International*, 2019. **125**: p. 350-364.
128. Lankveld, D.P., et al., *In vitro testing for direct immunotoxicity: state of the art*. *Methods Mol Biol*, 2010. **598**: p. 401-23.
129. *National Academies Press (NAP) Toxicity testing in the 21st century: a vision and a strategy*. 2007, National Research Council: National Academies Press (NAP)
130. Razumienko, E., et al., *Element-tagged immunoassay with ICP-MS detection: evaluation and comparison to conventional immunoassays*. *Journal of immunological methods*, 2008. **336**(1): p. 56-63.

131. Kay, A.W., D.M. Strauss-Albee, and C.A. Blish, *Application of Mass Cytometry (CyTOF) for Functional and Phenotypic Analysis of Natural Killer Cells*. Methods in molecular biology (Clifton, N.J.), 2016. **1441**: p. 13-26.
132. Nicholas, K.J., et al., *Multiparameter analysis of stimulated human peripheral blood mononuclear cells: A comparison of mass and fluorescence cytometry*. Cytometry. Part A : the journal of the International Society for Analytical Cytology, 2016. **89**(3): p. 271-280.
133. Bendall, S.C., et al., *Single-cell trajectory detection uncovers progression and regulatory coordination in human B cell development*. Cell, 2014. **157**(3): p. 714-25.
134. Bendall, S.C., et al., *Single-cell mass cytometry of differential immune and drug responses across a human hematopoietic continuum*. Science, 2011. **332**(6030): p. 687-96.
135. Horowitz, A., et al., *Genetic and environmental determinants of human NK cell diversity revealed by mass cytometry*. Sci Transl Med, 2013. **5**(208): p. 208ra145.
136. Mingueneau, M., et al., *Single-cell mass cytometry of TCR signaling: amplification of small initial differences results in low ERK activation in NOD mice*. Proc Natl Acad Sci U S A, 2014. **111**(46): p. 16466-71.
137. Newell, E.W., et al., *Cytometry by time-of-flight shows combinatorial cytokine expression and virus-specific cell niches within a continuum of CD8+ T cell phenotypes*. Immunity, 2012. **36**(1): p. 142-52.
138. Sen, N., et al., *Single-cell mass cytometry analysis of human tonsil T cell remodeling by varicella zoster virus*. Cell Rep, 2014. **8**(2): p. 633-45.
139. Polikowsky, H.G., et al., *Cutting Edge: Redox Signaling Hypersensitivity Distinguishes Human Germinal Center B Cells*. J Immunol, 2015. **195**(4): p. 1364-1367.
140. Ornatsky, O., et al., *Multiple cellular antigen detection by ICP-MS*. J Immunol Methods, 2006. **308**(1-2): p. 68-76.
141. Lou, X., et al., *Polymer-based elemental tags for sensitive bioassays*. Angewandte Chemie (International ed. in English), 2007. **46**(32): p. 6111-6114.
142. Gaudillière, B., et al., *Implementing Mass Cytometry at the Bedside to Study the Immunological Basis of Human Diseases: Distinctive Immune Features in Patients with a History of Term or Preterm Birth*. Cytometry. Part A : the journal of the International Society for Analytical Cytology, 2015. **87**(9): p. 817-829.
143. Bendall, S.C., et al., *A deep profiler's guide to cytometry*. Trends in immunology, 2012. **33**(7): p. 323-332.
144. Leipold, M.D., *Another step on the path to mass cytometry standardization*. 2015. **87**(5): p. 380-382.
145. Staser, K.W., et al., *OMIP-042: 21-color flow cytometry to comprehensively immunophenotype major lymphocyte and myeloid subsets in human peripheral blood*. Cytometry. Part A : the journal of the International Society for Analytical Cytology, 2018. **93**(2): p. 186-189.
146. Sabaredzovic, A., et al., *Determination of 12 urinary phthalate metabolites in Norwegian pregnant women by core-shell high performance liquid chromatography with on-line solid-phase extraction, column switching and tandem mass spectrometry*. J Chromatogr B Analyt Technol Biomed Life Sci, 2015. **1002**: p. 343-52.
147. Ramachandran, H., et al., *Optimal thawing of cryopreserved peripheral blood mononuclear cells for use in high-throughput human immune monitoring studies*. Cells, 2012. **1**(3): p. 313-324.
148. Smith, J.G., et al., *Development and validation of a gamma interferon ELISPOT assay for quantitation of cellular immune responses to varicella-zoster virus*. Clinical and diagnostic laboratory immunology, 2001. **8**(5): p. 871-879.
149. Amir, E.-a.D., et al., *visNE enables visualization of high dimensional single-cell data and reveals phenotypic heterogeneity of leukemia*. Nature biotechnology, 2013. **31**(6): p. 545-552.
150. Kimball, A.K., et al., *A Beginner's Guide to Analyzing and Visualizing Mass Cytometry Data*. J Immunol, 2018. **200**(1): p. 3-22.

151. Bruggner, R.V., et al., *Automated identification of stratifying signatures in cellular subpopulations*. Proc Natl Acad Sci U S A, 2014. **111**(26): p. E2770-7.
152. Hastie, T., et al., *PAM "Prediction Analysis of Microarrays" Users guide and manual*. 2002.
153. Grace, C. and E.P. Nacheva, *Significance Analysis of Microarrays (SAM) Offers Clues to Differences Between the Genomes of Adult Philadelphia Positive ALL and the Lymphoid Blast Transformation of CML*. Cancer informatics, 2012. **11**: p. 173-183.
154. Hoffman, J.I.E., *Chapter 22 - Comparison of Two Groups: t-Tests and Nonparametric Tests*, in *Biostatistics for Medical and Biomedical Practitioners*, J.I.E. Hoffman, Editor. 2015, Academic Press. p. 337-362.
155. Gad, S.C., *3.13 - Statistical Methods in Toxicology*, in *Comprehensive Toxicology (Second Edition)*, C.A. McQueen, Editor. 2010, Elsevier: Oxford. p. 183-197.
156. Riffenburgh, R.H., *Chapter 6 - Statistical Testing, Risks, and Odds in Medical Decisions*, in *Statistics in Medicine (Second Edition)*, R.H. Riffenburgh, Editor. 2006, Academic Press: Burlington. p. 93-114.
157. Riffenburgh, R.H., *Chapter 16 - Tests on Ranked Data*, in *Statistics in Medicine (Second Edition)*, R.H. Riffenburgh, Editor. 2006, Academic Press: Burlington. p. 281-303.
158. Handgretinger, R., et al., *Expression of an early myelopoietic antigen (CD33) on a subset of human umbilical cord blood-derived natural killer cells*. Immunology Letters, 1993. **37**(2): p. 223-228.
159. Lock, K., et al., *Expression of CD33-related siglecs on human mononuclear phagocytes, monocyte-derived dendritic cells and plasmacytoid dendritic cells*. Immunobiology, 2004. **209**(1): p. 199-207.
160. DeLeve, L.D., *Chapter 8 - Liver Sinusoidal Endothelial Cells and Liver Injury*, in *Drug-Induced Liver Disease (Third Edition)*, N. Kaplowitz and L.D. DeLeve, Editors. 2013, Academic Press: Boston. p. 135-146.
161. Naeim, F., et al., *2 - Principles of Immunophenotyping*, in *Atlas of Hematopathology*, F. Naeim, et al., Editors. 2013, Academic Press. p. 25-46.
162. Cytobank, I. *How to Configure and Run a CITRUS Analysis*. Cytobank 2019 01.02.2019 [cited 2019 05.06.2019]; Available from: <https://support.cytobank.org/hc/en-us/articles/226678087-How-to-Configure-and-Run-a-CITRUS-Analysis>.
163. Lin, D., S. Gupta, and H.T. Maecker, *Intracellular Cytokine Staining on PBMCs Using CyTOF™ Mass Cytometry*. Bio-protocol, 2015. **5**(1): p. e1370.
164. Subrahmanyam, P.B. and H.T. Maecker, *CyTOF Measurement of Immunocompetence Across Major Immune Cell Types*. Current protocols in cytometry, 2017. **82**: p. 9.54.1-9.54.12.
165. Leipold, M.D. and H.T. Maecker, *Phenotyping of Live Human PBMC using CyTOF™ Mass Cytometry*. Bio-protocol, 2015. **5**(2): p. e1382.
166. Ai, W., et al., *Optimal method to stimulate cytokine production and its use in immunotoxicity assessment*. International journal of environmental research and public health, 2013. **10**(9): p. 3834-3842.
167. Katial, R.K., et al., *Cytokine production in cell culture by peripheral blood mononuclear cells from immunocompetent hosts*. Clinical and diagnostic laboratory immunology, 1998. **5**(1): p. 78-81.
168. Schulz, A.R., et al., *Stabilizing Antibody Cocktails for Mass Cytometry*. **0**(0).
169. Yao, Y., et al., *CyTOF supports efficient detection of immune cell subsets from small samples*. Journal of immunological methods, 2014. **415**: p. 1-5.
170. Liang, H., Z. Xie, and T. Shen, *Monocyte activation and cardiovascular disease in HIV infection*. Cellular & Molecular Immunology, 2017. **14**: p. 960.
171. Sondag, C.M. and C.K. Combs, *Adhesion of monocytes to type I collagen stimulates an APP-dependent proinflammatory signaling response and release of Abeta1-40*. Journal of neuroinflammation, 2010. **7**: p. 22-22.
172. Kaur, M. and L. Esau, *Two-step protocol for preparing adherent cells for high-throughput flow cytometry*. 2015. **59**(3): p. 119-126.

173. Baran, J., et al., *Three-color flow cytometry detection of intracellular cytokines in peripheral blood mononuclear cells: comparative analysis of phorbol myristate acetate-ionomycin and phytohemagglutinin stimulation*. *Clinical and diagnostic laboratory immunology*, 2001. **8**(2): p. 303-313.
174. Srpan, K., et al., *Shedding of CD16 disassembles the NK cell immune synapse and boosts serial engagement of target cells*. 2018. **217**(9): p. 3267-3283.
175. Borrego, F., et al., *Downregulation of Fcγ Receptor IIIAα (CD16-II) on Natural Killer Cells Induced by Anti-CD16 mAb Is Independent of Protein Tyrosine Kinases and Protein Kinase C*. *Cellular Immunology*, 1994. **158**(1): p. 208-217.
176. Tibshirani, R., et al., *Diagnosis of multiple cancer types by shrunken centroids of gene expression*. *Proceedings of the National Academy of Sciences of the United States of America*, 2002. **99**(10): p. 6567-6572.
177. Wong, K.L., et al., *Gene expression profiling reveals the defining features of the classical, intermediate, and nonclassical human monocyte subsets*. *Blood*, 2011. **118**(5): p. e16-31.
178. Tillinger, W., et al., *Monocyte human leukocyte antigen-DR expression-a tool to distinguish intestinal bacterial infections from inflammatory bowel disease?* *Shock (Augusta, Ga.)*, 2013. **40**(2): p. 89-94.
179. Wildgruber, M., et al., *The "Intermediate" CD14(++)CD16(+) monocyte subset increases in severe peripheral artery disease in humans*. *Scientific reports*, 2016. **6**: p. 39483-39483.
180. Hijdra, D., et al., *Phenotypic characterization of human intermediate monocytes*. *Frontiers in immunology*, 2013. **4**: p. 339-339.
181. Sugimoto, C., et al., *Differentiation Kinetics of Blood Monocytes and Dendritic Cells in Macaques: Insights to Understanding Human Myeloid Cell Development*. *Journal of immunology (Baltimore, Md. : 1950)*, 2015. **195**(4): p. 1774-1781.
182. Nagasawa, T., et al., *Expression of CD14, CD16 and CD45RA on monocytes from periodontitis patients*. *J Periodontal Res*, 2004. **39**(1): p. 72-8.
183. Drutman, S.B., J.C. Kendall, and E.S. Trombetta, *Inflammatory spleen monocytes can upregulate CD11c expression without converting into dendritic cells*. *J Immunol*, 2012. **188**(8): p. 3603-10.
184. Amici, S.A., et al., *CD38 Is Robustly Induced in Human Macrophages and Monocytes in Inflammatory Conditions*. *Frontiers in immunology*, 2018. **9**: p. 1593-1593.
185. Gerhardt, T. and K. Ley, *Monocyte trafficking across the vessel wall*. *Cardiovascular research*, 2015. **107**(3): p. 321-330.
186. Nockher, W.A. and J.E. Scherberich, *Expanded CD14<sup>+</sup>CD16<sup>+</sup> Monocyte Subpopulation in Patients with Acute and Chronic Infections Undergoing Hemodialysis*. 1998. **66**(6): p. 2782-2790.
187. Fingerle, G., et al., *The novel subset of CD14<sup>+</sup>/CD16<sup>+</sup> blood monocytes is expanded in sepsis patients*. 1993. **82**(10): p. 3170-3176.
188. Thakral, B., J. Anastasi, and S.A. Wang, *17 - Myeloproliferative and "Overlap" Myelodysplastic/Myeloproliferative Neoplasms*, in *Hematopathology (Third Edition)*, E.D. Hsi, Editor. 2018, Content Repository Only!: Philadelphia. p. 488-538.e4.
189. Rice, L. and M. Jung, *Chapter 48 - Neutrophilic Leukocytosis, Neutropenia, Monocytosis, and Monocytopenia*, in *Hematology (Seventh Edition)*, R. Hoffman, et al., Editors. 2018, Elsevier. p. 675-681.
190. Hansen, J.F., et al., *Influence of phthalates on cytokine production in monocytes and macrophages: a systematic review of experimental trials*. *PLoS one*, 2015. **10**(3): p. e0120083-e0120083.
191. Bornehag, C.G. and E. Nanberg, *Phthalate exposure and asthma in children*. *Int J Androl*, 2010. **33**(2): p. 333-45.
192. Li, W., et al., *Regulation of development of CD56 bright CD11c + NK-like cells with helper function by IL-18*. *PLoS One*, 2013. **8**(12): p. e82586.

193. Poli, A., et al., *CD56bright natural killer (NK) cells: an important NK cell subset*. Immunology, 2009. **126**(4): p. 458-465.
194. Kurioka, A., et al., *CD161 Defines a Functionally Distinct Subset of Pro-Inflammatory Natural Killer Cells*. Frontiers in immunology, 2018. **9**: p. 486-486.
195. Damasceno, D., et al., *Expression profile of novel cell surface molecules on different subsets of human peripheral blood antigen-presenting cells*. Clinical & translational immunology, 2016. **5**(9): p. e100-e100.
196. Marshall, A.S.J., et al., *Human M1CL (CLEC12A) is differentially glycosylated and is down-regulated following cellular activation*. 2006. **36**(8): p. 2159-2169.
197. Lahoud, M.H., et al., *The C-Type Lectin Clec12A Present on Mouse and Human Dendritic Cells Can Serve as a Target for Antigen Delivery and Enhancement of Antibody Responses*. 2009. **182**(12): p. 7587-7594.
198. Fu, X., et al., *Human natural killer cells expressing the memory-associated marker CD45RO from tuberculous pleurisy respond more strongly and rapidly than CD45RO- natural killer cells following stimulation with interleukin-12*. Immunology, 2011. **134**(1): p. 41-49.
199. Diefenbach, A., *Chapter 4 - Natural Killer Cells*, in *Antibody Fc*, M.E. Ackerman and F. Nimmerjahn, Editors. 2014, Academic Press: Boston. p. 75-93.
200. Marcus, A. and D.H. Raulet, *Evidence for natural killer cell memory*. Current biology : CB, 2013. **23**(17): p. R817-R820.
201. Lund, F.E., *Cytokine-producing B lymphocytes-key regulators of immunity*. Current opinion in immunology, 2008. **20**(3): p. 332-338.
202. Rieckmann, P., J.M. Tuscano, and J.H. Kehrl, *Tumor Necrosis Factor- $\alpha$  (TNF- $\alpha$ ) and Interleukin-6 (IL-6) in B-Lymphocyte Function*. Methods, 1997. **11**(1): p. 128-132.
203. Eto, D., et al., *IL-21 and IL-6 are critical for different aspects of B cell immunity and redundantly induce optimal follicular helper CD4 T cell (Tfh) differentiation*. PLoS One, 2011. **6**(3): p. e17739.
204. Arkatkar, T., et al., *B cell-derived IL-6 initiates spontaneous germinal center formation during systemic autoimmunity*. J Exp Med, 2017. **214**(11): p. 3207-3217.
205. Thomas, P.S., *Tumour necrosis factor- $\alpha$ : The role of this multifunctional cytokine in asthma*. 2001. **79**(2): p. 132-140.
206. Busse, P.J., et al., *Decrease in airway mucous gene expression caused by treatment with anti-tumor necrosis factor alpha in a murine model of allergic asthma*. Annals of allergy, asthma & immunology : official publication of the American College of Allergy, Asthma, & Immunology, 2009. **103**(4): p. 295-303.
207. Utheim, T.P., *Chapter 7 - Why Test BCG in Sjögren's Syndrome?*, in *The Value of BCG and TNF in Autoimmunity*, D.L. Faustman, Editor. 2014, Academic Press: Amsterdam. p. 105-125.
208. Ye, J., *Regulation of PPARgamma function by TNF-alpha*. Biochemical and biophysical research communications, 2008. **374**(3): p. 405-408.
209. Schlezinger, J.J., et al., *Environmental and Endogenous Peroxisome Proliferator-Activated Receptor  $\gamma$  Agonists Induce Bone Marrow B Cell Growth Arrest and Apoptosis: Interactions between Mono(2-ethylhexyl)phthalate, 9-cis-Retinoic Acid, and 15-Deoxy- $\Delta^{12,14}$ -prostaglandin  $J_2$* . 2004. **173**(5): p. 3165-3177.
210. Tyagi, S., et al., *The peroxisome proliferator-activated receptor: A family of nuclear receptors role in various diseases*. Journal of advanced pharmaceutical technology & research, 2011. **2**(4): p. 236-240.
211. Banno, A., et al., *PPARs: Key Regulators of Airway Inflammation and Potential Therapeutic Targets in Asthma*. Nuclear receptor research, 2018. **5**: p. 101306.
212. Latini, G., et al., *Peroxisome proliferator-activated receptors as mediators of phthalate-induced effects in the male and female reproductive tract: epidemiological and experimental evidence*. PPAR research, 2008. **2008**: p. 359267-359267.
213. Hurst, C.H. and D.J. Waxman, *Activation of PPARalpha and PPARgamma by environmental phthalate monoesters*. Toxicol Sci, 2003. **74**(2): p. 297-308.

214. Peng, Y., et al., *Inhibitory effect of PPAR-Gamma activator on IL-6 and mPGES protein expression in PBMC induced by homocysteine*. 2005. **9**(s4): p. S15-S20.
215. Patzer, A., et al., *Peroxisome proliferator-activated receptors gamma (PPARgamma) differently modulate the interleukin-6 expression in the peri-infarct cortical tissue in the acute and delayed phases of cerebral ischaemia*. Eur J Neurosci, 2008. **28**(9): p. 1786-94.
216. Hokanson, R., et al., *DEHP, bis(2)-ethylhexyl phthalate, alters gene expression in human cells: possible correlation with initiation of fetal developmental abnormalities*. Hum Exp Toxicol, 2006. **25**(12): p. 687-95.
217. Grindler, N.M., et al., *Exposure to Phthalate, an Endocrine Disrupting Chemical, Alters the First Trimester Placental Methylome and Transcriptome in Women*. Scientific reports, 2018. **8**(1): p. 6086-6086.
218. Campbell, J.J., et al., *CCR7 expression and memory T cell diversity in humans*. J Immunol, 2001. **166**(2): p. 877-84.
219. Ichikawa, Y., et al., *T cells bearing gamma/delta T cell receptor and their expression of activation antigen in peripheral blood from patients with Sjogren's syndrome*. Clin Exp Rheumatol, 1991. **9**(6): p. 603-9.
220. Lawand, M., J. Déchanet-Merville, and M.-C. Dieu-Nosjean, *Key Features of Gamma-Delta T-Cell Subsets in Human Diseases and Their Immunotherapeutic Implications*. Frontiers in immunology, 2017. **8**: p. 761-761.
221. Kilmartin, D.J., et al., *CD69 Expression on Peripheral CD4+ T Cells Parallels Disease Activity and Is Reduced by Mycophenolate Mofetil Therapy in Uveitis*. Investigative Ophthalmology & Visual Science, 2001. **42**(6): p. 1285-1292.
222. Hosgood, H.D., 3rd, et al., *Decreased Numbers of CD4(+) Naive and Effector Memory T Cells, and CD8(+) Naive T Cells, are Associated with Trichloroethylene Exposure*. Frontiers in oncology, 2012. **1**: p. 53-53.
223. Lan, Q., et al., *Occupational exposure to trichloroethylene is associated with a decline in lymphocyte subsets and soluble CD27 and CD30 markers*. Carcinogenesis, 2010. **31**(9): p. 1592-1596.
224. Blossom, S.J. and K.M. Gilbert, *Epigenetic underpinnings of developmental immunotoxicity and autoimmune disease*. Current opinion in toxicology, 2018. **10**: p. 23-30.
225. Stubbe, M., et al., *Antigen-Specific Central Memory CD4<sup>+</sup> T Lymphocytes Produce Multiple Cytokines and Proliferate In Vivo in Humans*. 2006. **177**(11): p. 8185-8190.
226. Siegrist, C.-A. and P.-H. Lambert, *Chapter 2 - How Vaccines Work*, in *The Vaccine Book (Second Edition)*, B.R. Bloom and P.-H. Lambert, Editors. 2016, Academic Press. p. 33-42.
227. Riou, C., et al., *Convergence of TCR and cytokine signaling leads to FOXO3a phosphorylation and drives the survival of CD4+ central memory T cells*. The Journal of experimental medicine, 2007. **204**(1): p. 79-91.
228. Hardtke, S., L. Ohl, and R. Förster, *Balanced expression of CXCR5 and CCR7 on follicular T helper cells determines their transient positioning to lymph node follicles and is essential for efficient B-cell help*. 2005. **106**(6): p. 1924-1931.
229. Schaerli, P., et al., *CXC chemokine receptor 5 expression defines follicular homing T cells with B cell helper function*. The Journal of experimental medicine, 2000. **192**(11): p. 1553-1562.
230. Breitfeld, D., et al., *Follicular B helper T cells express CXC chemokine receptor 5, localize to B cell follicles, and support immunoglobulin production*. J Exp Med, 2000. **192**(11): p. 1545-52.
231. Schaerli, P., et al., *Cxc Chemokine Receptor 5 Expression Defines Follicular Homing T Cells with B Cell Helper Function*. 2000. **192**(11): p. 1553-1562.
232. Shete, A., et al., *A review on peripheral blood CD4+ T lymphocyte counts in healthy adult Indians*. The Indian journal of medical research, 2010. **132**(6): p. 667-675.
233. Merrill, J.E. and O. Martínez-Maza, *14 - Cytokines in AIDS-Associated Nervous and Immune System Dysfunction*, in *Methods in Neurosciences*, E.B. De Souza, Editor. 1993, Academic Press. p. 243-266.

234. González-Mariscal, L., E. Garay, and M. Quirós, *Chapter 6 - Regulation of Claudins by Posttranslational Modifications and Cell-Signaling Cascades*, in *Current Topics in Membranes*, A.S. L. Yu, Editor. 2010, Academic Press. p. 113-150.
235. Greenfeder, S., et al., *Th2 cytokines and asthma. The role of interleukin-5 in allergic eosinophilic disease*. *Respiratory research*, 2001. **2**(2): p. 71-79.
236. Tanaka, T., M. Narazaki, and T. Kishimoto, *IL-6 in inflammation, immunity, and disease*. *Cold Spring Harbor perspectives in biology*. **6**(10): p. a016295-a016295.
237. Punnonen, J., et al., *Interleukin 13 and its Receptor*, in *Encyclopedia of Immunology (Second Edition)*, P.J. Delves, Editor. 1998, Elsevier: Oxford. p. 1489-1492.
238. Jin, W. and C. Dong, *IL-17 cytokines in immunity and inflammation*. *Emerging Microbes & Infections*, 2013. **2**: p. e60.
239. Spolski, R. and W.J. Leonard, *Interleukin-21: a double-edged sword with therapeutic potential*. *Nature Reviews Drug Discovery*, 2014. **13**: p. 379.
240. Parrish-Novak, J., et al., *Interleukin 21 and its receptor are involved in NK cell expansion and regulation of lymphocyte function*. *Nature*, 2000. **408**: p. 57.
241. Dudakov, J.A., A.M. Hanash, and M.R.M. van den Brink, *Interleukin-22: immunobiology and pathology*. *Annual review of immunology*, 2015. **33**: p. 747-785.
242. Reeves, R.K. and S.E. Bosinger, *Chapter 8 - Innate Immunity in Simian Immunodeficiency Virus Infection*, in *Natural Hosts of SIV*, A.A. Ansari and G. Silvestri, Editors. 2014, Elsevier: Amsterdam. p. 135-172.
243. Rutz, S., C. Eidschenk, and W. Ouyang, *IL-22, not simply a Th17 cytokine*. *Immunol Rev*, 2013. **252**(1): p. 116-32.



# Appendix

## Figures

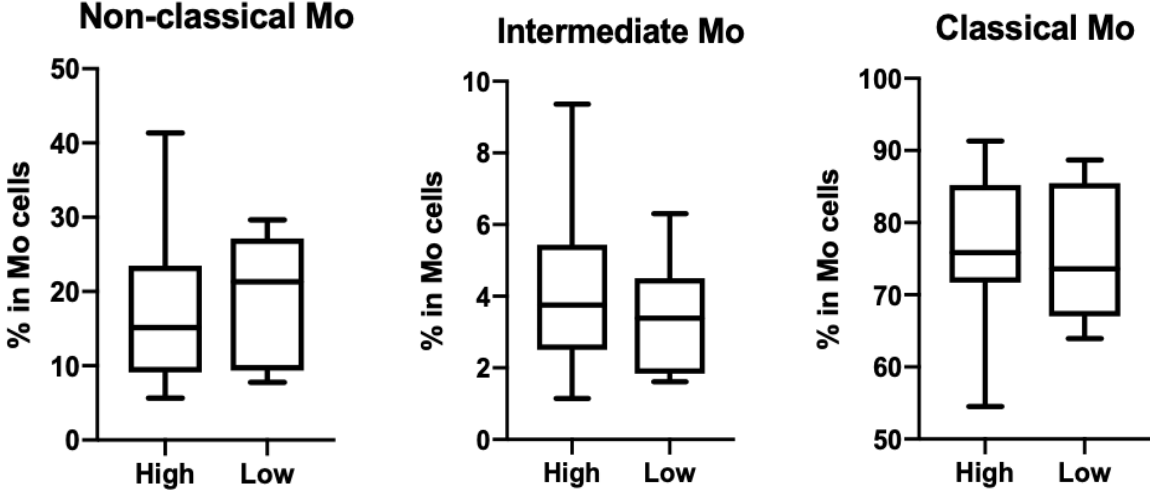


Figure 1: Box plots showing the percentages of Monocyte (Mo) subpopulations (non-classical (CD16++CD14dim), intermediate (CD16+CD14++) and Classical (CD16-CD14+++)) in the high and the low exposed group. The lines indicate the group median and the difference between the 75<sup>th</sup> and the 25<sup>th</sup> percentiles (the interquartile range (IQR)). We observed no significant between the two groups for neither of the subpopulations.

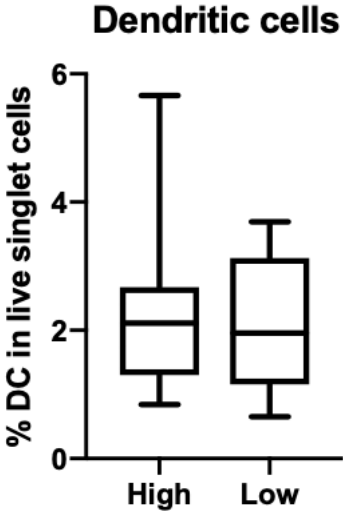


Figure 2: Box plot showing the percentage of DC in the high and the low exposed group. The percentages were calculated from the live singlet cell populations. The lines indicate the group median and the IQR. We observed no significant difference between the two groups.

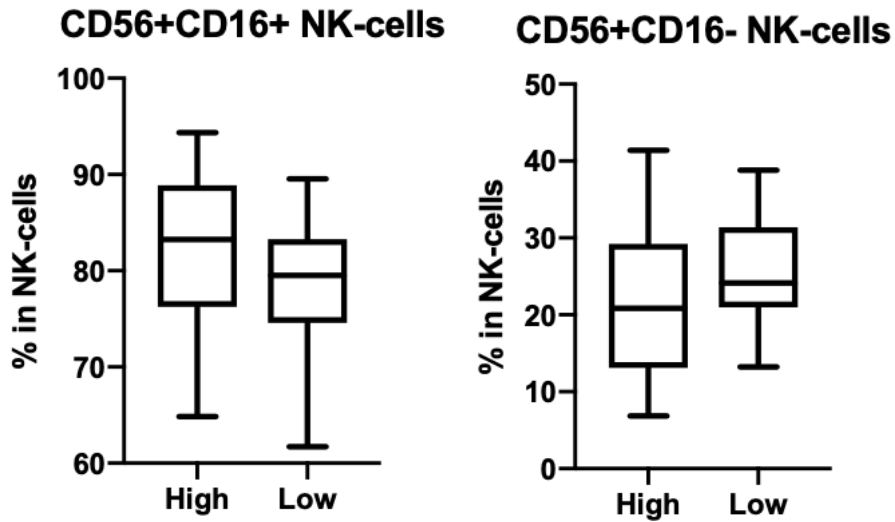


Figure 3: Box plots showing the percentages of NK-cell subpopulations (CD56+CD16+ NK-cells and CD56+CD16- NK-cells) in the high and the low exposed group. The lines indicate the group median and the IQR. We observed no significant between the two groups for neither of the subpopulations.

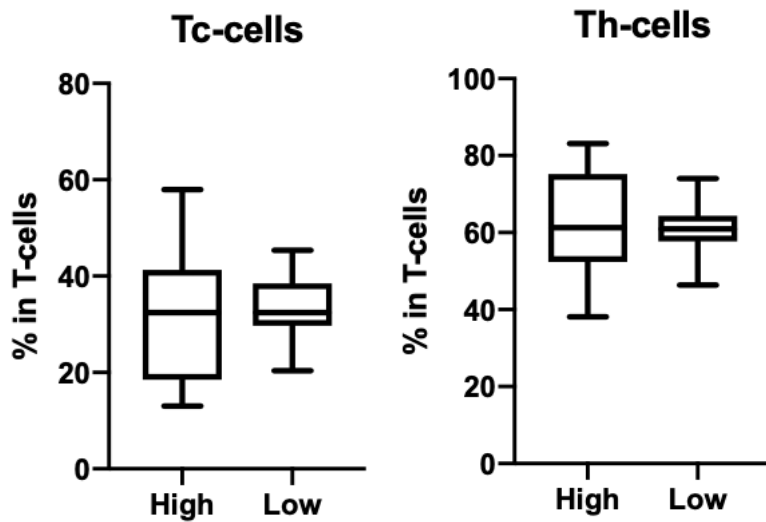


Figure 4: Box plot showing the percentages of T-cell subpopulations (Th- and Tc-cells) in the high and the low exposed group. The lines indicate the group median and the IQR. We observed no significant between the two groups for neither of the subpopulations.

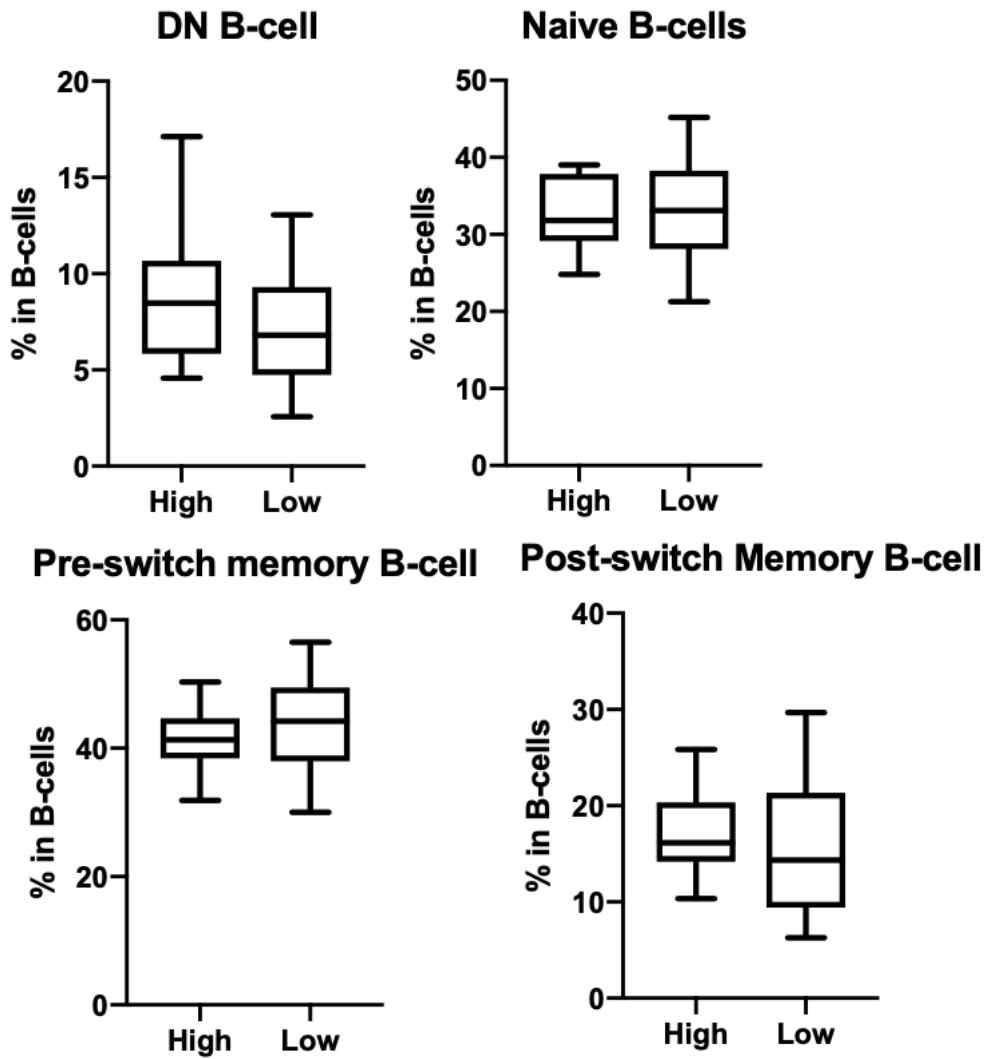


Figure 5: Box plots showing the percentages of B-cell subpopulations (double negative (DN), Naïve, Pre-switch memory and post-switch memory) in the high and the low exposed group. The lines indicate the group median and the IQR. We observed no significant between the two groups for neither of the subpopulations.

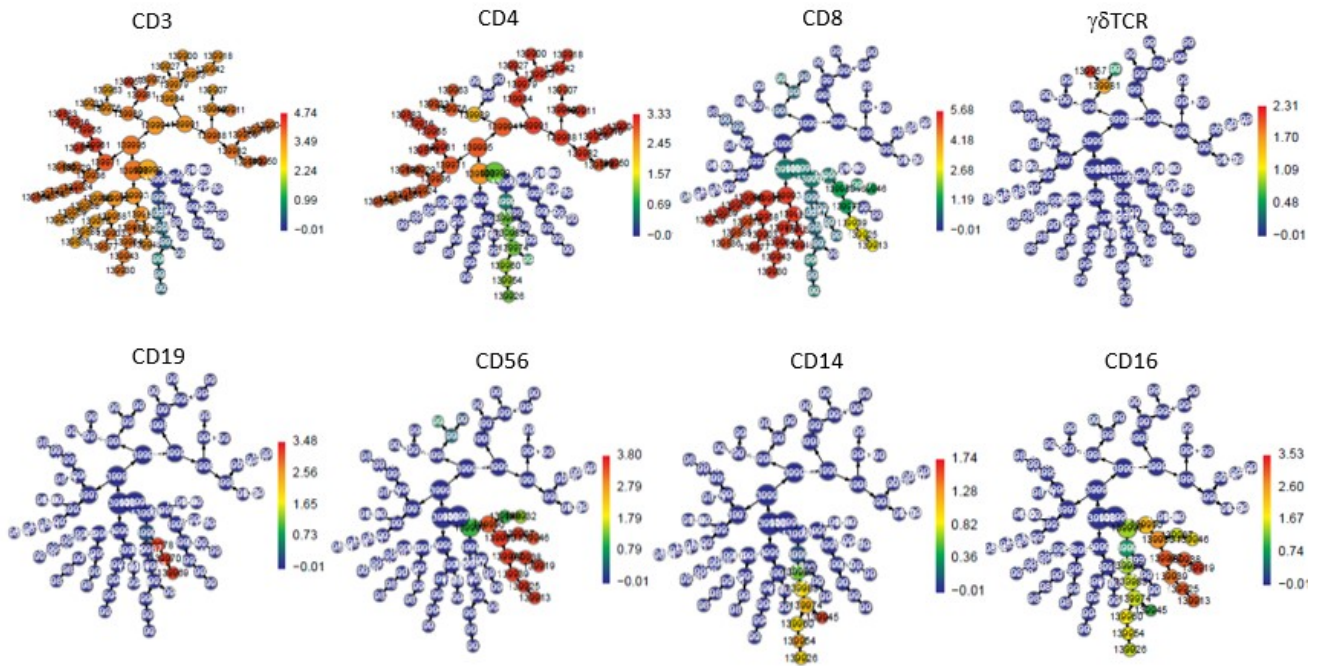


Figure 6: Example of how marker expression level for all cell clusters are illustrated by color scale by the CITRUS program. This coloring was used to identify and characterize each cell population. The coloring of the trees show the median marker expression in each node.

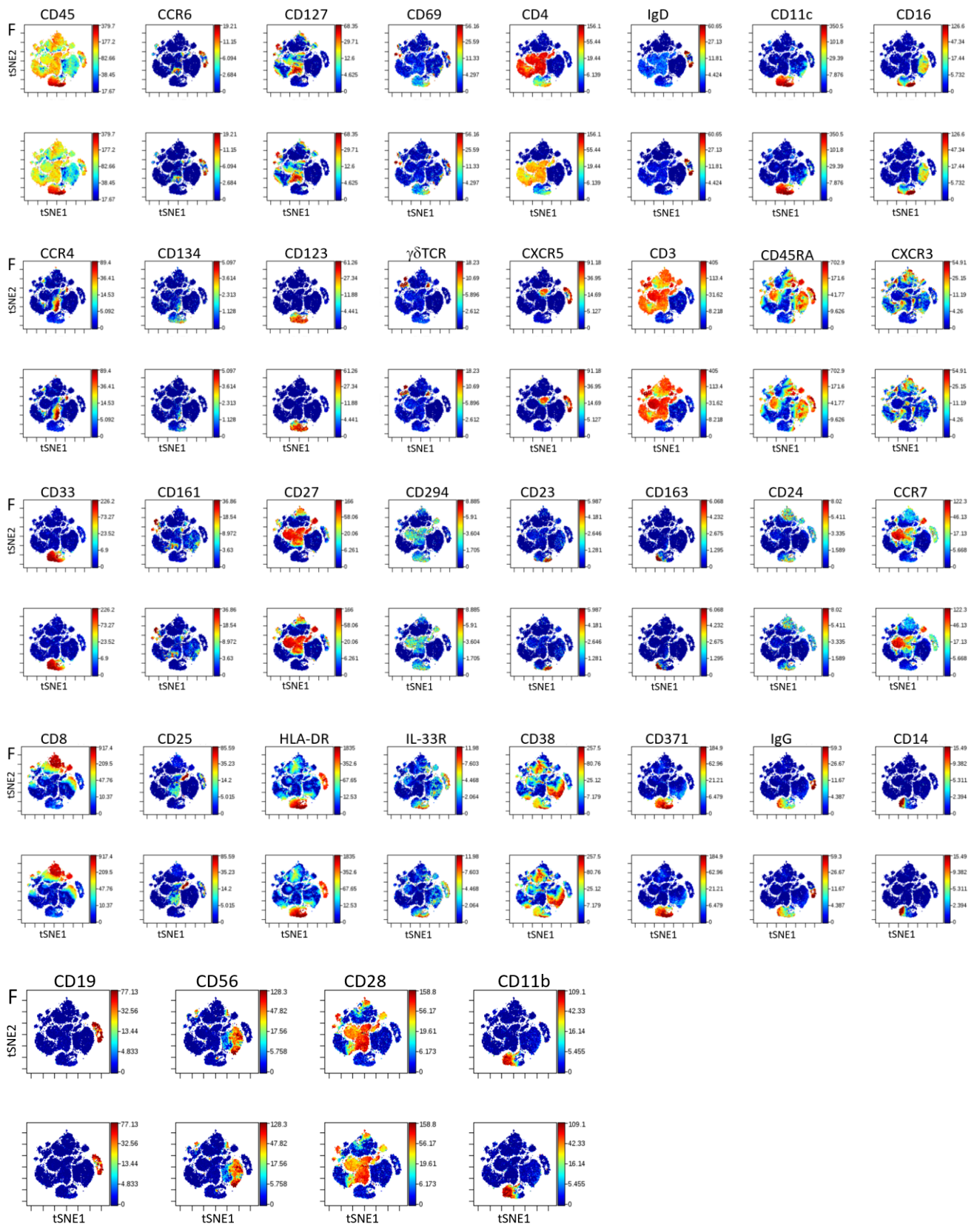


Figure 7: viSNE analysis from the unstimulated samples comparing the sample stained with a frozen antibody cocktail (F) and the sample from the same participant but colored with a fresh antibody cocktail. Each dot represents one cell and each cell are colored, on a gradient basis, by marker expression level (blue is low and red is high) for the given marker. The x- and y- axes are in arbitrary units. Clustering and marker expression analysis are done on the live singlet cell population.

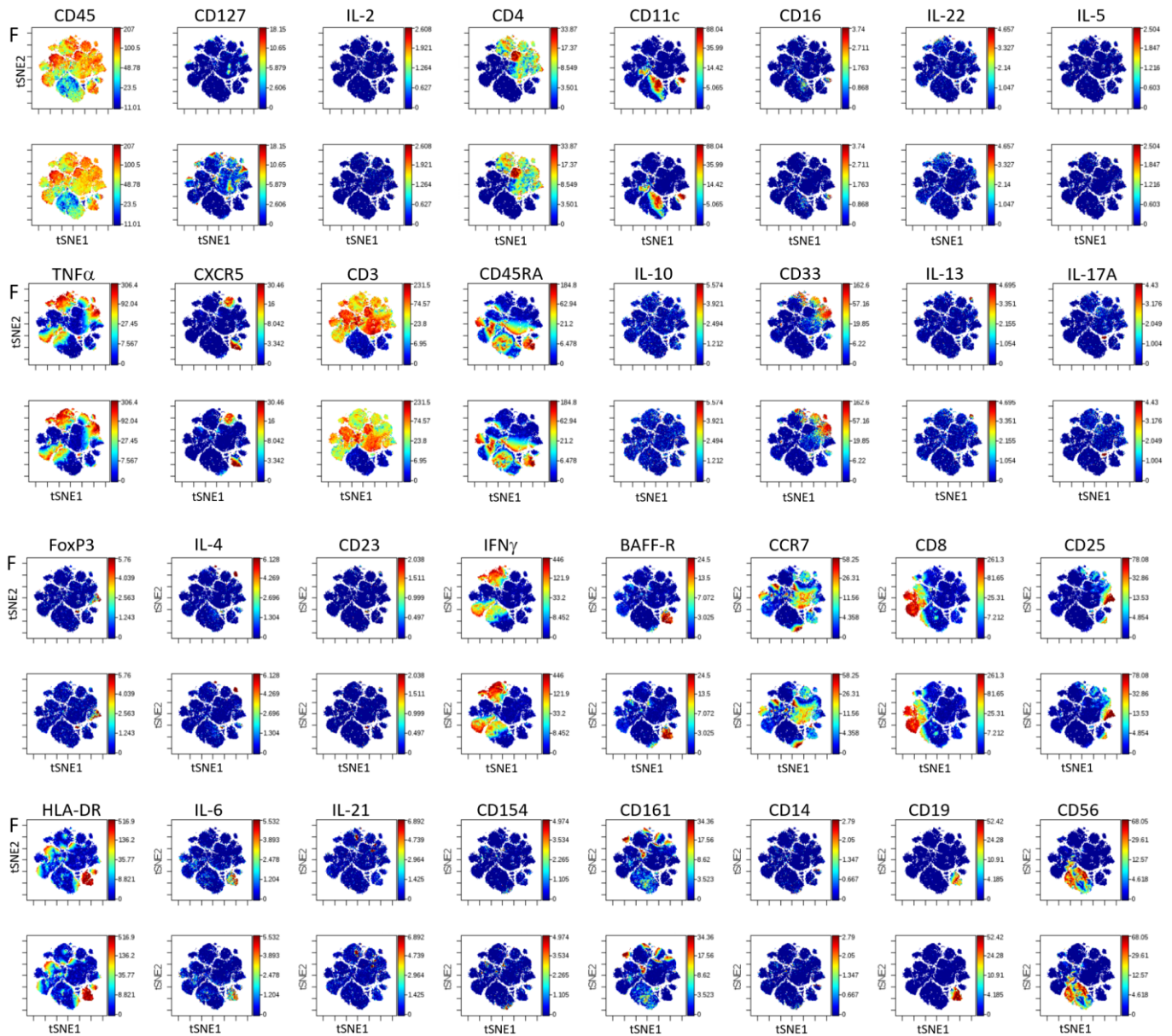


Figure 8: *viSNE* analysis from the stimulated samples comparing the sample stained with a frozen antibody cocktail (F) and the sample from the same participant but colored with a fresh antibody cocktail. Each dot represents one cell and each cell are colored, on a gradient basis, by marker expression level (blue is low and red is high) for the given marker. The x- and y- axes are in arbitrary units. Clustering and marker expression analysis are done on the live singlet cell population.

# Tables

Table 1: An overview of the cytokines investigated, the PBMC that produce them and their main effects [124].

<b>Cytokines</b>	<b>Produced by</b>	<b>Main effects</b>
<b>IFN<math>\gamma</math></b>	NK-cells, Tc1 and Th1 cells	Enhance MHC class I and II expression, activation of macrophages, antagonism of IL-4 actions and inhibition of Th2 cell proliferation
<b>TNF<math>\alpha</math></b>	DC, Mo, NK-cells, B-cells and Th-cells	Tumor cell cytotoxicity, induction of many other cytokines (e.g. IFN $\gamma$ ), E-selectin induction on endothelium, activating macrophages and antiviral activity
<b>IL-2</b>	Th1 cells	T-cell growth factor [233], enhancement of NK-cell cytotoxicity and monocyte activation
<b>IL-4</b>	NK cells, NKT-cells, $\gamma\delta$ T cells, Tc2 and Th2 cells	Induction of Th2-cells, stimulation of activated B- and T-proliferation, upregulation of MHC class II molecules on B-cells, downregulation of IL-12 production and thereby inhibiting Th1-cell differentiation, enhancement of macrophage phagocytosis and induction of switch to IgG1 and IgE and plays a key role in allergic responses [234]
<b>IL-5</b>	Th2 among others	Growth and proliferation factor for B-cells, maturation of eosinophils [235]
<b>IL-6</b>	DC, monocytes and Th2 among others	Maturation of B-cells, induction of acute phase reactants (plasma proteins that respond to elevated circulating levels of IL-1 and IL-6 when infection or tissue damage occurs) and involved in fever production [236].
<b>IL-10</b>	Mainly monocytes, (B-cells, Tc-cells, Th2-cells and T <sub>reg</sub> cells.)	Enhances B-cell survival, proliferation and antibody production, inhibit IL-2 secretion by Th1-cells, downregulation of MHC class II antigens and Th1 cytokines (e.g. IL-2) and anti-inflammatory properties [122]
<b>IL-13</b>	Th2 cells among others	Co-activation of B-cell proliferation, upregulation of MHC class II molecules and CD23 on B-cells and monocytes, induction of switch to IgG1 and IgE and anti-inflammatory properties [237]
<b>IL-17A</b>	Activated T-cells (Th17-cells, $\gamma\delta$ T cells, NKT-cells)	Pro-inflammatory action and stimulation of production of cytokines (e.g. TNF $\alpha$ , IL-6 and IL-8)[238]
<b>IL-21</b>	NKT-cells and Th-cells	Stimulation of B-cell proliferation, stimulation of NK cells and co-stimulation of T-cells [239, 240]
<b>IL-22</b>	NK-cells, Th17 cells and $\gamma\delta$ T cells[241]	Main impact is non-hematopoietic cells, promotes proliferation and differentiation [241-243]

Table 2: Urine sample concentration after correction for molecular weight for all DEHP and DiNP metabolites (as described in section 3.2). Concentration were estimated for 24 h collection period<sup>1</sup>. Reported as ng/mL.

	MEHP MOL COR.	MEHHP MOL COR.	MEOHP MOL COR.	MECPP MOL COR.	MMCHP MOL COR.	OH_MINP MOL COR.	OXO_MINP MOL COR.	CX_MINP MOL COR.	SUM MOL COR.
<b>H1</b>	20,2	55,5	31,9	82,4	53,5	18,2	13,9	19,0	294,6
<b>H2</b>	9,4	31,2	19,7	33,2	41,4	66,8	5,2	15,7	222,5
<b>H3</b>	7,4	41,4	33,2	60,4	54,4	4,4	2,1	8,7	212,0
<b>H4</b>	0,0	7,7	5,8	0,0	2,1	279,7	183,4	278,7	757,4
<b>H5</b>	16,7	73,6	45,6	90,9	72,9	9,5	5,8	13,4	328,5
<b>H6</b>	7,1	40,0	27,2	78,9	10,9	218,5	83,4	271,7	737,6
<b>H7</b>	7,7	27,4	18,9	38,3	34,5	32,3	10,3	20,5	189,9
<b>H8</b>	14,5	50,9	30,6	71,4	51,9	9,6	3,2	12,4	244,4
<b>H9</b>	48,8	53,4	30,8	74,9	48,2	6,9	4,9	11,9	279,8
<b>H10</b>	2,8	15,9	9,6	27,9	20,5	256,4	174,2	176,8	684,1
<b>H11</b>	6,9	14,1	8,3	16,8	11,2	150,4	77,5	69,7	354,9
<b>H12</b>	6,0	32,4	26,7	29,2	29,3	378,2	270,8	298,7	1071,2
<b>H13</b>	2,3	15,7	8,0	13,1	7,1	390,6	181,3	330,6	948,6
<b>H14</b>	26,0	111,2	61,0	87,2	76,9	8,7	3,2	7,5	381,6
<b>L1</b>	2,0	11,0	6,8	18,3	17,3	8,8	2,0	6,3	72,6
<b>L2</b>	3,1	9,8	5,8	17,1	17,9	9,6	3,6	11,8	78,7
<b>L3</b>	1,5	8,1	6,5	12,9	10,8	3,4	1,9	7,3	52,4
<b>L4</b>	2,3	10,0	7,1	13,9	20,1	8,8	4,2	11,4	77,8
<b>L5</b>	2,9	6,8	5,1	11,1	13,3	11,5	2,2	7,8	60,7
<b>L6</b>	0,0	12,8	7,9	23,4	12,7	2,2	1,2	4,9	65,1
<b>L7</b>	1,3	10,6	6,9	14,3	15,9	5,6	4,5	12,7	71,9
<b>L8</b>	1,5	12,3	5,9	15,6	13,3	6,9	5,0	7,5	68,2
<b>L9</b>	0,0	7,0	4,0	14,4	12,1	6,3	4,0	9,6	57,3
<b>L10</b>	0,7	7,2	5,6	14,3	11,3	1,9	1,9	5,5	48,4
<b>L11</b>	1,5	14,4	7,3	20,8	16,8	6,3	3,4	9,3	79,9
<b>L12</b>	2,8	8,9	5,3	10,3	13,8	4,2	2,8	8,9	57,0
<b>L13</b>	1,1	11,3	7,8	15,0	21,2	5,3	4,5	13,8	80,1
<b>L14</b>	1,2	9,1	6,1	12,9	12,2	8,8	4,2	9,2	63,7

<sup>1</sup> Mono-2-ethylhexyl phthalate (MEHP), Mono-2-ethyl-5-hydroxyhexyl phthalate (MEHHP), Mono-2-ethyl-5-oxohexyl phthalate (MEOHP), Mono-2-ethyl 5-carboxypentyl phthalate (MECPP), Mono-2-carboxymethyl hexyl phthalate (MMCHP), Mono-4-methyl-7-hydroxyoctyl phthalate (OH\_MiNP), Mono-4-methyl-7-oxooctyl phthalate (OXO\_MiNP) and Mono-4-methyl-7-carboxyoctyl phthalate (CX\_MiNP)



Table 3: Urine sample concentration (estimates for the 24 h collection period) of the other phthalate metabolite concentrations for the participants (DEP, DiBP, DnBP, BBzP, DINCH and DPHP)<sup>2</sup>. Measured as ng/mL

	MEP	MIBP	MNBP	MBZP	OH_MINCH	OXO_MINCH	OH_MPHP	SUM
<b>H1</b>	32,51	6,14	11,85	1,45	1,53	1,30	0,67	55,44
<b>H2</b>	5,21	9,57	17,14	5,08	0,76	0,59	0,26	38,60
<b>H3</b>	29,59	7,39	21,22	1,50	0,29	0,42	0,26	60,66
<b>H4</b>	4,58	3,35	13,59	1,10	0,37	0,29	0,06	23,34
<b>H5</b>	8,86	21,86	19,19	3,66	1,49	1,33	0,60	56,98
<b>H6</b>	29,66	7,70	12,01	2,28	1,05	0,83	0,30	53,83
<b>H7</b>	52,92	13,40	17,44	4,30	0,61	0,55	0,48	89,70
<b>H8</b>	15,80	8,64	15,46	0,77	0,38	0,46	0,58	42,08
<b>H9</b>	4,92	50,00	20,28	3,24	11,05	8,55	0,98	99,02
<b>H10</b>	9,50	15,38	7,94	2,73	18,55	14,63	0,32	69,06
<b>H11</b>	7,80	3,45	3,60	0,46	0,50	0,42	0,21	16,45
<b>H12</b>	33,49	4,25	8,75	1,82	0,06	0,15	0,06	48,58
<b>H13</b>	9,16	33,65	11,84	1,16	0,57	0,61	0,30	57,29
<b>H14</b>	29,81	3,61	8,38	0,60	0,35	0,29	0,38	43,42
<b>MEDIAN</b>								54,64
<b>L1</b>	6,55	3,81	5,28	1,00	1,43	1,07	0,38	19,50
<b>L2</b>	21,64	4,55	5,22	2,79	0,67	0,51	0,51	35,88
<b>L3</b>	22,40	5,87	9,49	1,71	0,52	0,39	0,41	40,80
<b>L4</b>	4,92	5,53	7,21	1,73	0,62	0,57	0,06	20,64
<b>L5</b>	4,70	4,95	7,82	2,00	0,65	0,59	0,39	21,10
<b>L6</b>	28,39	13,62	60,44	3,30	0,22	0,22	0,24	106,42
<b>L7</b>	5,78	4,94	7,26	0,66	0,79	0,71	0,42	20,56
<b>L8</b>	25,54	6,37	12,02	1,17	0,53	0,39	0,53	46,55
<b>L9</b>	7,85	11,76	9,41	1,52	0,46	0,40	0,09	31,48
<b>L10</b>	29,34	7,14	8,00	1,53	0,22	0,25	0,30	46,78
<b>L11</b>	1,75	10,77	5,44	0,47	0,74	0,57	1,04	20,79
<b>L12</b>	19,66	8,80	7,85	1,62	0,42	0,36	0,57	39,29
<b>L13</b>	5,01	11,39	9,82	1,88	0,92	0,90	0,11	30,04
<b>L14</b>	6,43	3,91	7,96	0,76	0,54	0,48	0,57	20,65
<b>MEDIAN</b>								30,76

<sup>2</sup> Diethyl phthalate (DEP)( Monoethyl phthalate (MEP)), Diisobutyl phthalate (DiBP) (Mono-iso-butyl phthalate (MiBP)), di-n-butyl phthalate (DNBP)( Mono-n-butyl phthalate (MNBP)), Benzyl butyl phthalate (BBzP) (Mono benzyl phthalate (MBZP)), 1,2-Cyclohexane dicarboxylic acid diisononyl ester (DINCH)( 2-(((Hydroxy-4-methyloctyl)oxy)carbonyl)cyclohexanecarboxylic Acid (OH\_MINCH)), 2-(((4-Methyl-7-oxooctyl)oxy)carbonyl)cyclohexanecarboxylic Acid (OXO\_MINCH)) and Di(2-propylheptyl) phthalate (DPHP) (6-Hydroxy Monopropylheptylphthalate (OH\_MPHP)).

Table 4: Urine sample concentrations of (estimates for the 24 h collection period) of the phenol and paraben for the participants (MEPA, ETPA, PRPA, BUPA, BPA, BSP, BPF, OXBE and TRCS)<sup>3</sup>. Measured as ng/mL.

	MEPA	ETPA	PRPA	BUPA	BPA	BPS	BPF	OXBE	TRCS
<b>H1</b>	46,95	0,51	22,67	0,19	2,82	0,37	0,13	1,10	1,67
<b>H2</b>	3,17	0,37	0,07	0,14	2,57	0,37	2,59	7,52	0,54
<b>H3</b>	11,99	7,64	1,81	0,54	1,39	12,74	0,08	0,45	0,45
<b>H4</b>	4,70	1,87	0,04	0,48	0,96	0,09	0,06	0,43	0,12
<b>H5</b>	5,48	0,50	0,04	0,18	1,92	0,65	0,08	3,60	0,28
<b>H6</b>	10,41	0,75	1,70	0,18	5,83	0,08	0,06	23,00	0,14
<b>H7</b>	4,65	1,19	0,89	0,15	9,97	0,11	0,08	13,00	301,21
<b>H8</b>	137,03	27,59	54,98	0,13	2,63	0,15	0,11	8,97	0,36
<b>H9</b>	15,64	1,03	14,07	0,10	1,09	0,90	0,10	19,92	0,80
<b>H10</b>	34,77	18,35	0,99	0,95	1,46	0,21	0,07	150,31	1,32
<b>H11</b>	50,60	15,11	8,70	13,45	1,42	0,36	0,07	5,60	0,11
<b>H12</b>	32,87	0,61	13,80	0,46	2,29	0,22	2,66	5,20	0,13
<b>H13</b>	3,86	2,10	0,05	0,07	1,63	0,11	0,07	8,03	0,36
<b>H14</b>	1,76	1,00	0,06	0,06	1,47	1,08	0,06	1,45	0,08
<b>L1</b>	2,78	1,06	0,62	0,20	0,67	0,06	0,04	0,54	0,17
<b>L2</b>	2,88	0,50	0,04	0,34	0,78	0,18	0,08	0,69	0,23
<b>L3</b>	3,01	0,87	0,04	0,09	0,90	0,17	0,07	44,67	0,10
<b>L4</b>	2,92	0,56	0,07	0,09	0,74	0,77	0,06	1,23	0,10
<b>L5</b>	4,91	1,91	0,08	0,07	2,36	0,29	0,07	0,88	0,63
<b>L6</b>	2,64	3,16	0,32	0,06	3,38	0,06	1,51	1,70	0,52
<b>L7</b>	2,36	1,02	0,04	0,10	0,47	0,99	0,08	1,09	0,32
<b>L8</b>	6,38	3,48	0,03	0,09	1,51	0,08	1,01	1,04	0,11
<b>L9</b>	8,55	0,16	0,09	0,09	1,70	0,12	0,09	7,16	0,17
<b>L10</b>	2,55	0,39	0,04	0,12	1,33	0,10	0,07	0,70	0,05
<b>L11</b>	3,91	0,22	0,08	0,14	0,25	0,21	0,14	1,04	0,14
<b>L12</b>	4,23	1,36	0,15	0,10	0,79	0,14	0,10	1,55	0,09
<b>L13</b>	7,10	2,93	0,06	0,13	0,41	0,16	0,11	0,25	0,06
<b>L14</b>	5,04	0,92	0,06	0,11	1,46	0,15	0,11	11,72	0,18

<sup>3</sup> Methyl paraben (MEPA), Ethyl paraben (ETPA), Propyl paraben (PRPA), Butyl paraben (BUPA), Bisphenol A (BPA), Bisphenol S (BPS), Bisphenol F (BPF), Oxybenzone (OXBE) and Triclosan (TRCS)

Table 5: Antibody panels used to identify surface and intracellular markers (proteins). The metal isotope tag, the target, and the volume used per sample are presented. Panel 1 was used on the unstimulated samples and contains 36 antibodies used for surface staining only. Panel 2 was used for the stimulated cells and contains 20 surface antibodies (denoted in the text as Panel 2A) and 12 intracellular antibodies (denoted in the text as Panel 2B), in total 32 antibodies.

Panel 1 (36 surface antibodies) – unstimulated cells				Panel 2 (20 surface + 12 intracellular antibodies) – stimulated cells			
Staining	Isotope	Target	Volume (µL)	Staining	Isotope	Target	Volume (µL)
Surface	141Pr	CD196 (CCR6)	0,5	Surface	142Nd	CD19	0,5
Surface	142Nd	CD19	0,5	Surface	143Nd	CD127 (IL-7Ra)	0,5
Surface	143Nd	CD127 (IL-7Ra)	0,5	Surface	145Nd	CD4	0,5
Surface	144Nd	CD69	0,5	Surface	147Sm	CD11c	0,5
Surface	145Nd	CD4	0,5	Surface	148Nd	CD16	0,5
Surface	146Nd	IgD	0,5	Surface	153Eu	CD185 (CXCR5)	0,5
Surface	147Sm	CD11c	0,5	Surface	154Sm	CD3	0,5
Surface	148Nd	CD16	0,5	Surface	155Gd	CD45RA	0,5
Surface	149Sm	CD194 (CCR4)	0,5	Surface	158Gd	CD33	0,5
Surface	150Nd	CD134 (Ox40)	0,5	Surface	164Dy	CD23	0,5
Surface	151Eu	CD123 (IL-3R)	0,5	Surface	166Er	BAFF-R (Cd268) (conj.)	0,5
Surface	152Sm	γδTCR	0,5	Surface	167Er	CD197 (CCR7)	0,5
Surface	153Eu	CD185 (CXCR5)	0,5	Surface	168Er	CD8	0,5
Surface	154Sm	CD3	0,5	Surface	169Tm	CD25 (IL-2R)	0,5
Surface	155Gd	CD45RA	0,5	Surface	170Er	HLA-DR	0,5
Surface	156Gd	CD183 (CXCR3)	0,5	Surface	173Yb	CD154(CD40L) (conj.)	0,5
Surface	158Gd	CD33	0,5	Surface	174Yb	CD161 (conj.)	1
Surface	159Tb	CD161	0,5	Surface	175Lu	CD14	0,5
Surface	160Gd	CD28	0,5	Surface	176Yb	CD56 (NCAM)	0,5
Surface	162Dy	CD27	0,5	Surface	89Y	CD45	0,5
Surface	163Dy	CD294 (CRTH2)	0,5	Intracellular	144Nd	IL-2	0,5
Surface	164Dy	CD23	0,5	Intracellular	150Nd	IL-22	0,5
Surface	165Ho	CD163	0,5	Intracellular	151Eu	IL-5	0,5
Surface	166Er	CD24	0,5	Intracellular	152Sm	TNFα	0,5
Surface	167Er	CD197 (CCR7)	0,5	Intracellular	156Gd	IL-10 (conj.)	0,5
Surface	168Er	CD8a	0,5	Intracellular	159Tb	IL-13 (conj.)	0,5
Surface	169Tm	CD25 (IL-2R)	0,5	Intracellular	161Dy	IL-17A	0,5
Surface	170Er	HLA-DR	0,5	Intracellular	162Dy	Foxp3	0,5
surface	171Yb	IL-33R /ST2 (conj.)	0,5	Intracellular	163Dy	IL-4	0,5

Surface	172Yb	CD38	0,5	Intracellular	165Ho	IFN $\gamma$	0,5
Surface	173Yb	CD371	0,5	Intracellular	171Yb	IL-6 (conj.)	0,5
Surface	174Yb	IgG (conj.)	0,5	3172011B	172Yb	IL-21	0,5
Surface	175Lu	CD14	0,5				
Surface	176Yb	CD56 (NCAM)	0,5				
Surface	209Bi	CD11b	0,5				
Surface	089Y	CD45	0,5				
Intracellular	191Ir	Cell-ID		Intracellular	191Ir	Cell-ID	
		Intercalator				Intercalator	
Intracellular	193Ir	Cell-ID		Intracellular	193Ir	Cell-ID	
		Intercalator				Intercalator	
Live/Dead	194Pt	Cisplatin – live/dead		Live/Dead	194Pt	Cisplatin – live/dead	

Table 6: Expression level (L; low, M; medium; H; high, N; none ) summarized for all markers in unstimulated cells, reported for the CITRUS identified significant clusters in this study<sup>4</sup>.

	CD 45	CD 196	CD 19	CD 127	CD 69	CD 4	IgD	CD 11c	CD 16	CD 194	CD 134	CD 123	γδTCR	CD 185	CD3	CD 45RA	CD 183	CD 33	CD 161	CD 28	CD 27	CD 294	CD 23	CD 163	CD 24	CD 197	CD8	CD 25	HLA-DR	IL33-R /ST2	CD 38	CD 371	IgG	CD 14	CD 56	CD 11b		
<b>NK#1</b>	H	N	N	N	M	N	N	H	H	N	N	N	N	N	L	H	M	N	M	L	N	N	L	N	N	N	N	H	N	N/L	L	H	M	N/L	N	H	L	
<b>NK#2</b>	H	N	N	N	N/L	N	N	M	L	L	N	N	N	N	N/L	H	L	N	L	L	N/L	N	N	N	N	N	L	L	N	L	N/L	H*	N/L	N	N	H	L	
<b>MO#1</b>	H	N	N	N	H	H	N	H	H	L	N/L	H	L	L	L/M*	M	L	H	L	L/	N/L	M	N/L	L	L	N/L	M	N/	H	H	H*	H	H	H*	H	H	N/	H
<b>Th#1</b>	H	N	N	H*	L	H	L	N	N	M	N	N	L	H	H	L/M	M	N	L	H	H	M	N	N	N	H	N/L	H/	N/L	N	L/	M	N	N	N	N	N	N
<b>Th#2</b>	H	N	N	H	N/	H	L	N	N	N	N	N	N/L	N	H	H	M	N	N	H	H	H*	N	N	N	H	M	N	N	L++	H	N/L	N	N	N	N	N	
<b>gdTCR</b>	H	N	N	L	N/	N	N	L	L	N	N	N	H	N	H	H*	H	N	L	L	N	N	N	N	N	N	M	N	M	N/L	L	N	N	N	N	M	N/	L
<b>Tc#1</b>	H	N	N	H	L	N	N	N	N	N	N	N	N	N	H	H	H	N	N	H	H	H*	N/L	N	L	H	H	N/	N	H+	M/	N	N	N	N	N	N	N
<b>Tc#2</b>	H	N	N	M	N	N	N	N	N	N	N	N	N	N	H	H	H	N	N	H	H	H*+	N/L	N	M	H	H	N/	L	H	M/	N	N	N	N	N	N+	

<sup>4</sup>\*; Two tops, +; higher expression than other cluster from the same branch, --; lower expression than parent cluster (data not shown), ++; higher expression than parent cluster (data not shown).

Table 7: Expression level (L; low, M; medium; H; high, N; none) summarized for all markers in stimulated cells, reported for the CITRUS identified significant clusters in this study<sup>5</sup>.

	CD 45	CD 19	CD 127	IL- 2	CD 4	CD 11c	CD 16	IL- 22	IL- 5	TNFα	CD185 (CXCR5)	CD3	CD 45RA	IL- 10	IL- 13	IL- 17A	Foxp3	IL-4	CD 23	IFNγ	BAFF-R	CD197	CD8	CD 25	HLA-DR	IL-6	IL-21	CD 154	CD 161	CD 14	CD 56				
<b>B#1</b>	H	H	N	N	N	N	N	N	N	H	H*	N	H	N	N	N	N	N	N	N	N	H*	H*	L	L+	H	H+	N	N	N	N	N	N		
<b>B#2</b>	H	H	N	N	N	N	N	N	N	M	H*	N	H	N	N	N	N	N	N	N	N	H	H*	L*	L	H	H	N	N	N	N	N	N		
<b>NK#3</b>	H	N	N	N	N	H*	N	N	N	N/L--	N	N	H*	N	N	N	N	N	N	N	H	N	N	L	N	L	N	N	N	N	H	N	H		
<b>Tc#3</b>	H	N	M	N	N	N	N	N	N	L	N	H	H	N/L	N	N	N	N	N	N	N/L	N/L	H	H	N	L	M	N	N	N	N	N	N	N	
<b>Th#3</b>	H	N	N/L	N	H	N	N	N	N	N/L	N	H	H	N	N	N	N	N	N	N	N/L	N	H*	N	N	N/L	L	N	N	N	N	N	N	N	N

<sup>5</sup>\*; Two tops, +; higher expression than other cluster from same cell population, --; lower expression than parent cluster (data not shown), ++; higher expression than parent cluster (data not shown).

Table 8: Expression level (low, medium, high) summarized for activation markers in the unstimulated samples of CITRUS identified significant clusters. (med; medium)

	<b>CD69</b>	<b>CD134</b>	<b>CD123</b>	<b>CD28</b>	<b>CD23</b>	<b>CD163</b>	<b>CD25</b>	<b>HLA-DR</b>	<b>CD371</b>
<b>TH#1</b>	Low	Low	Low	High	Low	Low	High/Med	Low/Med	Low
<b>TH#2</b>	Low/Med	Low	Low	High	Low/Med	Low	Low	Low	Low/Med
<b>TC#1</b>	Low	Low	Low	High	Low	Low	Low/Med	Med	Low
<b>TC#2</b>	Low/Med	Low/Med	Low	High	Low	Low	Low/Med	Low	Low
<b>GDT</b>	Med	Low	Low	Med	Low	Low	None	Med	Low
<b>NK#1</b>	Med	None/Low	Low	Med	Med	Low	Low	Low/Med	Med/High
<b>NK#2</b>	Low/Med	Low	Low	Low/Med	Low	Low	Low/med	Low/Med	Low/med
<b>MO#1</b>	Medium	Low	High	Medium	Low/Med	Med/Low	Low	High	High(Two)

Table 9: Expression level (low, medium, high) summarized for the functional markers and cytokines in the stimulated samples of CITRUS identified significant clusters. (med; medium)

	IL-2	IL-22	IL-5	TNFA	IL-10	IL-13	IL-17A	FOXP3	IL-4	CD23	IFN $\gamma$	BAFF-R	CD25	IL-6	IL-21
<b>B#2</b>	Low	Low	Low	Med	Low	Low	Low	Low	Low	Low	Low/ Med	High	Med	High	Low/ Med
<b>B#1</b>	Low	Low	Low	Med	Low	Low	Low	Low	Low	Low	Low/ Med	High(Two)	Med/ High	High+	Low/ Med
<b>NK#3</b>	Low	Low	Low	Low	Low	Low	Low	Low/ Med	Low	Low	High	Low	Low	Low	Low
<b>TC#3</b>	Low/ None	Low	Low	Low/ Med	Low	Low	Low	Low/ None	Low	Low	Low/ Med	Low/Med	Low	Med	Low
<b>TH#3</b>	Low	Low	Low	Low/ Med	Low	Low	Low	Low	Low	Low	Low/ Med	Low	Low	Med	Low